Bimetallic Silver Catalysts for the Reformate-Assisted Selective Catalytic Reduction of NO_x

by

Richard C. Ezike

A dissertation submitted in partial fulfillment
of the requirements for the degree of
Doctor of Philosophy
(Chemical Engineering)
in The University of Michigan
2011

Doctoral Committee:

Professor Levi T. Thompson, Jr., Chair
Professor Arvind Atreya
Professor Erdogan Gulari
Professor Phillip E. Savage
Adjunct Professor Galen B. Fisher

© Richard C. Ezike 2011
All Rights Reserved

To The Almighty, who gives me strength to endure and succeed. Everything is for Him and Him alone. And to my parents, for their love and support through this journey.

ACKNOWLEDGEMENTS

I would like to thank my advisor, Professor Levi T. Thompson, for providing me with guidance and mentorship and the opportunity to do research in environmental catalysis. I thank him for his encouragement and the belief he had in me to complete this research, even during times I did not believe I could do so. He not only helped me to grow as a researcher, but to mature as a person as well. I am also grateful to my doctoral committee, Professors Arvind Atreya, Galen Fisher, Erdogan Gulari, and Phillip Savage for their insights and suggestions during my committee meetings.

I also want to thank the many members of the Thompson Research Group including Dr. William Johnson, Dr. Chang Hwan Kim, Dr. Timothy King, Dr. Worajit (Sai) Setthapun, Dr. Easwar Ranganathan, Dr. Maha Hammoud, Dr. Saemin Choi, Dr. Neil Schweitzer, Dr. Peter Aurora, Dr. Andre Taylor, Dr. Alice Sleightholme, Dr. Sang Ok Choi, Professor Paul Rasmussen, Dr. Josh Schaidle, Dr. Adam Lausche, Priyanka Pande, Aaron Shinkle, Josh Grilly, Binay Prassad, Kana Weiss, Allison Wilson, Yuan Chen, and Steve Blodgett, who all have provided me with assistance and ideas to further my research. I would also like to thank my undergrads Cynthia Wang and Reinald Deda for their assistance in preparing my experiments. I also would like to acknowledge financial support from Quantum Sciences Incorporated, Michigan Memorial Phoenix Energy Institute and the Rackham Graduate School.

There are many people who have helped me to develop personally throughout my research experience. The people in SMES-G, SCOR, Men of Valor, and New Genesis Bible Study have all provided me with personal guidance and support and

the means to rejuvenate when I needed it. I want to give special thanks to Dr. Susan Montgomery and Debby Mitchell. Dr. Montgomery served as my longtime AGEP advisor, and she helped me to navigate many difficult times I faced during my graduate studies. She has been instrumental in my success here at Michigan. Debby has been a personal mentor to me in so many ways; I cannot even begin to count. She has encouraged me when I was down, applauded me when I have been successful and was stern with me when I needed to get back on track. Thank you so much Debby.

I would to acknowledge my parents, James M. Ezike and Felicia N. Ezike. Without them I could not have completed this process. They believed in me and my ability to finish my degree, even in times when I did not believe I could do so. They always encouraged me to see my strengths and use them to my advantage. They uplifted me in the worst times - which seemed to be many - and never, ever stopped loving me. I also want to acknowledge my little sister Vivian and brother Michael, who were there for me during those late night talks when I was frustrated to no end. Thank you so much for your love and caring.

TABLE OF CONTENTS

LIST OF FIGURES

Figure

LIST OF TABLES

Table

ABSTRACT

Bimetallic Silver Catalysts for the Reformate-Assisted Selective Catalytic Reduction of NO_x

by

Richard C. Ezike

Chair: Levi T. Thompson, Jr.

The objective in this dissertation was to investigate a strategy to improve the low-temperature performance of Ag/Al_2O_3 for hydrocarbon selective catalytic reduction of NO_x, or HC-SCR. The overall goal was to determine a set of conditions that would make an active Ag/Al_2O_3 catalyst between 200-400°C. Two approaches were studied. The first approach was to add H_2 into the reactant stream. The presence of H_2 has been shown to reduce the light-off reaction temperature for Ag/Al_2O_3 nearly 200°C. The second approach was to impregnate Pd, Pt, or Rh (platinum group metals, or PGMs) onto the Ag/Al_2O_3 catalyst. Pd, Pt, and Rh are active for NO_x at 400°C and lower, so it was believed that the addition of these metals could interact with the Ag active sites and make them more active below 400°C. Specifically, the two approaches were combined to maximize the low-temperature catalytic performance.

A series of bimetallic catalysts were synthesized and a full factorial design experimental design was conducted to determine the conditions in which the low temperature performance of the Ag/Al_2O_3 catalyst for HC-SCR would be maximized. These factors included (1) HC/NO_x ratio; (2) H_2/CO ratio; (3) second metal loading; (4)

second metal type; and (5) temperature. The NO_x conversion and N_2 selectivity generally decreased as the loading of the second metal increased. The NO_x conversion was affected by second metal type specifically at a temperature of 300°C, in which the order of performance was Pd < Pt < Rh. In response to the detrimental effect of second metal loading, the loading order was switched. The loading order independently did not significantly affect the NO_x conversion or N_2 selectivity. However, the loading order did affect NO_x conversion and N_2 selectivity performance with regard to Pd. The NO_x conversion improved by 6% and the N_2 selectivity by 12% when the Pd precursor was added before the Ag precursor.

It was hypothesized that the detrimental effect of the second metal on the NO_x conversion was caused by the unselective combustion of the C_3H_6 to CO_2. When the loading of the second metal was increased, the combustion of the C_3H_6 increased to 100%, yet the conversions to NO_x decreased. With regard to the N_2 selectivity, the platinum group metal catalysts are known to produce N_2O. It was believed that the PGMs did not interact with the Ag significantly. Therefore, the catalytic surface was populated with separate domains of Ag and PGM sites. In regards to the loading order, the interaction between Ag and the second metal type was significant due to the presence of Pd on the surface. The NO_x conversion and N_2 selectivity improved when Pd was added before Ag. Pd is known to be miscible with Ag, and therein, it was believed that the extent of alloying changed, resulting in improved conversion and selectivity.

In summary, the addition of the PGMs did not improve the NO_x conversion or N_2 selectivity even in the presence of H_2. The presence of the PGMs enhanced the unselective combustion of the hydrocarbon to CO_2 and increased production of N_2O on the catalyst surface, inhibiting both the conversion and selectivity. Switching the loading order resulted in an improvement for the Pd bimetallic catalysts.

CHAPTER I

Introduction

1.1 Summary

This chapter provides an overall introduction in the field of catalytic reduction of nitrogen oxides, or NO_x, from mobile sources. First, the reasons for diesel exhaust aftertreatment and the shortcomings that exist with the current technologies are discussed. Next, the advantages and disadvantages of the technologies that have been investigated to date for reduction of NO_x are described. Hydrocarbon selective catalytic reduction of NO_x (HC-SCR) is the technology of greatest interest, and the case for further research into HC-SCR is explained. Bimetallic catalysts have been utilized for a number of chemical reactions, and the relevance in HC-SCR is introduced. In conclusion, the scope of the thesis is described and each chapter of the thesis is briefly summarized.

1.2 Vehicle Exhaust Treatment

According to the emissions inventory taken by the U.S. EPA in 2008, 58% of the total NO_x emissions released into the atmosphere in 2008 originated from mobile sources (see Figure 1.1) [1].

When NO_x and volatile organic compounds mix in the atmosphere, they react

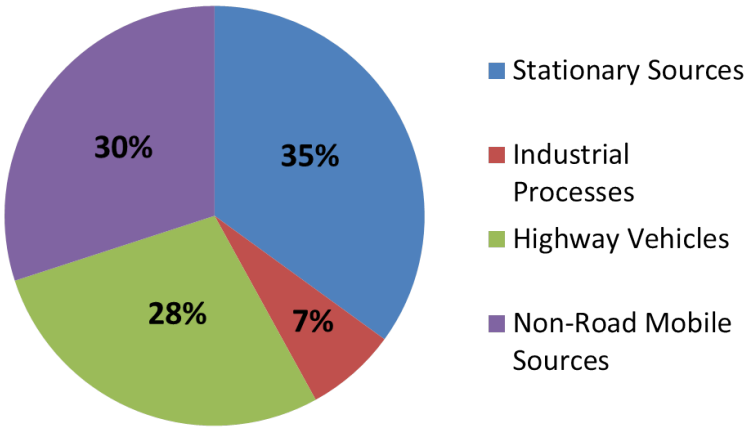

Figure 1.1: Man-made emissions of NO_x produced in 2008. Data taken from http://www.epa.gov/airtrends/2010/report/airpollution.pdf.

with sunlight to produce photochemical smog (which consists of airborne particulate matter and ground-level ozone). The presence of photochemical smog is common in urban areas and contributes to problems such as emphysema, asthma, bronchitis, and shortness of breath [2]. The production of NO_x occurs in all types of engines, but is most prevalent in the operation of diesel engines.

Diesel engines operate under lean conditions (air-to-fuel ratios above the stoichiometric ratio of 14.7:1 observed in an internal-combustion spark-ignition gasoline engine) and have better fuel efficiencies compared to the internal combustion engines. However, the excess air also increases the concentration of emitted NO_x from the engine tailpipe. For gasoline engines, NO_x is reduced using a three-way catalytic converter (TWC). These converters use a combination of Pt, Pd, and Rh to remove hydrocarbons, CO, and NO_x [3]. TWCs are efficient in the removal of these pollutants between 400-800°C at which these reactions readily proceed [4]. However, TWCs cannot be used in a lean environment because the net oxidizing condition of the exhaust severely inhibits NO_x reduction.

In addition to the inability of TWCs to reduce NO_x in diesel engines, legislation

also drives the development of technologies to reduce NO_x. The U.S. Environmental Protection Agency (EPA) set new NO_x emission standards that were phased into effect from 2004-2009. In 2010, the California Air Resources Board adopted new NO_x regulations that call for a fleet average requirement of 0.03 g/mile of total NO_x and non-methane organic gases (NMOG) by the year 2022. The total would consist of 0.01 grams of NMOG and 0.02 grams of NO_x [5]. The EPA currently does not have any proposed updates in NO_x emission standards past the 2009 model year, but it is possible that when the next update is announced, it will be based on the new CARB standards. Figure 1.2 shows the change in the EPA NO_x standards from 1975 to 2009 and the CARB standard for 2022. Updating to the 2009 standard from the 1999 standard required a 77% reduction in NO_x. The new CARB standard will require an additional 72% reduction in NO_x. The need to meet these new stringent regulations has sparked investigations of several technologies for NO_x reduction, of which some will be discussed in this chapter. These technologies include NO_x decomposition, NO_x storage-reduction, selective catalytic reduction of NO_x with urea, and selective catalytic reduction of NO_x with hydrocarbons [6].

1.3 Technologies for NO_x Reduction

1.3.1 NO_x Decomposition

Although the decomposition of NO_x to N_2 and O_2 would be the most direct route to convert NO_x because the method does not require a reductant, the thermodynamic barriers and the low turnover frequencies make the method unfeasible for commercial application. The Cu/ZSM-5 catalyst was initially considered an attractive candidate for catalyzing NO_x decomposition. Iwamoto *et al.* analyzed the ability of Cu/ZSM-5 to directly decompose NO using a concentration of 1000 ppm NO balanced with He. They observed that light-off for NO decomposition occurred 300°C and that

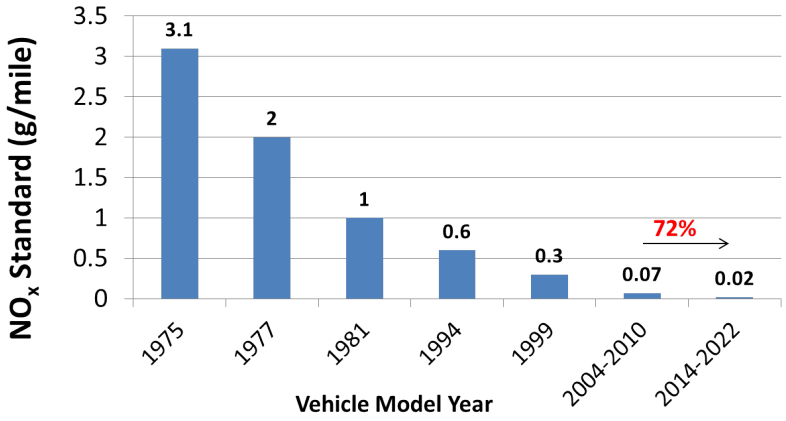

Figure 1.2: Change in EPA NO_x emission standards from 1975-2009 and percentage reductions from the previous standard. The CARB standard for the year 2022 is also listed, although the EPA has not officially adopted any new standards past the 2009 model year. The CARB standard is to be phased in between the 2014 and 2022 vehicle model years. Taken from the U.S. EPA Federal Register No. 65.

Cu/ZSM-5 achieved a 25% maximum conversion of NO at 500°C [7]. However, the presence of SO_2 deactivated the catalyst. When 220 ppm of SO_2 was introduced into the system, the catalyst deactivated completely after 40 minutes of reaction time. The catalyst could be regenerated by introducing He at 700°C [7]. They suggested that the reduction in activity was due to the competition of adsorption sites between SO_2 and NO [7, 8]. In response, Ishihara *et al.* synthesized a $La_{0.7}Ba_{0.3}Mn_{0.8}In_{0.2}O_3$ catalyst and found that the catalyst was active for NO_x decomposition in the presence of H_2O, SO_2, and O_2; however, the temperatures tested were at 800°C and higher [9], which is much higher than the temperature range for commercial diesel exhaust. In addition, the O_2 concentration in diesel exhaust is too high for NO_x decomposition to be an effective solution because thermodynamically, the oxidation of NO to NO_2 is significantly more favorable than its decomposition to N_2. Therein, significantly more NO_2 would be formed than N_2, as concluded by Goralski and Schneider using free-energy minimization calculations [10].

1.3.2 NO_x Storage-Reduction

NO_x storage-reduction catalysis (NSR), or lean NO_x trapping, is another possible method of reducing NO_x [11–13]. Figure 1.3 depicts a schematic of NSR [14]. The catalyst functions in lean and rich conditions. Under lean conditions, the NO_x is adsorbed on the surface of a catalyst containing Pt and BaO supported on γ-Al_2O_3. The role of Pt is to oxidize NO to NO_2 while the BaO stores the NO_x as $BaNO_3$. Under rich conditions (less than the stoichiometric air-to-fuel ratio of 14.7 maintained in internal combustion engines), the stored NO_x is reduced to N_2 and desorbs from the catalyst. The Pt is reduced using H_2, CO, and the hydrocarbons in the exhaust and fuel, resulting in the regeneration of the trap.

The most common NO adsorption pathway is called the nitrate route. In this pathway, NO is first oxidized to NO_2, then the NO_2 is adsorbed onto the catalyst surface via disproportion, resulting in the formation of nitrates (NO_3^-) [15, 16]. Nova *et al.* suggested a two-step parallel process for adsorption in which the NO oxidizes to NO_2 and subsequently disproportionates to form nitrates or is oxidized in the presence of O_2 to form adsorbed nitrite species, which are then oxidized to nitrates [17]. The oxidization to the adsorbed nitrites was dependent on the coupling of Pt and Ba sites. The nitrite process occurs due to the activation of oxygen by Pt, which in turn transfers to the Ba sites [18]. For reduction, it was proposed that the nitrate species decomposes into NO, which is then dissociated by the reduced metal [19]. NH_3 is also formed in the process due to the reaction of H_2 with decomposed NO or by hydrolysis of isocyanate (NCO) [20].

Several problems exist with NSR catalysts. The NSR catalyst is deactivated by SO_2 [21]. When NO is oxidized under lean conditions, undesirable SO_2 oxidation can occur and form $BaSO_4$. $BaSO_4$ is more stable than $BaNO_3$ on Pt and blocks the reaction with NO_x on the metal [22]. In addition, SO_2 can compete with NO_x for adsorption sites, reducing the efficiency of the reduction [23]. The deactivation

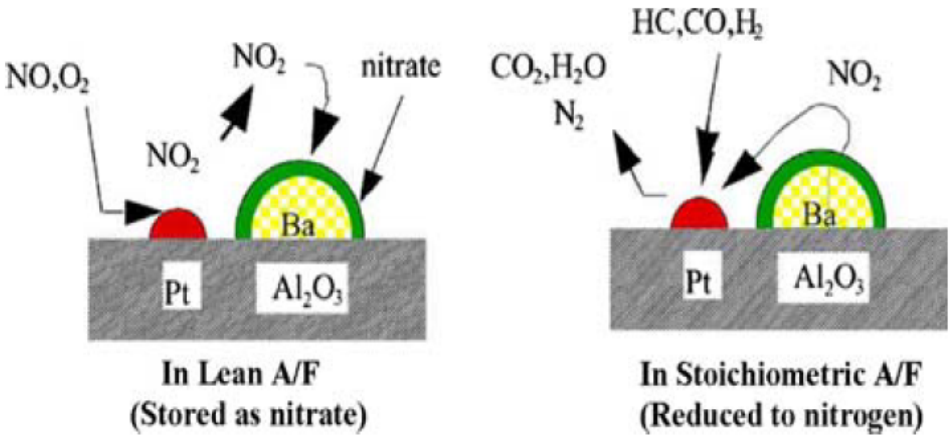

Figure 1.3: Schematic mechanism of NO_x storage reduction using over a Pt-BaO/γ-Al_2O_3 catalyst.

is more likely to occur under rich conditions as compared to lean conditions. The deactivation is attributed to the formation of PtS species [23]. Another issue is thermal deactivation. The NSR catalyst is at its optimum efficiency near 350°C, but as temperatures increase to around 600°C, the Pt begins to sinter. Therefore, fewer sites are available for NO and O_2 to adsorb and react and the rate of key catalytic steps, such as the oxidation of NO, decreases. Furthermore, the catalyst is subject to sintering [24]. Another problem is that at low temperatures, outlet hydrocarbon concentration at cold start is an issue. The concentrations could be reduced by placing a pre-turbo oxidation catalyst in the NSR system [5].

1.3.3 Selective Catalytic Reduction(SCR)

1.3.3.1 SCR with NH_3/Urea

The selective catalytic reduction with NH_3 is another means to reduce NO_x. This method has been widely used for the reduction of NO_x from stationary sources since the 1970s [25]. Common catalysts for this reaction include V_2O_5, WO_3, and MoO_3 [26]. However, NH_3 cannot directly be used as a selective reductant on a diesel- or lean-burn engine-powered vehicle. In gaseous phase, NH_3 is corrosive, toxic, and is

difficult to handle [27]. Furthermore, slip and corrosion prevent NH_3 from being used directly [6]. As an alternative, urea is used because it is a benign chemical that can be stored safely on-board and can be hydrolyzed to make NH_3 [26]. For heavy-duty trucks and bus engines, urea is the choice reductant for meeting Euro IV and Euro V NO_x limits [26].

However, there are some notable drawbacks with the use of NH_3/urea as a reductant. Several side reactions occur during urea-SCR, leading to the formation of undesired products such as N_2O, NO, NH_4NO_3, NH_4NO_2, and NH_4HSO_4 [28]. At low temperatures (100-200°C), ammonium nitrate can form and deposit in the pores of the catalyst, causing temporary deactivation [25]. Another notable drawback is that urea freezes at -10°C, which makes SCR difficult to conduct at temperatures typical of winter and cold climates [29]. Also at low temperatures, the high hydrocarbon concentration can poison sites on the catalysts. These hydrocarbons form carbonaceous deposits, which can only be removed by oxidizing that catalyst in air at high temperatures [25]. Because diesel engines work in highly transient conditions, the issues that occur at low temperatures are a significant barrier. Sulfur can also act as a catalyst poison. Sulfur in diesel fuel is a source for the formation of SO_2 and SO_3 in a highly oxidizing environment. Ammonium sulfates can form when SO_3 reacts with NH_3, which can irreversibly foul the catalyst [25]. Finally, SCR technology with urea presents enforcement issues in the United States in that (1) urea must be ensured to be available along with diesel fuel throughout the current distribution network and that (2) urea has to be timely replenished, which is a responsibility to EPA is concerned to place on drivers [25].

1.3.3.2 HC-SCR

An alternative strategy for meeting NO_x emission regulations that does not exhibit the difficulties of the aforementioned NO_x reduction methods is Hydrocarbon Selective

Catalytic Reduction, or HC-SCR. The equations below display the reaction using propylene (C_3H_6) as the reductant:

$$4NO + 2C_3H_6 + 7O_2 \Rightarrow 2N_2 \text{ (desired product)} + 6CO_2 + 6H_2O$$

$$2NO + C_3H_6 + 4O_2 \Rightarrow N_2O \text{ (undesired product)} + 3CO_2 + 3H_2O$$

This method requires the introduction of excess hydrocarbons into the exhaust to reduce the NO_x, as the concentration of total hydrocarbons from diesel exhaust is not enough to reduce the NO_x at an acceptable level. Therefore, the hydrocarbons would have to originate from the unburned fuel in the vehicle. However, because the source of the hydrocarbons comes from the fuel, there is no need for an extra reductant-containing tank to be installed on board, which is required for urea-SCR. N_2 is the primary desired product; however, the formation of undesired N_2O may also occur. Minimizing the amount of N_2O formed is important because N_2O has a global warming potential 270 times that of CO_2 [30].

A variety of catalysts have been tested for HC-SCR, such as zeolites [31–34] and supported metal oxides using both base metals (such as Fe and Co) and platinum group metals such as Pd, Pt, and Rh [35–39]. Zeolites are characterized by high activities for NO_x reduction to with wide reaction temperature windows [6]. The type of zeolite has a significant effect on the activity. For example, when comparing zeolites impregnated with Ni, Mosqueda-Jimenez *et al.* observed that Ni/ZSM-5 exhibited higher activity for NO_x reduction compared with Ni/MOR and Ni/MCM-22. They attributed the improvement of NO_x reduction on Ni/ZSM-5 to the high concentration of acid sites on the Ni/ZSM-5 when using propane as the reductant. With propane, the amount of olefin available on the catalyst surface is limited during NO reduction and, therefore, it reacts more efficiently with the adsorbed nitrites and nitrates to form N_2 [40]. However, when using propylene, the acid sites caused the formation of carbonaceous deposits on the catalyst surface, resulting in deactivation [41]. The main

factor inhibiting the widespread use of zeolites for commercial applications is their low hydrothermal stability. The reduction of the activity is caused by the competitive adsorption of H_2O, reducing the ability of the reactant gases to reach the active site for reaction [6]. This loss can be reversible; however, irreversible deactivation can also occur when the metal ions are removed from the ion-exchange zeolite sites or if crystallites begin to form in the zeolite pores [42]. Although catalysts have been proposed that are less susceptible to hydrothermal breakdown, much more research needs to be done in order to bring zeolites to market.

Base metal catalysts typically have high selectivities to N_2, but low NO_x conversions, especially at low temperatures. One of the most promising materials is $Ag/\gamma\text{-}Al_2O_3$ due to its high activity and selectivity to N_2. Miyadera was the first to report on $Ag/\gamma\text{-}Al_2O_3$ for NO_x reduction [43]. The extent of activity and selectivity is dependent on a number of factors such as reductant type and preparation method. The activity can vary among different reductants. As carbon number increases, the NO_x reduction activity for $Ag/\gamma\text{-}Al_2O_3$ has been reported to shift to lower temperatures [44]. Shimizu *et al.* also observed that the inhibitive effect of H_2O on HC-SCR is lessened as carbon number is increased. For propane and n-butane, the presence of H_2O inhibited the reaction over $Ag/\gamma\text{-}Al_2O_3$. However, the effect was mitigated when using n-hexane as a reductant. Furthermore, they observed a slight promotion of the activity in the presence of H_2O when using n-octane [44]. The use of alcohols as reductants have resulted in improved low temperature activity compared to unsaturated and saturated hydrocarbons. Zhu *et al.* observed a 20% improvement in the NO_x reduction activity in the presence of SO_2 when using methanol as a reductant. Furthermore, the temperature at which the maximum conversion was achieved shifted from approximately 250°C (at a maximum conversion of 60%) to 350°C (at a maximum conversion of 80%) [45]. Using ethanol as a reductant, Miyadera observed conversions between 80% and 85% over $Ag/\gamma\text{-}Al_2O_3$ at temperatures between 200

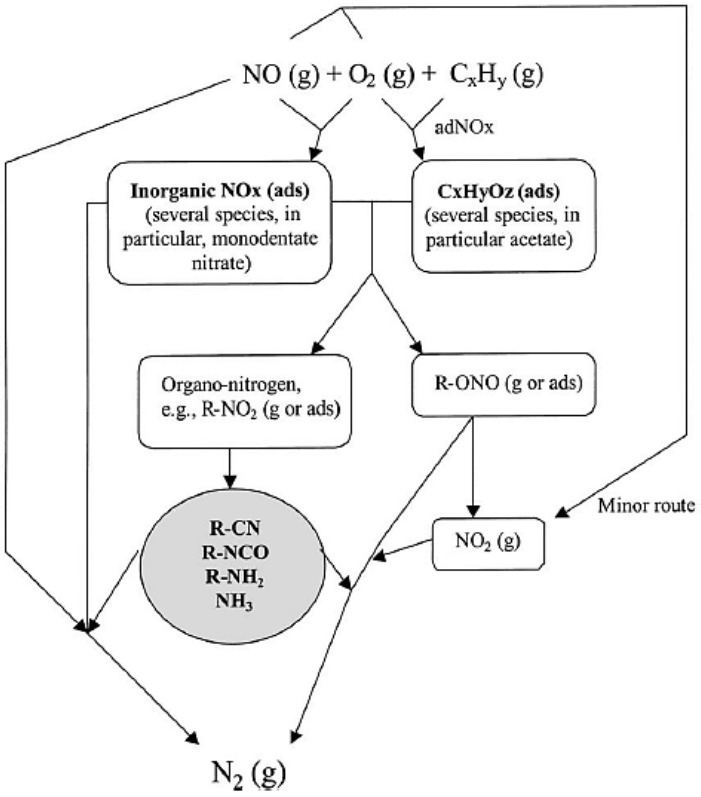

Figure 1.4: Simplified reaction scheme of the SCR of NO_x with C_3H_6 over oxide catalysts with species that are likely to be involved. It was proposed that the formation of N_2 occurs through the transformation of oxidized and reduced nitrogen species, which are in the gray-shaded circle.

and 400°C [43]. A significant issue with ethanol is the formation of nonselective side products in the reaction. Sumiya *et al.* attempted to reduce NO_x with ethanol in the presence of H_2O and SO_2. They observed the formation of CH_3CHO, CO, C_3H_6, C_2H_4, C_2H_2 and CH_4 along with NH_3 and N_2O [46].

A number of reaction pathways have been proposed for NO_x reduction over Ag/Al_2O_3 [39, 47–50]. Figure 1.4 displays the most widely accepted pathway this catalyst and other base metal catalysts [4]. Under lean environments, the excess O_2 plays an important role. The proposed first step is the formation of adsorbed hydrocarbon species onto the surface sites, followed by adsorption of NO onto a surface site to form ad-NO_x species.

Most researchers have reported that O_2 participates in the oxidation of NO and hydrocarbons to form various reaction intermediates [4, 25]. O_2 may also help to prevent coking of the surface by removing hydrocarbons that can bind strongly to the surface and block active sites. The adsorbed NO_x, acetates, and O_2 react to form various organo-nitro and organo-nitrito species on the surface and in the gas phase [39, 50, 51]. These species further react to produce cyanates (R-CN), isocyanates (R-NCO), amines (R-NH_2), and NH_3 that are adsorbed on the surface and further react to form N_2 [4].

Platinum group metal based catalysts are generally characterized as having high activities for NO_x reduction at temperatures below 300°C, but produce significant amounts of N_2O, resulting in low selectivities to N_2 [4]. Pd. Pt, Rh, and Ir all have displayed activity for the reduction of NO_x on a variety of supports [32]. Burch and Millington tested Pd/Al_2O_3, Pt/Al_2O_3, and Rh/Al_2O_3 at a 1% weight loading to compare differences in the activity of the metal catalysts at similar conditions. Pd/Al_2O_3 attained a maximum NO_x conversion of 25% with a full width half maximum (FWHM) temperature window from 225-275°C, Pt/Al_2O_3 attained a maximum NO_x conversion of 60% with a FWHM temperature window from 250-300°C, and Rh/Al_2O_3 attained a maximum NO_x conversion of 30% with a FWHM temperature window from 325-400°C [38].

The dissociation-reduction pathway was proposed for platinum group metal catalysts by Burch and Millington and is the generally accepted pathway over platinum group metals [52]. This pathway is displayed in the following equations below, where Z represents a surface adsorption site on the PGM [52]:

$$NO(g) + Z = NO(ads)$$

$$NO(ads) + 2Z = N(ads) + O(ads)$$

$$N(ads) + N(ads) = N_2(g)$$

$$NO(ads) + N(ads) = N_2O(g)$$

$$O_2(g) + 2Z = 2O(ads)$$

$$C_xH_y(g) + nZ = C_xH_y(ads)$$

$$C_xH_y(ads) + (2x + \tfrac{1}{2}y)O(ads) = xCO_2(g) + \tfrac{1}{2}yH_2O(g)$$

The first step involves the adsorption of NO on the surface of the catalyst, followed by the dissociation of NO into adsorbed N and O species. Two adsorbed N atoms can form N_2 or an adsorbed N atom can react with an adsorbed, non-dissociated NO to form N_2O. The hydrocarbon reduces the platinum group metal sites by removing adsorbed oxygen species on the surface. This reduction is important because the dissociation of NO happens on the reduced metallic sites.

Selective catalytic reduction of NO_x with hydrocarbons appears to be a promising method to achieve the reductions in NO_x emissions needed to meet future standards. Nevertheless, issues remain that have to be addressed. The extra hydrocarbon needs to be injected into the exhaust aftertreatment system to achieve the reduction. This would require rerouting fuel typically used for powering the engine. This rerouting results in a fuel penalty and a reduction in the fuel economy. In addition, the Ag/Al_2O_3 catalyst has shortcomings. Miyadera reported that the Ag/Al_2O_3 catalyst displayed negligible activity at temperatures below 400°C [43]. The lack of activity is of concern because the temperature of diesel exhaust is between 150-400°C [53]. Theinnoi *et al.* concluded that the primary causes for the lack of low-temperature performance were that Ag/Al_2O_3 self-poisons by forming stable surface nitrates and that gas-phase hydrocarbons can produce carbonaceous species that block active sites [54]. Furthermore, Ag/Al_2O_3 can be inhibited by sulfur species, although it is much more resistant than the $Pt/BaO/\gamma\text{-}Al_2O_3$ catalyst for NO_x storage reduction [54].

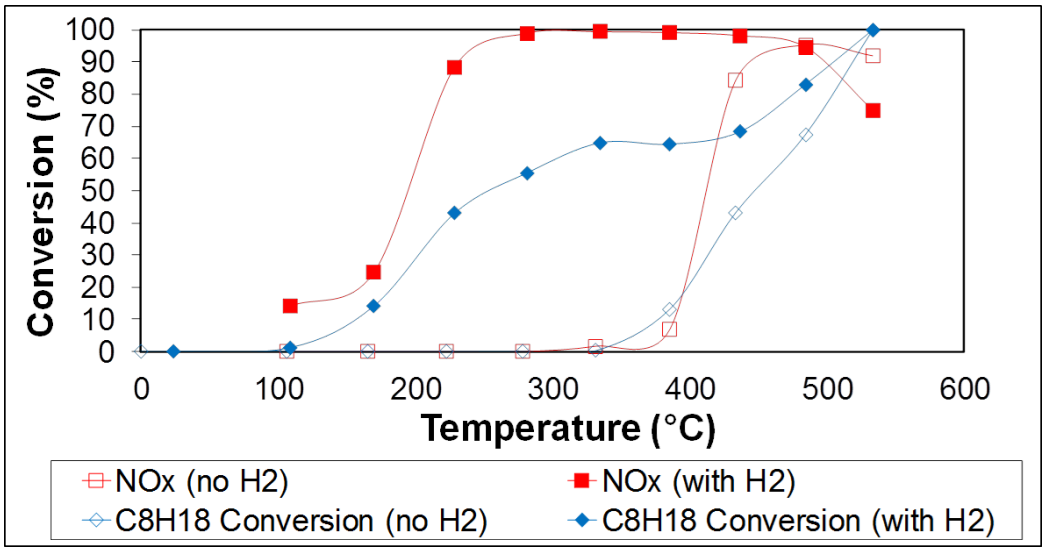

Figure 1.5: Effect of H_2 on the SCR of NO_x with n-octane. The experiment was conducted with a total flow rate of 276 cm^3/minute using 266 mg of catalyst. The inlet concentration was as follows: 720 ppm NO, 4340 ppm C_3H_6 (as C_1), 4.3% O_2, 7.2% H_2O, He balance.

1.3.3.3 Reformate-Assisted HC-SCR

In response to the difficulties reported by Miyadera, Satokawa *et al.* proposed that NO_x conversion on Ag/Al_2O_3 could be promoted by the addition of H_2. The added H_2 improved the tolerance of the catalyst to sulfur and H_2O and widened the temperature window at which NO_x reduction occurred [55, 56]. According to Burch *et al.*, the temperature at which the reduction of NO_x began to occur decreased from 400°C to 200°C when H_2 was added as shown in Figure 1.5 [57]. The effect of the reduction of the light-off temperature has been observed for when both non-oxygenated and oxygenated hydrocarbons have been used as reductants [58].

Satokawa *et al.* and Shibata *et al.* suggested two reasons for the H_2 effect. Satokawa *et al.* believed that the presence of H_2 resulted in higher concentrations of isocyanate surface species, which are believed to be key intermediates in the reaction mechanism with H_2 [59]. Shibata *et al.* postulated that H_2 promoted oxidation of the hydrocarbon to form surface-bound acetates. Because Shibata *et al.* proposed that

the formation of the acetates is viewed as the rate-determining step in HC-SCR in the absence of H_2, they believed the acetates were key intermediates in the reaction mechanism [60]. In addition to the two reasons above, Breen *et al.* and Kannisto *et al.* also suggested that H_2 removed strongly adsorbed nitrate species that poisoned the Ag/Al_2O_3 catalyst [61, 62].

When H_2 is added, certain reaction steps in the reaction pathway for Ag/Al_2O_3 are enhanced. Figure 1.6 displays the H_2-enhanced reaction pathway [25]. The adsorption of NO and hydrocarbons to the catalytic surface and the formation of organo-nitro and organo-nitrito species are enhanced by the presence of H_2. The rate-determining step, which is proposed to be the formation of isocyanate, is also accelerated in the presence of H_2. The increased rate of formation of isocyanate results in the promotion of the production of NH_3, eventually leading to an increase in the rate of N_2 production.

Hydrocarbon selective catalytic reduction of NO_x with Ag/Al_2O_3 appears to be the most promising of the currently studied technologies. HC-SCR does not require any extra tank for a reductant, which is a requirement for NH_3-SCR. Furthermore, H_2-assisted HC-SCR with Ag/Al_2O_3 appears to be more resistant to sulfur and does not require to use of expensive precious metals. However, some key challenges need to be addressed before the system can be implemented commercially. The need for H_2 requires the installation of a reformer, and therein more study is required to determine how the reformer will fit into the aftertreatment system. In addition, complete conversion of NO_x is not achieved until 250°C even in the presence of H_2 [57] and the low-temperature conversion is dependent on the H_2 concentration. It is desired that the H_2 concentration required should be as minimal as possible. Since diesel exhaust is between 150-400°C, more research is required to determine how to maximize conversion in this temperature range.

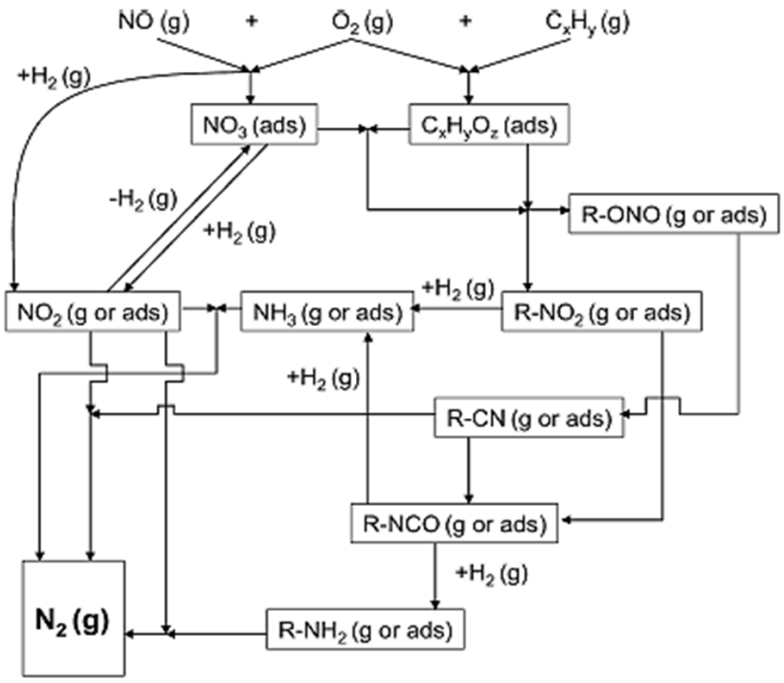

Figure 1.6: Proposed reaction scheme of NO_x reduction over Ag/Al_2O_3 with H_2. H_2 accelerates the adsorption of gas-phase NO and C_3H_6 onto the surface and the activation of adsorbed NO to more reactive NO_2, which can be adsorbed on the surface or in gas phase. In turn, the formation of N-containing species, specifically isocyanate (R-NCO), is enhanced, resulting in improved NO_x performance.

1.4 Bimetallic Catalysts for HC-SCR of NO_x

The performance of a catalyst for a given reaction depends on many factors, including the surface chemistry. Most catalysts consists of some active species, such as a metal that is impregnated onto a high surface area support. By adding multiple metallic components on the surface, the performance of a catalyst for a reaction can be greatly altered [63–66]. Transition metal catalysts have garnered interest because many pairs can form alloys over large composition ranges [67]. The surface of a bimetallic catalyst can significantly vary based on a number of factors, such as atomic size, surface energies, and temperature [68, 69].

There have been a number of studies for HC-SCR of NO_x using multi-metallic catalysts, particularly with combinations of Ag and PGMs [70–73]. Sato *et al.* added 0.05% Rh onto a previously prepared 4% Ag catalyst. They observed an increase in the conversion of NO_x to N_2 between 250-400°C, reaching a maximum of 50% at 300°C [70]. Wang *et al.* added small amounts of Pd, Pt and Au (0.01% and 0.05%) to a 5% Ag/Al_2O_3 catalyst under the following conditions: 800 ppm NO, 1714 ppm C_3H_6, 10% O_2, 10% H_2O, balanced with N_2. The addition of 0.01% Pd and Pt resulted in an increase in the NO_x conversion between 300°C and 400°C. However, the improvement was negligible in this temperature range. Furthermore, the conversions did not exceed 20% until 350°C [71].

1.5 Scope of Thesis

This thesis describes an effort to improve the low temperature activity of Ag/Al_2O_3 by (1) adding H_2 to the diesel exhaust mixture and (2) adding Pd, Pt, or Rh onto the Ag/Al_2O_3 surface, with the goal of developing a highly active and selective catalyst for the HC-SCR of NO_x at temperatures between 200-400°C. The objectives of the research were to

- develop active and selective bimetallic catalysts for NO_x reduction;
- define effects of H_2 and PGMs on the activity and selectivity of Ag/Al_2O_3, and;
- examine the effect of impregnation order on NO_x reduction performance.

An extensive screening experiment was conducted to determine factors that affected the NO_x conversion. After these effects were identified, various characterization techniques were employed in an effort to explain these effects.

Chapter 2 describes the experimental tools utilized in the catalyst screening and characterization. Chapter 3 introduces the experimental design and presents the results for the screening experiments. Chapter 4 discusses the identified factors of interest - loading and loading order - in greater detail using various characterization techniques, such as temperature-programmed reduction, H_2 chemisorption, and O_2 chemisorption. Finally, Chapter 5 summarizes the major conclusions resulting from the research and outlines possible directions for future work.

Bibliography

[1] United States Environmental Protection Agency. Our nation's air: Status and trends through 2008. `http://www.epa.gov/airtrends/2010/report/airpollution.pdf`, November 2008.

[2] J.A. Bernstein, N. Alexis, C. Barnes, I.L. Bernstein, A. Nel, D. Peden, D. Diaz-Sanchez, S.M. Tarlo, and P.B. Williams. Health effects of air pollution. *Journal of Allergy and Clinical Immunology*, 114(5):1116–1123, 2004.

[3] H. Shinjoh, T. Tanabe, K. Yokota, and M. Sugiura. Comparative NO_x Reduction Behavior of Pt, Pd, and Rh Supported Catalysts in Simulated Exhaust Gases as a Function of Oxygen Concentration. *Topics in Catalysis*, 30(1):319–323, 2004.

[4] R. Burch, J.P. Breen, and F.C. Meunier. A review of the selective reduction of NO_x with hydrocarbons under lean-burn conditions with non-zeolitic oxide and platinum group metal catalysts. *Applied Catalysis B: Environmental*, 39(4):283–303, 2002.

[5] T.V. Johnson. Review of diesel emissions and control. *SAE International Journal of Fuels and Lubricants*, 3(1):16, 2010.

[6] Z. Liu and S.I. Woo. Recent advances in catalytic $DeNO_x$ science and technology. *Catalysis Reviews*, 48(1):43–89, 2006.

[7] M. Iwamoto, H. Yahiro, S. Shundo, Y. Yu-u, and N. Mizuno. Influence of sulfur dioxide on catalytic removal of nitric oxide over copper ion-exchanged ZSM-5 zeolite. *Applied Catalysis*, 69(1):L15–L19, 1991.

[8] Y. Teraoka, K. Shimanoe, and N. Yamazoe. Simultaneous catalytic removal of NO and SO_2 over Pt/ZSM-5 and V_2O_5-MoO_3/TiO_2 catalysts. *Chemistry Letters*, (10):2047–2050, 1987.

[9] T. Ishihara, K. Anami, K. Takiishi, H. Yamada, H. Nishiguchi, and Y. Takita. Direct decomposition of No on Cu-doped La(Ba)Mn(In)O_3 perovskite oxide under coexistence of O_2, H_2O, and SO_2. *Chemistry Letters*, 32(12):1176–1177, 2003.

[10] C.T. Goralski et al. Analysis of the thermodynamic feasibility of NO_x decomposition catalysis to meet next generation vehicle NO_x emissions standards. *Applied Catalysis B: Environmental*, 37(4):263–277, 2002.

[11] J.R. Theis, J.A. Ura, C.T. Goralski, J. Caine, M. Davies, D. Kay, A. Todd, and S. Dinsdale. The effects of aging temperature and PGM loading on the NO_x storage capacity of a lean NO_x trap. *SAE Transactions*, 114(4):614–627, 2005.

[12] T.V. Johnson et al. Diesel emission control in review. 2006.

[13] J.H. Kwak, D.H. Kim, J. Szanyi, and C.H.F. Peden. Excellent sulfur resistance of $Pt/BaO/CeO_2$ lean NO_x trap catalysts. *Applied Catalysis B: Environmental*, 84(3-4):545–551, 2008.

[14] J.H. Park, S.J. Park, and I.S. Nam. Fast Colorimetric Assay for Screening NSR Catalyst. *Catalysis Surveys from Asia*, 14(1):11–20, 2010.

[15] N.W. Cant and M.J. Patterson. The storage of nitrogen oxides on alumina-supported barium oxide. *Catalysis Today*, 73(3-4):271–278, 2002.

[16] C. Hess and J.H. Lunsford. Mechanism for NO_2 storage in barium oxide supported on magnesium oxide studied by in situ Raman spectroscopy. *The Journal of Physical Chemistry B*, 106(25):6358–6360, 2002.

[17] L. Castoldi, I. Nova, L. Lietti, and P. Forzatti. Study of the effect of Ba loading for catalytic activity of $Pt/Ba/Al_2O_3$ model catalysts. *Catalysis Today*, 96(1-2):43–52, 2004.

[18] I. Nova, L. Castoldi, L. Lietti, E. Tronconi, P. Forzatti, F. Prinetto, and G. Ghiotti. NO_x adsorption study over Pt-Ba/alumina catalysts: FT-IR and pulse experiments. *Journal of Catalysis*, 222(2):377–388, 2004.

[19] D. James, E. Fourre, M. Ishii, and M. Bowker. Catalytic decomposition/regeneration of $Pt/Ba(NO_3)_2$ catalysts: NO_x storage and reduction. *Applied Catalysis B: Environmental*, 45(2):147–159, 2003.

[20] T. Lesage, C. Verrier, P. Bazin, J. Saussey, and M. Daturi. Studying the NO_x-trap mechanism over a $Pt\text{-}Rh\text{-}Ba/Al_2O_3$ catalyst by operando FT-IR spectroscopy. *Phys. Chem. Chem. Phys.*, 5(20):4435–4440, 2003.

[21] S. Matsumoto. Recent advances in automobile exhaust catalysts. *Catalysis Today*, 90(3-4):183–190, 2004.

[22] S. Matsumoto, Y. Ikeda, H. Suzuki, M. Ogai, and N. Miyoshi. NO_x storage-reduction catalyst for automotive exhaust with improved tolerance against sulfur poisoning. *Applied Catalysis B: Environmental*, 25(2-3):115–124, 2000.

[23] E. Fridell, A. Amberntsson, L. Olsson, A.W. Grant, and M. Skoglundh. Platinum Oxidation and Sulphur Deactivation in NO_x Storage Catalysts. *Topics in Catalysis*, 30(1):143–146, 2004.

[24] D. Uy, A.E. O'Neill, J. Li, and W.L.H. Watkins. UV and visible Raman study of thermal deactivation in a NO_x storage catalyst. *Catalysis Letters*, 95(3):191–201, 2004.

[25] F. Klingstedt, K. Arve, K. Eranen, and D.Y. Murzin. Toward improved catalytic low-temperature NO_x removal in diesel-powered vehicles. *Accounts of Chemical Research*, 39(4):273–282, 2006.

[26] M. Koebel, M. Elsener, and M. Kleemann. Urea-SCR: a promising technique to reduce NO_x emissions from automotive diesel engines. *Catalysis Today*, 59(3-4):335–345, 2000.

[27] J.A. Sullivan and J.A. Doherty. NH_3 and urea in the selective catalytic reduction of NO_x over oxide-supported copper catalysts. *Applied Catalysis B: Environmental*, 55(3):185–194, 2005.

[28] M. Koebel, G. Madia, and M. Elsener. Selective catalytic reduction of NO and NO_2 at low temperatures. *Catalysis Today*, 73(3-4):239–247, 2002.

[29] K. Hirata, N. Masaki, H. Ueno, and H. Akagawa. Development of Urea-SCR System for Heavy-Duty Commercial Vehicles. *SAE TRANSACTIONS*, 114(4):678, 2005.

[30] T.N. Angelidis and V. Tzitzios. Promotion of the catalytic activity of a Ag-Al_2O_3 catalyst for N_2O decomposition by the addition of Rh. A comparative activity and kinetic study. *Industrial & engineering chemistry research*, 42(13):2996–3000, 2003.

[31] C. Rottlander, R. Andorf, C. Plog, B. Krutzsch, and M. Baerns. Selective NO reduction by propane and propene over a Pt/ZSM-5 catalyst: a transient study of the reaction mechanism. *Applied Catalysis B: Environmental*, 11(1):49–63, 1996.

[32] R. Burch and S. Scire. Selective catalytic reduction of nitric oxide with ethane and methane on some metal exchanged ZSM-5 zeolites. *Applied Catalysis B: Environmental*, 3(4):295–318, 1994.

[33] H.Y. Chen, Q. Sun, B. Wen, Y.H. Yeom, E. Weitz, and W.M.H. Sachtler. Reduction over zeolite-based catalysts of nitrogen oxides in emissions containing excess oxygen: Unraveling the reaction mechanism. *Catalysis Today*, 96(1-2):1–10, 2004.

[34] Y. Traa, B. Burger, and J. Weitkamp. Zeolite-based materials for the selective catalytic reduction of NO_x with hydrocarbons. *Microporous and Mesoporous Materials*, 30(1):3–41, 1999.

[35] M. Huuhtanen, T. Kolli, T. Maunula, and R.L. Keiski. *In situ* FTIR study on NO reduction by C_3H_6 over Pd-based catalysts. *Catalysis Today*, 75(1-4):379–384, 2002.

[36] A. Kotsifa, D.I. Kondarides, and X.E. Verykios. Comparative study of the chemisorptive and catalytic properties of supported Pt catalysts related to the

selective catalytic reduction of NO by propylene. *Applied Catalysis B: Environmental*, 72(1-2):136–148, 2007.

[37] E.A. Efthimiadis, S.C. Christoforou, A.A. Nikolopoulos, and I.A. Vasalos. Selective catalytic reduction of NO with C_3H_6 over Rh/alumina in the presence and absence of SO_2 in the feed. *Applied Catalysis B: Environmental*, 22(2):91–106, 1999.

[38] R. Burch and P.J. Millington. Selective reduction of NO_x by hydrocarbons in excess oxygen by alumina-and silica-supported catalysts. *Catalysis Today*, 29(1-4):37–42, 1996.

[39] K. Eranen, F. Klingstedt, K. Arve, L.E. Lindfors, and D.Y. Murzin. On the mechanism of the selective catalytic reduction of NO with higher hydrocarbons over a silver/alumina catalyst. *Journal of Catalysis*, 227(2):328–343, 2004.

[40] B.I. Mosqueda-Jiménez, A. Jentys, K. Seshan, and J.A. Lercher. Structure-activity relations for Ni-containing zeolites during NO reduction I. Influence of acid sites. *Journal of Catalysis*, 218(2):348–353, 2003.

[41] B.I. Mosqueda-Jiménez, A. Jentys, K. Seshan, and J.A. Lercher. Structure-activity relations for Ni-containing zeolites during NO reduction: II. role of the chemical state of Ni. *Journal of Catalysis*, 218(2):375–385, 2003.

[42] K. Sato, T. Fujimoto, S. Kanai, Y. Kintaichi, M. Inaba, M. Haneda, and H. Hamada. Catalytic performance of silver ion-exchanged saponite for the selective reduction of nitrogen monoxide in the presence of excess oxygen. *Applied Catalysis B: Environmental*, 13(1):27–33, 1997.

[43] T. Miyadera. Alumina-supported silver catalysts for the selective reduction of nitric oxide with propene and oxygen-containing organic compounds. *Applied Catalysis B: Environmental*, 2(2-3):199–205, 1993.

[44] K. Shimizu, A. Satsuma, and T. Hattori. Catalytic performance of Ag-Al_2O_3 catalyst for the selective catalytic reduction of NO by higher hydrocarbons. *Applied Catalysis B: Environmental*, 25(4):239–247, 2000.

[45] T. Zhu, J. Hao, and W. Li. Enhancing Effect of SO_2 on Selective Catalytic Reduction of NO by Methanol over Ag-Al_2O_3. *Chemistry Letters*, 29(5):478–479, 2000.

[46] S. Sumiya, M. Saito, H. He, Q.C. Feng, N. Takezawa, and K. Yoshida. Reduction of lean NO_x by ethanol over Ag-Al_2O_3 catalysts in the presence of H_2O and SO_2. *Catalysis Letters*, 50(1):87–91, 1998.

[47] K. Shimizu and A. Satsuma. Selective catalytic reduction of NO over supported silver catalysts-practical and mechanistic aspects. *Physical Chemistry Chemical Physics*, 8(23):2677–2695, 2006.

[48] H. He and Y. Yu. Selective catalytic reduction of NO_x over Ag/Al_2O_3 catalyst: from reaction mechanism to diesel engine test. *Catalysis Today*, 100(1-2):37–47, 2005.

[49] Y. Yu, H. He, Q. Feng, H. Gao, and X. Yang. Mechanism of the selective catalytic reduction of NO_x by C_2H_5OH over Ag/Al_2O_3. *Applied Catalysis B: Environmental*, 49(3):159–171, 2004.

[50] F.C. Meunier, J.P. Breen, V. Zuzaniuk, M. Olsson, and J.R.H. Ross. Mechanistic aspects of the selective reduction of NO by propene over alumina and silver-alumina catalysts. *Journal of Catalysis*, 187(2):493–505, 1999.

[51] P. Sazama, L. Capek, H. Drobna, Z. Sobalik, J. Dedecek, K. Arve, and B. Wichterlova. Enhancement of decane-SCR-NO_x over Ag/alumina by hydrogen. Reaction kinetics and *in situ* FTIR and UV-vis study. *Journal of Catalysis*, 232(2):302–317, 2005.

[52] R. Burch, P.J. Millington, and A.P. Walker. Mechanism of the selective reduction of nitrogen monoxide on platinum-based catalysts in the presence of excess oxygen. *Applied Catalysis B: Environmental*, 4(1):65–94, 1994.

[53] B. Wichterlova, P. Sazama, J.P. Breen, R. Burch, C.J. Hill, L. Capek, and Z. Sobalik. An *in situ* UV-vis and FTIR spectroscopy study of the effect of H_2 and CO during the selective catalytic reduction of nitrogen oxides over a silver alumina catalyst. *Journal of Catalysis*, 235(1):195–200, 2005.

[54] K. Theinnoi, S. Sitshebo, V. Houel, R.R. Rajaram, and A. Tsolakis. Hydrogen promotion of low-temperature passive hydrocarbon-selective catalytic reduction (SCR) over a silver catalyst. *Energy & Fuels*, 22(6):4109–4114, 2008.

[55] S. Satokawa. Enhancing the NO/C_3H_8 reaction by using H_2 over Ag/Al_2O_3 catalysts under lean-exhaust conditions. *Chemistry Letters*, 29(3):294–295, 2000.

[56] M. Richter, U. Bentrup, R. Eckelt, M. Schneider, M.M. Pohl, and R. Fricke. The effect of hydrogen on the selective catalytic reduction of NO in excess oxygen over Ag/Al_2O_3. *Applied Catalysis B: Environmental*, 51(4):261–274, 2004.

[57] R. Burch, J.P. Breen, C.J. Hill, B. Krutzsch, B. Konrad, E. Jobson, L. Cider, K. Eranen, F. Klingstedt, and L.E. Lindfors. Exceptional activity for NO_x reduction at low temperatures using combinations of hydrogen and higher hydrocarbons on Ag/Al_2O_3 catalysts. *Topics in Catalysis*, 30(1-4):19–25, 2004.

[58] G.B. Fisher, C.L. DiMaggio, D. Trytko, K.M. Rahmoeller, and M. Sellnau. Effects of fuel type on dual SCR aftertreatment for lean NO_x reduction. *SAE International Journal of Fuels and Lubricants*, 2(2):313, 2010.

[59] S. Satokawa, J. Shibata, K. Shimizu, A. Satsuma, and T. Hattori. Promotion effect of H_2 on the low temperature activity of the selective reduction of

NO by light hydrocarbons over Ag/Al_2O_3. *Applied Catalysis B: Environmental*, 42(2):179–186, 2003.

[60] J. Shibata, K. Shimizu, S. Satokawa, A. Satsuma, and T. Hattori. Promotion effect of hydrogen on surface steps in SCR of NO by propane over alumina-based silver catalyst as examined by transient FT-IR. *Physical Chemistry Chemical Physics*, 5(10):2154–2160, 2003.

[61] J.P. Breen and R. Burch. A review of the effect of the addition of hydrogen in the selective catalytic reduction of NO_x with hydrocarbons on silver catalysts. *Topics in Catalysis*, 39(1):53–58, 2006.

[62] H. Kannisto, H.H. Ingelsten, and M. Skoglundh. Aspects of the role of hydrogen in H_2-assisted HC-SCR over Ag-Al_2O_3. *Topics in Catalysis*, 52(13):1817–1820, 2009.

[63] R.J. Fenoglio, G.M. Nunez, and D.E. Resasco. Selectivity changes in the ring-opening reaction of methylcyclopentane over rhodium catalysts caused by the addition of silver and metal–support interactions. *Applied Catalysis*, 63(1):319–332, 1990.

[64] S. Yuvaraj, S.C. Chow, and C.T. Yeh. Characterization of Silver-Rhodium Bimetallic Nanocrystallites Dispersed on [gamma]-Alumina. *Journal of Catalysis*, 198(2):187–194, 2001.

[65] I. Eswaramoorthi and N. Lingappan. Hydroisomerisation of n-hexane over bimetallic bifunctional silicoaluminophosphate based molecular sieves. *Applied Catalysis A: General*, 245(1):119–135, 2003.

[66] Y. Shu, L.E. Murillo, J.P. Bosco, W. Huang, A.I. Frenkel, and J.G. Chen. The effect of impregnation sequence on the hydrogenation activity and selectivity of supported Pt/Ni bimetallic catalysts. *Applied Catalysis A: General*, 339(2):169–179, 2008.

[67] S. Jaatinen, P. Salo, M. Alatalo, V. Kulmala, and K. Kokko. Structure and reactivity of Pd doped Ag surfaces. *Surface Science*, 529(3):403–409, 2003.

[68] AV Ruban, H.L. Skriver, and J.K. Nørskov. Surface segregation energies in transition-metal alloys. *Physical review B*, 59(24):15990, 1999.

[69] J.A. Anderson and M.F. Garcia. *Supported Metals in Catalysis*, volume 5. Imperial College Press London, 2005.

[70] K. Sato, T. Yoshinari, Y. Kintaichi, M. Haneda, and H. Hamada. Remarkable promoting effect of rhodium on the catalytic performance of Ag/Al_2O_3 for the selective reduction of NO with decane. *Applied Catalysis B: Environmental*, 44(1):67–78, 2003.

[71] J. Wang, H. He, Q. Feng, Y. Yu, and K. Yoshida. Selective catalytic reduction of NO_x by C_3H_6 over Ag/Al_2O_3 catalyst with a small quantity of noble metal. *Catalysis Today*, 93:783–789, 2004.

[72] A. Kotsifa, T.I. Halkides, D.I. Konarides, and X.E. Verykios. Activity enhancement of bimetallic Rh-Ag/Al_2O_3 catalysts for selective catalytic reduction of NO by C_3H_6. *Catalysis Letters, 79*, 1(4):113–117, 2002.

[73] J. Wang, H. He, S. Xie, and Y. Yu. Novel Ag-Pd/Al_2O_3-SiO_2 for lean NO_x reduction by C_3H_6 with high tolerance of SO_2. *Catalysis Communications*, 6(3):195–200, 2005.

CHAPTER II

Experimental Techniques

2.1 Summary

This chapter provides a detailed description of the experimental techniques used in this thesis and the underlying principles that govern their operation. First, the method used to synthesize the monometallic and bimetallic catalysts is described. Next, the various characterization tools that were employed in this work are introduced and explained in detail. Furthermore, a description of the reactor used to test the catalysts is introduced. Finally, a description of the design of experiments (DOE) is explained.

2.2 Introduction

The goal of research described in this dissertation was to explore the possibility of generating a highly active and selective catalyst for the HC-SCR of NO_x at temperatures between 200°C and 400°C by employing two approaches: (1) adding H_2 into the reactant stream, and (2) adding a platinum group metal (Pd, Pt, or Rh) onto Ag/Al_2O_3. The following objectives of the research were to:

- prepare monometallic and bimetallic catalysts for NO_x reduction;

- define effects of H_2 and the presence of platinum group metals on the activity and selectivity of Ag/Al_2O_3, and;
- examine the effect of impregnation order on NO_x reduction performance over Ag/Al_2O_3.

The first objective was achieved using dry impregnation to prepare the catalysts and the catalysts were characterized using nitrogen physisorption method for surface area, inductively coupled plasma-optical emission spectroscopy (ICP-OES) for elemental analysis, x-ray diffraction (XRD) for crystalline structure, and pulse chemisorption experiments to determine metal site density. The second and third objectives required a comprehensive analysis of a number of possible conditions that could be important in defining the effects of H_2, PGMs, and impregnation order on NO_x reduction and N_2 selectivity. Any experiment of this complexity can be best analyzed by using DOE, or design of experiments. DOE allows one to analyze a number of factors simultaneously to determine what conditions most affect the activity and/or selectivity.

2.3 Catalysis Synthesis

Ag, Pt, Pd, and Rh were supported on γ-Al_2O_3 using an impregnation technique. The support material was commercial γ-Al_2O_3 powder (3 μm flakes, 99.97% purity, 80-120 m^2/g BET surface area, Alfa Aesar). The flakes were compressed under 4000 psi in a Carver Model 4350-L compressor to cylindrical blocks of about 1 cm^3 in volume before being crushed and sieved to particle sizes of 125-250 μm. Before impregnation, the support material was calcined in 90 cm^3/minute of dry-grade air in a horizontal quartz tube furnace at 600°C for 3 hours.

The metals were impregnated onto surfaces of the support using the dry impregnation technique [1, 2]. Just enough precursor solution is used to fill the total pore

volume of the support, which is measured using nitrogen physisorption and was calculated to be 0.383 cm^3/g. The solutions were prepared by dissolving a metal precursor in water. The metal precursors were $AgNO_3$ (Johnson Matthey), $Pt(NH_3)_4(NO_3)_2$ (Johnson Matthey), $Pd(NH_3)_4(NO_3)_2$ (10% solution, Sigma-Aldrich), and $Rh(NO_3)_3$ (Johnson Matthey) for Ag, Pt, Pd, and Rh respectively. The precursor solution volume was adjusted to fill the support pore volume of 0.383 cm^3. After impregnation, the solution was allowed to diffuse into the support for 1 hour, then the catalysts were dried in a Fisher Scientific vacuum oven at a pressure of -30 mm Hg at 100°C for 8-12 hours and subsequently calcined at 600°C for 3 hours in 90 cm^3/minute of dry-grade air. The time and temperature were chosen based on previous work [3, 4]; these calcination parameters were shown to maximize the activity of bimetallic Ag-Pt group metal NO_x catalysts.

The bimetallic catalysts were prepared using sequential dry impregnation. The Ag metal precursor solution was impregnated before the Pd, Pt, or Rh precursor solutions. After each step the catalysts were dried in a Fisher Scientific vacuum oven at a pressure of -30 mm Hg at 100°C for 8-12 hours and subsequently calcined at 600°C for 3 hours in 90 cm^3/minute of dry-grade air.

2.4 Surface Area

Nanostructured catalysts consist of micropores, mesopores, and macropores. Microporous materials have average pore diameters less than 2 nm, mesoporous materials between 2 and 50 nm, and macroporous materials above 50 nm. N_2 cooled to temperatures of 77 K is often used as a probe molecule, at which physical adsorption occurs on the total surface of the catalyst [5]. Adsorbed N_2 is recorded as a function of the partial pressure of N_2 producing an adsorption isotherm. Depending on the average pore size diameter of the support, the isotherm can vary significantly [5].

The surface area can be calculated using the Brunauer, Emmett, and Teller, or

BET method. For adsorption at a free surface, the BET equation is given as [5]:

$$\frac{P}{V(P_o - P)} = \frac{1}{V_m C} + \frac{(C-1)P}{V_m C P_o} \tag{2.1}$$

where V is the volume of adsorbed gas at equilibrium pressure P, V_m is the volume of a monolayer coverage of adsorbed gas, P_o is the vapor pressure of the probe gas in its condensed state at the adsorption temperature, and C is a constant related to the enthalpy change in the first layer ΔH_1 and heat of condensation of the adsorbate ΔH_c. The equation for C is given as [5]:

$$C = exp[(\Delta H_1 - \Delta H_c)/RT] \tag{2.2}$$

A strong linear relationship is usually observed when $\frac{P}{V(P_o - P)}$ is plotted as a function of the relative pressure $\frac{P}{P_o}$. The monolayer volume is determined from the slope $\frac{C-1}{C}V_m$. The intercept $\frac{1}{V_m}C$ is divided by the weight of the sample to determine the surface area (m^2/gram). The determination is valid for ranges of the relative pressure from 0.05 to 0.3 [5]. The surface areas and average pore radii were measured using a Micromeritics ASAP 2010 instrument. Prior to these measurements, the catalysts were degassed at 200°C for 3 hours under 5 μm Hg of vacuum. Approximately 100 mg of catalyst was used for each run.

2.5 Elemental Analysis

The metal loading was determined via inductively coupled plasma-optical emission spectrometry, or ICP-OES [6]. In ICP-OES, a hot plasma breaks down compounds into atoms and ions. The atoms and ions inside the plasma are excited to emit

Table 2.1: Wavelengths utilized during elemental loading analysis with ICP-OES. Two wavelengths were used to examine each element for reproducibility purposes.

Element	Wavelength 1 (nm)	Wavelength 2 (nm)
Ag	328.068	338.289
Pd	340.458	360.955
Pt	214.424	217.468
Rh	249.078	343.488

electromagnetic radiation in the form of light. The light is resolved through diffractive optics, and a detector measures the intensity of the light. An element can be identified from a specific wavelength resolved through the optics, and the intensity can be directly correlated with the element's concentration [6]. Multiple elements can be measured simultaneously. Samples can be liquids, solids or gases. Solid samples are typically dissolved in acids such as HCl, HF, or HNO_3. The degree of dissolution depends on factors such as the type of sample, time, and temperature. ICP-OES is useful over a large concentration working range, from μg/L up to g/L.

Metal loadings were calculated using an Agilent Technologies axial 710-ES series ICP-OES instrument.Prior to analysis, the instrument was calibrated with standard solutions of Ag (1005 $\pm$ 3 μg/mL), Pd (1005 $\pm$ 5 μg/mL), Pt (1000 $\pm$ 3 μg/mL), and Rh (999 $\pm$ 3 μg/mL)(Inorganic Ventures). First, the powder samples were dissolved in 3 mL of a 1:1:1 volumetric mixture of deionized H_2O, HF, and HNO_3. Then the samples were sonicated for 1 hour at a temperature of 55°C. The samples were introduced into the ICP using peristaltic pumping and collected using an autosampler. Table 2.1 lists the wavelengths chosen in the analysis. Two wavelengths were used to examine each element for reproducibility purposes.

2.6 Thermal Sorption Spectroscopy Methods

2.6.1 Temperature Programmed Reduction

Temperature programmed reduction (TPR) experiments were employed to study the reduction of catalysts. The reduction temperatures are important because the active site can vary depending on the oxidation state of the metal. In TPR, a H_2-containing stream is passed over a metal oxide, which is reduced into its metallic state when exposed to elevated temperatures. Depending on the metal oxide, a peak will be generated at a specific temperature corresponding to the reduction of the oxide. The temperature at which the reduction of a metal occurs is essential to know for the method of pulse chemisorption, for the metal oxide needs to be reduced before doing any adsorbate probing. In the case of bimetallic catalysts, TPR possibly helps to understand the effect of one metal on the reducibility of the other. The area under the peak can be integrated to give the total H_2 consumed from the reduction of the metal oxide. Experiments were conducted using a Micromeritics ASAP 2910 sorption analyzer. Figure 2.1 shows a schematic of the 2910 system used for TPR. For the experiments, approximately 150 milligrams of the catalyst was loaded into a quartz U-tube reactor and heated from 25 °C to 500°C at a rate of 40°C/min in a mixture of 10% H_2/Ar flowing at 90 mL/min. H_2 consumption was monitored using a thermal conductivity detector (TCD). A cold trap placed before the TCD was used to remove water from the exit stream.

2.6.2 Chemisorption

Chemisorption measures the number of metallic sites on the surface of a catalyst by pulsing an adsorbate gas - such as H_2, O_2, CO, or N_2O - over a catalytic surface until all sites are occupied by the adsorbate. Depending on the uptake of gas, the active surface area, percent metal dispersion, and active metal particle size can be

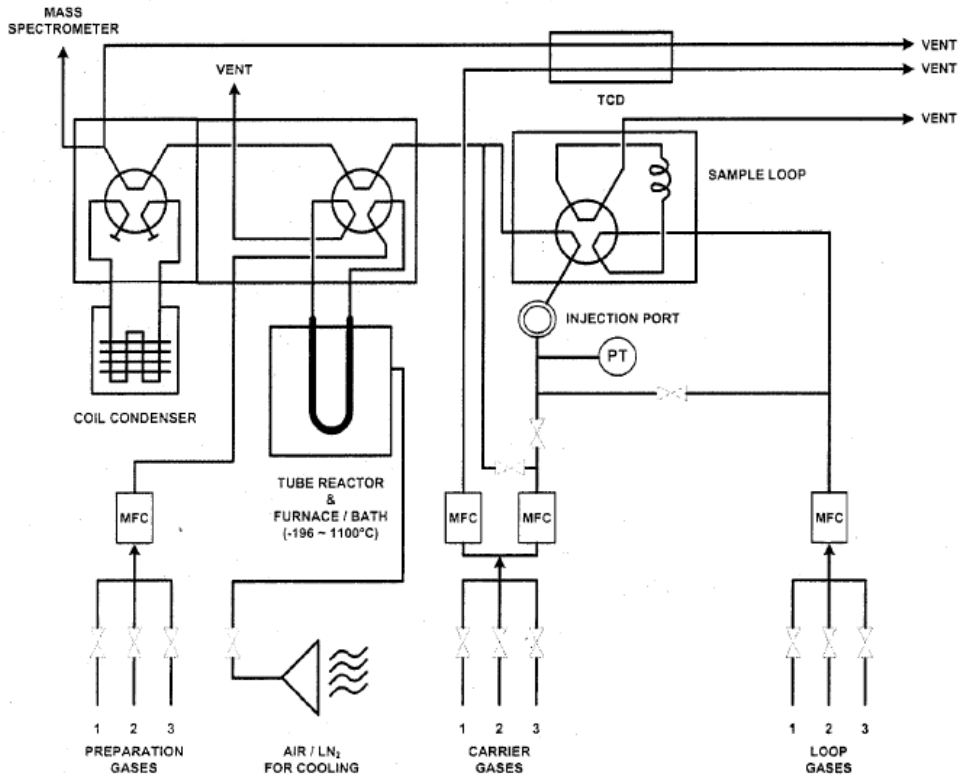

Figure 2.1: Schematic of the Micromeritics Autochem 2910. Taken from the AutoChem 2910 manual.

calculated. The catalysts must be reduced before chemisorption. A fraction of the metal may still be in an unreduced state, thus it is important to confirm that the metal is completely reduced [1, 5].

Dynamic pulse chemisorption is a common technique employed to measure the metal site density in a catalyst. In this method, the reduced catalyst is exposed to pulses of adsorbate gas from a calibrated loop in a flow of an inert carrier gas at atmospheric pressure. The quantity of gas not adsorbed is measured by TCD (thermal conductivity detector). The first few pulses may be completely adsorbed by the sample and no change in the TCD detector signal will be observed. As the sample approaches saturation, peaks representing concentrations of non-adsorbed molecules appear. When saturation occurs, each injected gas volume emerges from the sample apparatus unchanged and peaks become constant in area. The number of molecules chemisorbed is the difference between the total amount of gas injected and the total amount of the gas that did not adsorb on the active sites. The quantity of each pulse is determined by a fixed-volume loop connected to an electronically controlled valve.

For the platinum group metals (Pd, Pt, and Rh), H_2 was used as the adsorbate gas, whereas for Ag, O_2 was used. H_2 does not adsorb on Ag [7–10]. The adsorption temperature for O_2 was 170°C. This temperature was selected because effective removal of O_2 occurs without sintering the metal [11, 12]. Samples (approximately 150 mg) were first oxidized in air at 600°C for 1 hour, degassed in a inert gas at 600°C for 30 minutes, reduced in a mixture of 10% H_2/Ar at 250°C for 2 hours, degassed in an inert gas at 300°C for 30 minutes, and cooled to the desired temperature. Pt and Rh measurements were taken at ambient temperature, and Pd measurements were taken at 70°C. This temperature was selected to avoid formation of palladium hydride [13, 14]. Then 20-30 pulses of 10% H_2/Ar or 1% O_2/He were passed over the catalyst until saturation was reached. The loop size used was 300 μL.

2.7 X-Ray Diffraction

X-ray diffraction (XRD) is used to identify bulk crystalline phases and to estimate particle sizes of crystalline materials. X-rays are emitted from a source to the sample. These x-rays undergo scattering with a set of incident angles when they make contact with the sample, and those angles are unique for a particular crystallographic structure. From the scattering, a pattern of the intensity as a function of the scattering angle is obtained, and can be compared to known patterns to identify crystal structures of elements. Via the Scherrer equation, the pattern can obtain mean particle sizes [5]:

$$d_c = \frac{K\lambda}{B\cos\theta} \tag{2.3}$$

where d_c is the diameter of the crystallite, K is a constant, B is the breadth of the diffraction peak, λ is the wavelength of the incident x-rays, and θ is the angle of the diffraction peak.

The measurements were conducted using a Rigaku Miniflex DMAX-B diffractometer with a Cu-Kα radiation source, operated at 40 kV and 100 mA. Patterns were recorded in the θ range from 20^o to 90^o at 4θ/minute. JADE software (version 9) was used to interpret the patterns.

2.8 Reaction Rate System Setup

The HC-SCR experiments were carried out using a Altimara Instruments Celero^{TM} high-throughput screening reactor system with 8 parallel flow-through reactor wells (Figure 2.2). The catalyst was loaded into each reactor well using two swabs of quartz wool surrounding the material. The 8 reactors were inserted into a stainless steel reactor block that held the reactor wells. The temperature of each reactor well was

controlled by a band heater surrounding the reactor block. There were two thermocouples; one was inserted into the bottom of the reactor block while another was inserted between the band heater and the reactor block. The maximum rated temperature of the heating block was 550°C. All lines before and after the reactor block were heated to 200°C via an oven to ensure vaporization of H_2O. Five mass flow controllers, one rotameter (for O_2) and one high-pressure liquid chromatograph (HPLC) pump were used to control the gas and liquid flow rates. The flow distribution across the reactor wells was controlled by pressure drop over independent capillaries of 500 μm diameter. An 8-way Valco selection valve was used to select which reactor well was to be analyzed. To remove H_2O, the gas outlet stream flowed through a stainless steel condenser held at 0°C and an A+ Corporation Genie membrane filter before going into a Thermo Scientific 42C-High Level NO_x analyzer and an Agilent Technologies CP-4900 micro-gas chromatograph. The H_2O traps were required to prevent H_2O from damaging the components in the analytical instruments.

The 42C-High Level NO_x analyzer has the ability to measure NO and NO_2 separately. Figure 2.3 displays the analyzer schematic. A gas sample from the testing system is directed into the reaction chamber inside the analyzer, where chemiluminescence is used to measure concentrations. For NO analysis, the NO reacts with ozone to produce NO_2, excited NO_2^*, and O_2. The ozone is produced by an ozonator device located inside the analyzer. The air is dried by a desiccant trap before entering the analyzer. A vacuum pump is used to draw in air for the ozonator. The excited NO_2^* molecules instantaneously revert to ground level NO_2, and the resulting light emission from the grounding is directly proportional to the NO concentration in the feed stream. A photomultiplier (PMT) tube, at a temperature of -3°C, measures the intensity of the emitted light. For determination of the NO_x (NO + NO_2) concentration, the sample gas containing both molecules is directed to an internal converter catalyst (T = 625°C) where the NO_2 is reduced to NO. The NO-only sample gas is

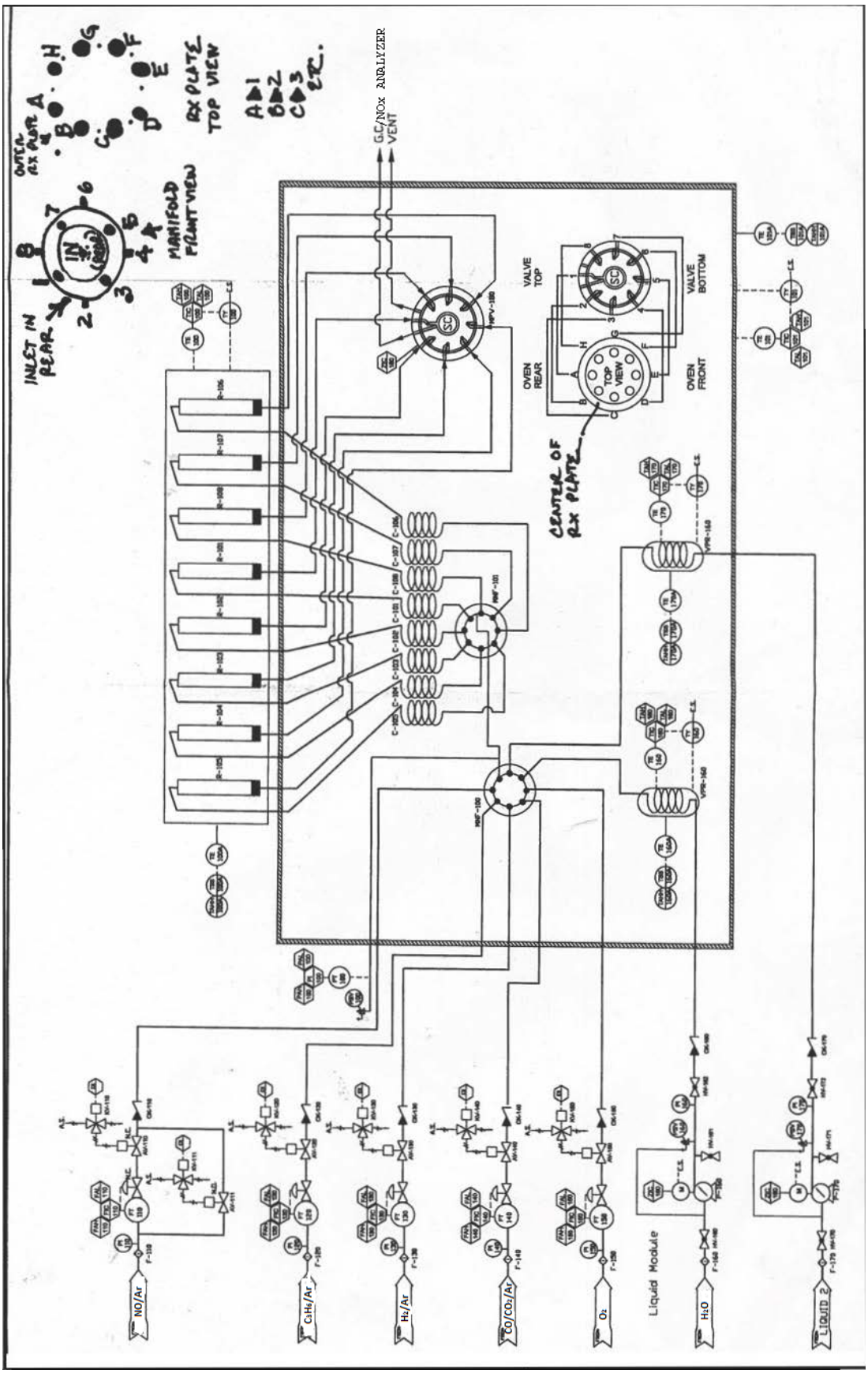

Figure 2.2: Piping and instrumentation diagram of the Celero. Provided by Altamira Technologies.

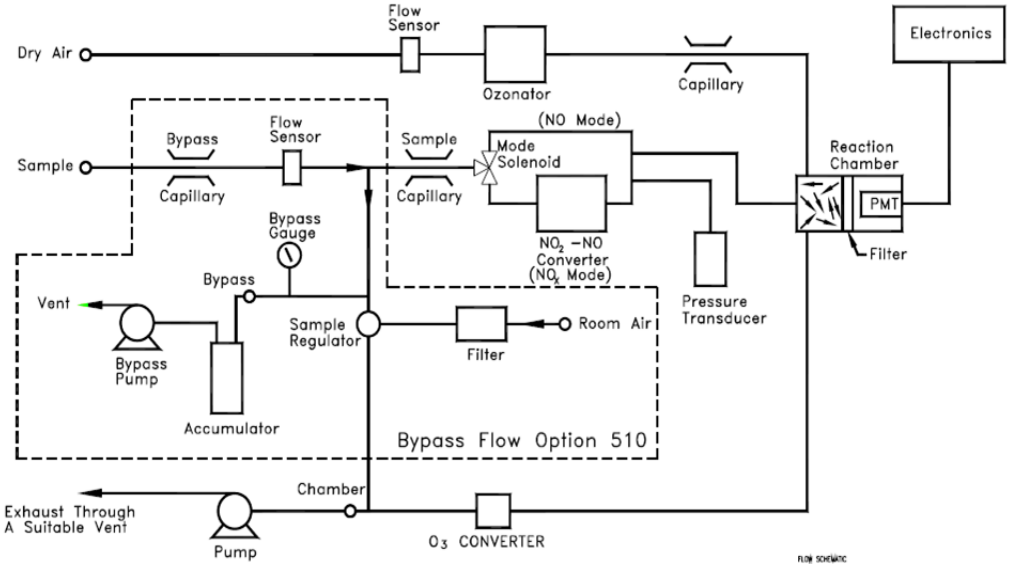

Figure 2.3: Schematic of the Model 42C High Level NO_x Analyzer. Provided by Thermo Fisher Scientific.

analyzed by the chemiluminescence method. The NO_x concentration is determined by the difference in the NO_x and NO concentrations.

The column modules inside the micro-GC were a MolSieve 5A Plot (MS) with argon as the carrier gas (column temperature = 100°C) and a PoraPLOT Q (PPQ) with helium as the carrier gas (column temperature = 40°C). The MS column was used to quantify H_2, O_2, N_2, and CO, and the PPQ column was used to quantify CO_2, N_2O, and C_3H_6. Analysis of a sample took 4 minutes. The system was fully automated using Impressionist Software developed by Altamira^{TM} Technologies, allowing for time-on-stream data collection. The flow rates of the wells were measured before each run. Depending on the well flow rate, the catalyst weight was in the range of 50-70 mg in order to maintain a gas hourly space velocity of 60000 hr^{-1}. The reaction was conducted at reaction temperatures of 200°C, 300°C, and 400°C using simulated diesel exhaust feed. The total flow rate through the system was 600 ml/min. The NO_x analyzer and micro-GC were calibrated to the simulated diesel exhaust concentrations before each run. The catalysts were re-oxidized at 400°C for 30 minutes before each

run to remove any carbonaceous species from the catalysts.

2.9 Experimental Design

Design of Experiments (DOE) methods enable the identification of variables that influence characteristics of interest in a process. Through DOE, one can systematically test the effect of a dependent variable, called a *response*, by varying the levels of an independent variable, called a *factor*. This approach can yield important information about the performance of a process. One such design is the factorial design. Factorial designs are divided into full and fractional designs. In a full design, every combination of factor and level is tested. For example, in a design with 4 factors with 3 levels each, a total of $3^4 = 81$ total treatments are carried out. In the full factorial design, all effects (one, two, three and four-factor) can be calculated. In a fractional factorial design, a specific fraction of the full design is conducted. The fraction eliminates the ability to calculate higher-order interactions, specifically above two [15]. These higher-order interactions are typically lumped into the calculation of the error because they are assumed to be negligible [16].

If time and resources permit, the full factorial design is the most desirable plan to follow. These experiments can be designed and analyzed using a number of software packages, such as MINITAB^{TM} and SPSS^{TM}. Assume a n^k design with k factors and n levels. A combination of factor levels is called a *run*. The total number of runs would be n^k. Table 2.2 displays a planning matrix with two factors and two levels. The notation (+, -) is used to represent the two factor levels. Two key properties in a design are balance and orthogonality. Balance means that each factor level appears in the same number of runs, and orthogonality means that two factors have all their level combinations appear in the same number of runs [15].

When the data collection for the factorial experiment is completed, main and interaction effects can be calculated. A main effect is the influence of one factor on the

Table 2.2: A sample full factorial planning matrix with two factors and two levels.

Experiment	Factor A	Factor B
1	+	+
2	+	-
3	-	+
4	-	-

response, whereas an interaction effect is the combined and simultaneous influence of two or more factors on the response. Both main and interaction effects can be plotted graphically.

An analysis of variance (ANOVA) can be done to test for statistical significance of the main and interaction effects on the response. The ANOVA tests if a null hypothesis H_o is rejected. The p-value is used to test the statistical significance of a hypothesis. In statistics, A p-value of 0.05 signifies a 95% confidence interval; the data in a set would make the null hypothesis true 5% of the time if at this value. Other p-values may also be used depending on the desired accuracy of the analysis. If the p-value is below the desired confidence interval, then H_o is rejected and the alternate hypothesis H_a is accepted, i.e. the effect is significant on the response. The mean square coefficients can be used to rank the influence of the main and interaction effects on the response. The mean square coefficients is the quotient of the residual sum of square and the degrees of freedom. The residual sum of squares is a measure of the discrepancy between the data and an estimation model. Therefore, if the sum of squares for a factor is large, then a significant amount of the variance (deviation) in the model can be explained by the influence of the factor, and therein the factor affects the behavior of the response significantly. The degrees of freedom for a main effect is (n-1), where n is the number of levels for the factor related to the main effect. The degrees of freedom for an interaction effect is the product of the degrees of freedom for each individual main effect.

The factorial method for the DOE analysis employed five factors: HC/NO_x ratio,

H_2/CO ratio, second metal loading, second metal type, and reaction temperature. The hydrocarbon to inlet NO_x ratio (HC/NO_x) is the ratio of the concentration of hydrocarbon on a carbon atom basis to the inlet NO_x concentration. The H_2/CO ratio is the ratio of the concentration of H_2 to the concentration of inlet CO. The second metal loading is the amount of additional Pd, Pt, or Rh impregnated onto the Ag/Al_2O_3 catalyst. Each factor was tested at three different levels for a total of 243 independent treatments. The data was analyzed using the MINITAB^{TM} software package to identify which factors were most significant in affecting the NO_x conversion and N_2 selectivity. The p-value was used to determine effect significance. The p-value is used in a significance test to assess the hypothesis' validity. A p-value target of 0.05 was used; any main or interaction factor that had a p-value of 0.05 or less was statistically significant. The mean squares were used to rank the influence of the factors on the responses. MINITAB^{TM} was also utilized to generate main effect and interaction effect plots.

Bibliography

[1] J.A. Anderson and M.F. Garcia. *Supported Metals in Catalysis*, volume 5. Imperial College Press London, 2005.

[2] J. Hagen. *Industrial Catalysis: A Practical Approach*. Wiley-VCH, 2006.

[3] S. Xie, J. Wang, and H. He. Poisoning effect of sulphate on the selective catalytic reduction of NO_x by C_3H_6 over Ag-Pd/Al_2O_3. *Journal of Molecular Catalysis A: Chemical*, 266(1-2):166–172, 2007.

[4] J. Wang, H. He, Q. Feng, Y. Yu, and K. Yoshida. Selective catalytic reduction of NO_x by C_3H_6 over Ag/Al_2O_3 catalyst with a small quantity of noble metal. *Catalysis Today*, 93:783–789, 2004.

[5] J.R. Anderson and K.C. Pratt. *Introduction to Characterization and Testing of Catalysts*. Academic Press North Ryde, Australia, 1985.

[6] J. Nolte. ICP Emission Spectroscopy: A Practical Guide. 2003.

[7] A. Noordermeer, G.A. Kok, and B.E. Nieuwenhuys. A comparative study of the behaviour of the PdAg (111) and Pd (111) surfaces towards the interaction with hydrogen and carbon monoxide. *Surface Science*, 165(2-3):375–392, 1986.

[8] L.G. Petersson, H.M. Dannetun, and I. Lundstrom. Hydrogen desorption versus electronic structure studied on Ag-covered Pd with photoemission and a hydrogen-sensitive metal-oxide-semiconductor structure. *Physical Review B*, 30(6):3055, 1984.

[9] S. Yuvaraj, S.C. Chow, and C.T. Yeh. Characterization of Silver-Rhodium Bimetallic Nanocrystallites Dispersed on [gamma]-Alumina. *Journal of Catalysis*, 198(2):187–194, 2001.

[10] C. Mijoule and V. Russier. Theoretical study of physisorption and chemisorption of hydrogen on Ag (111) from LSD calculations. *Surface Science*, 254(1-3):329–340, 1991.

[11] T.E. Hoost, R.J. Kudla, K.M. Collins, and M.S. Chattha. Characterization of Ag/[gamma]-Al_2O_3 catalysts and their lean-NO_x properties. *Applied Catalysis B: Environmental*, 13(1):59–67, 1997.

[12] K. Arve, K. Svennerberg, F. Klingstedt, K. Eranen, L.R. Wallenberg, J.O. Bovin, L. Capek, and D.Y. Murzin. Structure-Activity Relationship in HC-SCR of NO_x by TEM, O_2-Chemisorption, and EDXS Study of Ag/Al_2O_3. *The Journal of Physical Chemistry B*, 110(1):420–427, 2006.

[13] P.C. Aben. Palladium areas in supported catalysts:: Determination of palladium surface areas in supported catalysts by means of hydrogen chemisorption. *Journal of Catalysis*, 10(3):224–229, 1968.

[14] J.E. Benson, H.S. Hwang, and M. Boudart. Hydrogen-oxygen titration method for the measurement of supported palladium surface areas. *Journal of Catalysis*, 30(1):146–153, 1973.

[15] C.F.J. Wu, M. Hamada, and C.F. Wu. *Experiments: Planning, Analysis, and Parameter Design Optimization*. Wiley New York, 2000.

[16] W.S. Connor and M. Zelen. *Fractional factorial experiment designs for factors at three levels*. US Govt. Print. Off., 1959.

CHAPTER III

Synthesis and Performance Evaluation Silver-Based Catalysts for the Reformate-Assisted Selective Catalytic Reduction of NO_x

3.1 Summary

The development of better performing catalysts for the hydrocarbon selective catalytic reduction of NO_x is a major challenge in the advancement of exhaust aftertreatment systems in diesel and lean-burn gasoline engines. A significant number of studies have focused on low-loading Ag/Al_2O_3 catalysts, which are active for the reduction of NO_x and are selective to N_2. However, the catalysts are active only at temperatures above 400°C if using propylene as a reductant [1]. Therefore, we studied the effects of (1) adding H_2 to the exhaust environment, and (2) adding a second metal - specifically platinum group metals - along with the Ag. A full factorial experimental design was conducted to screen catalysts and determine which factors affect the NO_x conversion and N_2 selectivity. Five factors were studied: HC/NO_x ratio, H_2/CO ratio, second metal loading, second metal type, and reaction temperature. For the NO_x conversion and N_2 selectivity, all five main effects were statistically significant with p values ≤ 0.05. Increasing the loading of the second metal inhibited the NO_x conversion and N_2 selectivity. Pd bimetallic catalysts performed marginally worse for

NO_x reduction compared to Pt and Rh bimetallic catalysts and significantly worse for N_2 selectivity. The effect of impregnation order was also studied. The impregnation order had two levels - Ag-loaded first and Ag-loaded second. The impregnation order by itself did not have any significant effect on the NO_x conversion and N_2 selectivity. However, when interacting with second metal type, it was observed that for the Pd bimetallic catalysts, the NO_x conversion and N_2 selectivity were significantly affected by the impregnation order.

3.2 Introduction

Hydrocarbon Selective Catalytic Reduction (HC-SCR) of NO_x is a catalytic process in which NO_x is reduced to N_2 by a hydrocarbon reductant [2]. Since the tailpipe concentration of hydrocarbons from a diesel engine is not sufficient enough to reduce NO_x, some fuel has to be rerouted from the engine to the exhaust aftertreatment system. HC-SCR is important for reducing NO_x emissions from mobile sources such as diesel and lean-burn gasoline cars. Ag/Al_2O_3 is one of the most researched catalysts for HC-SCR [3–5]. However, Ag/Al_2O_3 does not exhibit significant activity or selectivity to N_2 below 400°C when using propylene as a reductant [3, 6]. The addition of H_2 improves the performance for NO_x reduction by reducing the light-off temperature [7]. Factors that can affect the extent of conversion include H_2 concentration, the presence of H_2O and/or CO, and catalyst loading.

Platinum group metals, such as Pd, Pt, and Rh, have displayed activity for HC-SCR below 400°C. Burch and Millington tested Pd/Al_2O_3, Pt/Al_2O_3, and Rh/Al_2O_3 at 1% weight loading. Pd/Al_2O_3 attained a maximum NO_x conversion of 25% with a full width half maximum (FWHM) temperature window from 225°C - 275°C, Pt/Al_2O_3 attained a maximum NO_x conversion of 60% with a FWHM temperature window from 250°C - 300°C, and Rh/Al_2O_3 attained a maximum NO_x conversion of 30% with a FWHM temperature window from 325°C - 400°C [8]. In addition, Pd, Pt,

and Rh have been proven to reduce NO_x in the presence of H_2, CO, or both H_2 and CO [9–11]. Accordingly, it is hypothesized that the addition of platinum group metals to the surface of Ag/Al_2O_3 would lower the light-off temperature and increase low-temperature activitiy for NO_x reduction. This work focuses on combining the NO_x light-off improvement observed with the presence of H_2 with the low-temperature performance of the platinum group metals to formulate a bimetallic Ag-based catalyst that will improve the NO_x conversion at temperatures below 400°C.

In this chapter, a design of experiments (DOE) was used to quantify the effects of several factors on the NO_x reduction performance. The factors studied were HC/NO_x ratio, H_2/CO ratio, second metal loading, second metal type, and reaction temperature. The dependent variables, or *responses*, of interest were NO_x conversion and N_2 selectivity. An analysis of variance (ANOVA) was conducted to determine significant effects, and main effect and interaction effects plots were generated to assess the magnitude of the effect changes. The influence of the factors on the responses was ranked using the mean square error generated by the ANOVA.

3.3 Experimental

3.3.1 Catalyst Synthesis

Catalysts consisting of Ag, Pt, Pd, and Rh were supported on a commercial γ-Al_2O_3 powder purchased from Alfa Aesar (3 μm flakes, 99.99% purity, 80-120 m^2/g surface area). The metals were loaded onto the surface of the support using a dry impregnation technique [12, 13]. The metal precursors were $AgNO_3$ (Johnson Matthey), $Pt(NH_3)_4(NO_3)_2$ (Johnson Matthey), $Pd(NH_3)_4(NO_3)_2$ (10% solution, Sigma-Aldrich), and $Rh(NO_3)_3$ (Johnson Matthey). The metal precursors were dissolved in H_2O and impregnated onto the support. After impregnation, the monometallic catalysts were dried at a pressure of -30 mm Hg at 100°C for 8-12 hours and sub-

sequently calcined at 600°C for 3 hours in 90 cm^3/minute of dry grade air. For the bimetallic catalysts, the Ag metal precursor solution was impregnated before Pd, Pt, or Rh. After each impregnation step the catalysts were dried overnight at a pressure of -30 mm Hg at 100°C for 8-12 hours and then calcined at 600°C for 3 hours in 90 cm^3/minute of dry grade air.

3.3.2 Catalyst Characterization

3.3.2.1 Surface Areas

The catalyst surface areas were measured via N_2 physisorption using a Micromeritics ASAP 2010 instrument. Prior to these measurements, the catalysts were degassed at 200°C for 3 hours until the sample pressure achieved 5 μm Hg. Approximately 100 mg of catalyst was used for each run.

3.3.2.2 Elemental Analysis

The metal content was measured using an Agilent Technologies axial 710-ES series ICP analyzer. Prior to analysis, the instrument was calibrated with standard solutions of Ag (1005 $\pm$ 3 μg/mL), Pd (1005 $\pm$ 5 μg/mL), Pt (1000 $\pm$ 3 μg/mL), and Rh (999 $\pm$ 3 μg/mL)(Inorganic Ventures). The samples were dissolved in 3 mL of a 1:1:1 volumetric mixture of deionized H_2O, 49% HF, and concentrated HNO_3. Then the samples were sonicated for 1 hour at a temperature of 55°C. The dissolved samples were introduced into the ICP using peristaltic pumping and collected using an autosampler.

3.3.2.3 X-Ray Diffraction

Bulk structures of the catalysts were characterized using powder X-ray diffraction (XRD). XRD measurements were conducted using a Rigaku Miniflex DMAX-B rotating anode diffractometer with a Cu-Kα radiation source, operated at 40 kV and

100 mA. The powder samples were mounted on glass slides using double-side tape. XRD patterns were recorded over diffraction angles (2θ) range from 20^o to 90^o at 4θ/minute. A multifunction software, JADE (version 9), was used to interpret the patterns.

3.3.3 Conversion Measurements

3.3.3.1 Calculations

Catalytic activity measurements were performed using a Celero^{TM} high-throughput screening reactor system (Altamira Instruments) with 8 parallel flow-through reactor wells made of stainless steel. The catalyst was supported in each reactor well with quartz wool (Waite Glass Inc.). The 8 reactors were inserted into a stainless steel block. The temperature of each reactor well was controlled by a band heater surrounding the reactor block. An 8-way Valco selection valve was used to select which reactor well was to be measured. To remove water, the gas outlet stream passed through a stainless steel condenser held at 0°C and an A+ Corporation Genie membrane filter before going into a Thermo Scientific 42C-High Level NO_x analyzer and an Agilent Technologies CP-4900 micro-gas chromatograph. The condenser and Genie filter were required to prevent H_2O from damaging the gas phase analyzers. The column modules inside the micro-GC were a MolSieve 5A with Ar as the carrier gas (operation temperature = 100°C) and a PoraPLOT Q with he as the carrier gas (operation temperature = 40°C). The MolSieve column quantified H_2, O_2, N_2, and CO, and the PoraPLOT Q column quantified CO_2, N_2O, and C_3H_6. Analyses of the gas mixtures were performed every 4 minutes. The system was fully automated using Impressionist^{TM} software.

The gas space velocity was 60000 hr^{-1}. This gas space velocity is within the range of commercial systems, as the space velocity range of testing for the FTP-75 Federal Test Cycle for emission certification of light-duty vehicles made after 2000 is between

10000 - 120000 hr^{-1} [14]. The flow rates of the wells were measured before each run. Depending on the well flow rate, the catalyst weight was in the range of 50-70 mg. The reaction was conducted at reaction temperatures of 200°C, 300°C, and 400°C using a simulated diesel exhaust feed that consisted of 600 ppm NO, 800 ppm CO, 3200 ppm H_2, 1800 ppm C_3H_6, 4% CO_2, 10% O_2, and 4% H_2O, with Ar as the balance gas. The total flow rate through the system was 600 ml/min. The NO_x analyzer and micro-GC were calibrated to the simulated diesel exhaust concentrations before each run. The catalysts were re-oxidized at 400°C for 30 minutes before each run to remove any carbonaceous species from the catalysts.

The HC-SCR performance of the catalyst was reported as conversions to NO_x and selectivity to N_2. The equations used to calculate the NO_x conversion and N_2 selectivity are displayed below.

$$Conversion = (\frac{NOx_{in} - NOx_{out}}{NOx_{in}}) \times 100 \tag{3.1}$$

$$Selectivity = (\frac{NOx_{in} - NOx_{out} - N_2O_{out}}{NOx_{in} - NOx_{out}}) \times 100 \tag{3.2}$$

3.3.3.2 Factors and Levels for DOE analysis

The factorial method for the DOE analysis employed five factors: HC/NO_x ratio, H_2/CO ratio, second metal loading, second metal type, and reaction temperature. The hydrocarbon to inlet NO_x ratio (HC/NO_x) is the ratio of the concentration of hydrocarbon on a carbon atom basis to the inlet NO_x concentration. The H_2/CO ratio is the ratio of the concentration of H_2 to the concentration of inlet CO. The second metal loading is the amount of additional Pd, Pt, or Rh impregnated onto the

Table 3.1: Components in the simulated diesel exhaust with constant concentrations.

Component	Concentration
NO	600 ppm
CO	800 ppm
CO_2	4%
H_2O	4%
O_2	10%
Ar	balance

Ag/Al_2O_3 catalyst. Each factor was tested at three different levels for a total of 243 independent observations. The concentrations of NO, CO, CO_2, H_2O, and O_2 were held constant. The concentrations are displayed in Table 3.1.

Table 3.2 lists the factors and levels tested in the experimental design. The HC/NO_x ratio was tested at 3:1, 6:1, and 9:1. Equivalent HC/NO_x ratios have been tested in literature for HC-SCR on Ag/Al_2O_3 catalysts [15]. In this range, Ag/Al_2O_3 is highly active for NO_x conversion and selective to N_2. The H_2/CO ratio was investigated at ratios of 0:1, 2:1, and 4:1. Conducting tests without H_2 (the 0:1 H_2/CO ratio) was done for the purpose of elucidating the promoting effect of H_2 with Ag/Al_2O_3 and to investigate the effect of CO by itself as a possible reductant. The selection of the H_2/CO ratios of 2:1 and 4:1 were based on a typical reformate stream that produces a stoichiometric excess of H_2 compared to CO. The concentrations of H_2 and hydrocarbon are listed in Table 3.3.

The second metals employed were Pd, Pt, and Rh. These metals were chosen because they have demonstrated to be active for SCR with hydrocarbons, H_2, and/or CO [10, 16–18]. The loading levels tested were 0%, 1%, and 10%. The values are calculated based on the amount of Ag atoms contained in a 2% Ag/Al_2O_3 catalyst, which was calculated to be 1.1×10^{20} atoms and is accepted as the ideal loading for HC-SCR by dry impregnation methods [19]. For example, a loading of 1% Pt means that the value of 1% of 1.1×10^{20} - or 1.1×10^{18} - of additional atoms of Pt were added onto the 2% Ag/Al_2O_3 catalyst. In this work, the 1% loading is referred to

Table 3.2: Factors and levels employed in the full factorial analysis.

Factors	Level 1	Level 2	Level 3
HC/NO_x Ratio	3	6	9
H_2/CO Ratio	0	2	4
Second Metal Loading	0%	1%	10%
Second Metal Type	Pd	Pt	Rh
Reaction Temperature (°C)	200	300	400

Table 3.3: H_2 and C_3H_6 concentrations at the tested HC/NO_x and H_2/CO ratios.

H_2	C_3H_6
0 ppm (0:1)	600 ppm (3:1)
1600 ppm (2:1)	1200 ppm (6:1)
3200 ppm (4:1)	1800 ppm (9:1)

as the low-loading level and the 10% loading is referred to as the high-loading level. The catalysts were tested at 200°C, 300°C, and 400°C. The lower temperature resides within the range of diesel exhaust where Ag/Al_2O_3 exhibits low to negligible activity [6].

The data was analyzed using the MINITAB^{TM} software package to identify which factors were most significant in affecting the NO_x conversion and N_2 selectivity. The p-value was used to determine effect significance. The p-value is used in a significance test to assess the hypothesis' validity. A p-value target of 0.05 was used; any main or interaction factor that had a p-value of 0.05 or less was statistically significant. The mean squares were used to rank the influence of the factors on the responses. The mean square is the quotient of the residual sum of square and the degrees of freedom. The residual sum of squares is a measure of the discrepancy between the data and an estimation model. Therefore, if the sum of squares for a factor is large, then a significant amount of the variance (deviation) in the model can be explained by the influence of the factor, and therein the factor affects the behavior of the response significantly.

3.4 Results and Discussion

3.4.1 Surface Areas and Elemental Analysis

Table 3.4 lists the BET surface areas and actual metal loadings for the tested catalysts. Impregnation of the metal precursor did not result in a significant change in the overall surface area, and the areas were identical within error for all impregnated catalysts. Ag loadings varied between 1.3-2.1%, with a target value of 2%. Platinum group metal content was typically 50-60% of the target loading.

3.4.2 Structure Characterization

Figure 3.1 shows the diffraction patterns of all tested catalysts. The presence of γ-Al_2O_3 is visible with peaks at 39°, 46°, and 67°. Any peaks corresponding to the metal were not visible, indicating that the metal particles were likely well dispersed on the support.

3.4.3 Conversions/Selectivities of Tested Catalysts

3.4.3.1 HC-SCR of NO_x Activity for Monometallic Catalysts

The blank reactors in the Celero and the Al_2O_3 support were inactive under all tested conditions. Figure 3.2 shows the NO_x conversion as a function of temperature for the Ag/Al_2O_3 and monometallic platinum group metal catalysts. The PGM catalysts were not as active for NO_x conversion compared to Ag/Al_2O_3. The catalysts were not significantly active at 200°C. At 300°C, the NO_x conversion activity of Ag/Al_2O_3 increased to 92% and to 97% at 400°C. At low loadings, there is no difference in NO_x conversion between the monometallic catalysts at 200°C and 300°C. At 400°C, the NO_x conversion improved over all the PGM catalysts, and the Rh catalyst exhibited the greatest increase to 50% conversion. At high loadings at 200°C, the NO_x conversion mirrors the performance at low loadings. At 300°C, both the

Table 3.4: Surface areas and metal loadings for the catalysts studied in this work.

Catalyst	Target Metal Loading	Actual Metal Loading	Surface Area (m^2/g)
Al_2O_3	-	-	67 ± 3
Ag/Al_2O_3	2.00% Ag	1.55 ± 0.03% Ag	58 ± 3
Ag-1% Pd/Al_2O_3	2.00% Ag, 0.02% Pd	2.13 ± 0.01% Ag, 0.01 ± 0.001% Pd	59 ± 3
Ag-1% Pt/Al_2O_3	2.00% Ag, 0.04% Pt	1.27 ± 0.01% Ag, 0.02 ± 0.003% Pt	59 ± 3
Ag-1% Rh/Al_2O_3	2.00% Ag, 0.02% Rh	1.82 ± 0.02% Ag, 0.01 ± 0.001% Rh	59 ± 3
Ag-10% Pd/Al_2O_3	2.00% Ag, 0.20% Pd	2.10 ± 0.02% Ag, 0.17 ± 0.01% Pd	61 ± 3
Ag-10% Pt/Al_2O_3	2.00% Ag, 0.40% Pt	1.83 ± 0.02% Ag, 0.24 ± 0.01% Pt	61 ± 3
Ag-10% Rh/Al_2O_3	2.00% Ag, 0.20% Rh	1.47 ± 0.03% Ag, 0.10 ± 0.01% Rh	59 ± 3

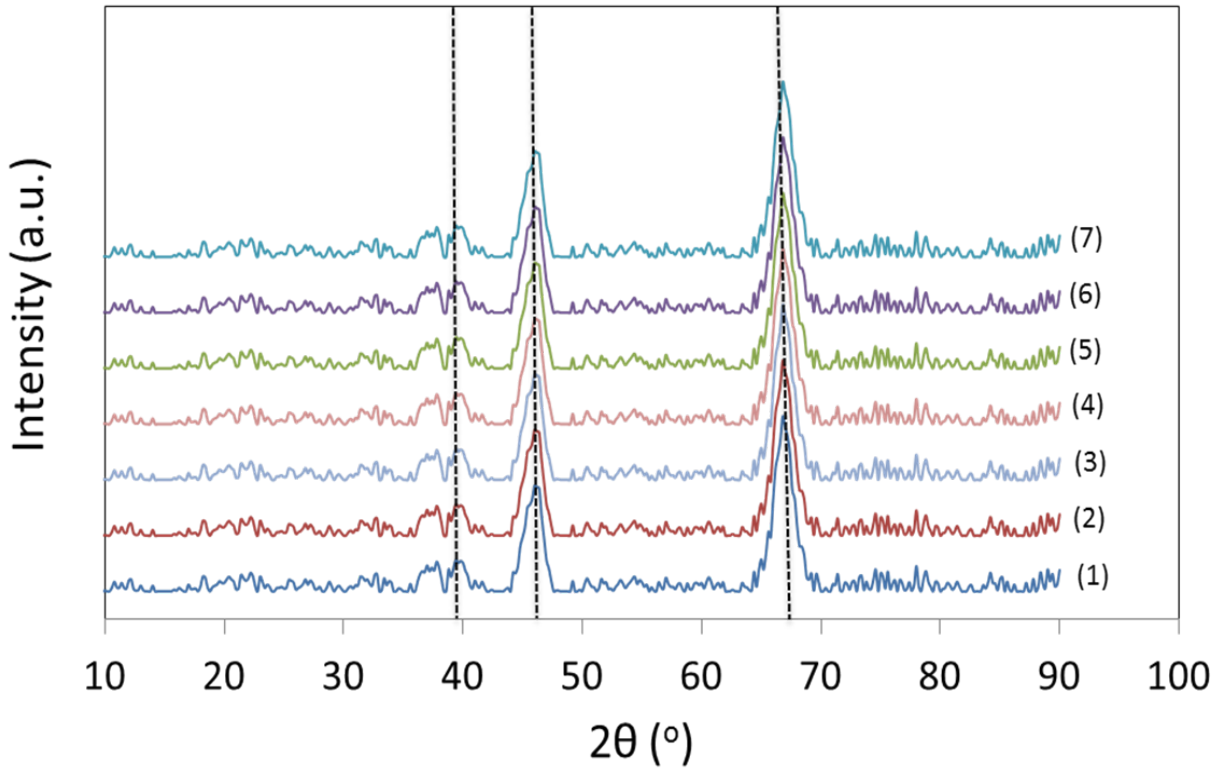

Figure 3.1: X-ray diffraction patterns for the catalysts studied in this work. (1) Ag/Al_2O_3, (2) Ag-1% Pd/Al_2O_3, (3) Ag-1% Pt/Al_2O_3, (4) Ag-1% Rh/Al_2O_3, (5) Ag-10% Pd/Al_2O_3, (6) Ag-10% Pt/Al_2O_3, (7) Ag-10% Rh/Al_2O_3. The dotted lines correspond to the major peaks obtained in the γ-Al_2O_3 support.

Pd and Pt catalysts achieved their maximum NO_x conversions (32% and 52%, respectively) before decreasing to 13% and 35% at 400°C. The conversion over the Rh catalyst continued increasing from 14% at 300°C to 40% at 400°C. The NO_x conversion profiles over the Pd and Pt catalysts exhibited volcano-like behavior, which can be viewed as the competition between two oxidation reactions in which either molecular O_2 or adsorbed oxygen atoms occurring from the dissociation of NO is the source of oxygen that oxidizes the hydrocarbon [1]. At temperatures above 300°C, where the peak in NO_x conversion occurs, molecular O_2 is the main source and the hydrocarbon reductant is consumed unproductively to CO_2. At temperatures below 300°C, the source of oxygen is from the adsorbed oxygen atoms occurring from the dissociation of NO. The reaction in which NO_x is converted to N_2 or N_2O over platinum group metal catalysts was suggested to occur on a reduced surface [1]. Burch and Millington also observed this volcano-like trend over a 1% Rh/Al_2O_3 catalyst. However, the peak NO_x conversion temperature for a Rh/Al_2O_3 was observed to be 50-100°C higher than Pd or Pt. Since the NO_x conversion over the Rh/Al_2O_3 catalyst tested in this study continues to increase with increasing temperature, it is possible that the maximum NO_x conversion for Rh/Al_2O_3 may occur at a temperature above 400°C [8].

Figure 3.3 displays the effect of increasing loading on N_2 selectivity over the monometallic catalysts as a function of temperature. Ag/Al_2O_3 exhibited high selectivity to N_2 across the entire temperature range of interest, from 90% at 200°C to 99% at 400°C. The low-loading platinum group metal catalysts exhibited decreasing selectivity to N_2 as temperature increased. The high-loading Pd and Pt catalysts showed high selectivity (although negligible NO_x conversion) at 200°C before decreasing significantly to 77% and 70%, respectively, at 300°C. The selectivity increased to 92% and 95%, respectively, at 400°C. The high-loading Rh catalyst achieved the lowest selectivity to N_2 compared to the other PGM metal catalysts, reaching 90% selectivity

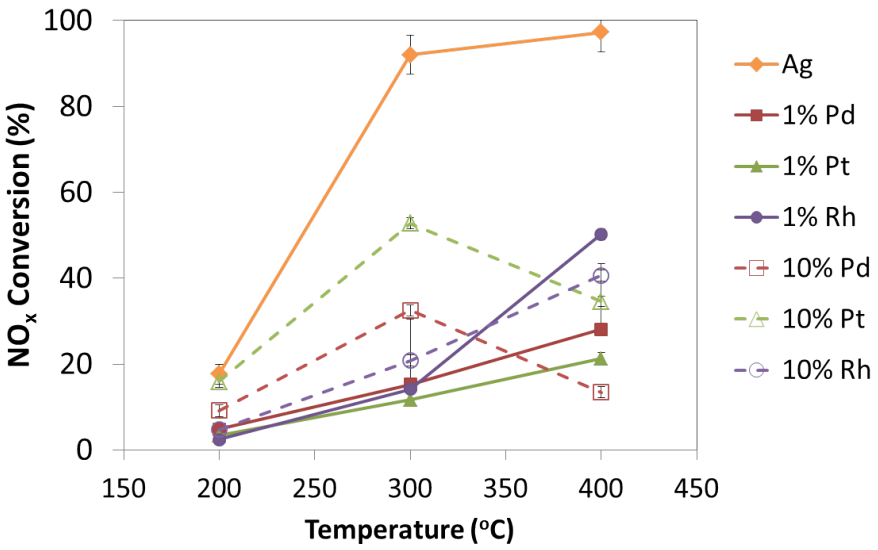

Figure 3.2: Effect of metal loading on NO_x conversion for the monometallic catalysts supported on γ-Al_2O_3. The feed consisted of 600 ppm NO, 800 ppm CO, 3200 ppm H_2, 1800 ppm C_3H_6, 4% CO_2, 10% O_2, and 4% H_2O, with Ar as the balance gas.

at 400°C.

Figure 3.4 displays the effect of increasing loading on C_3H_6 conversion. The conversion of C_3H_6 was less than 5% across all the catalysts at 200°C. Since activation of the hydrocarbon is required to initiate NO_x reduction, the low conversion of C_3H_6 is related to the low conversion of NO_x. At 300°C, C_3H_6 reacted over the Ag/Al_2O_3 and high-loading catalysts. The C_3H_6 is completely consumed at 300°C over the 10% Pd and 10% Pt catalysts. Consequently, the NO_x conversion decreased at 300°C over these catalysts because there is no reductant left to initiate NO_x reduction on the surface of the catalyst. In comparison, the C_3H_6 conversion over the 10% Rh catalyst is 13%. For all the catalysts except Ag/Al_2O_3 and 10% Rh, the C_3H_6 is completely consumed at 400°C.

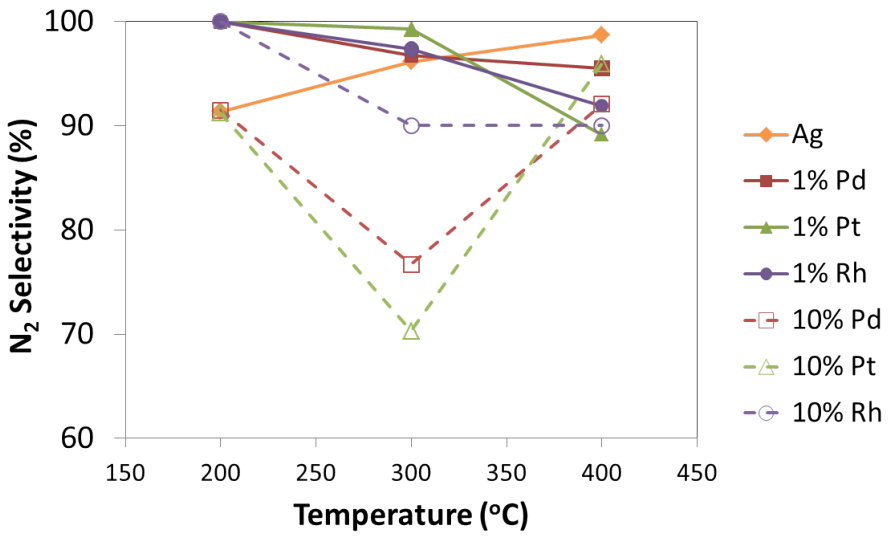

Figure 3.3: Effect of metal loading on N_2 selectivity for the monometallic catalyst supported on γ-Al_2O_3.The feed consisted of 600 ppm NO, 800 ppm CO, 3200 ppm H_2, 1800 ppm C_3H_6, 4% CO_2, 10% O_2, and 4% H_2O, with Ar as the balance gas.

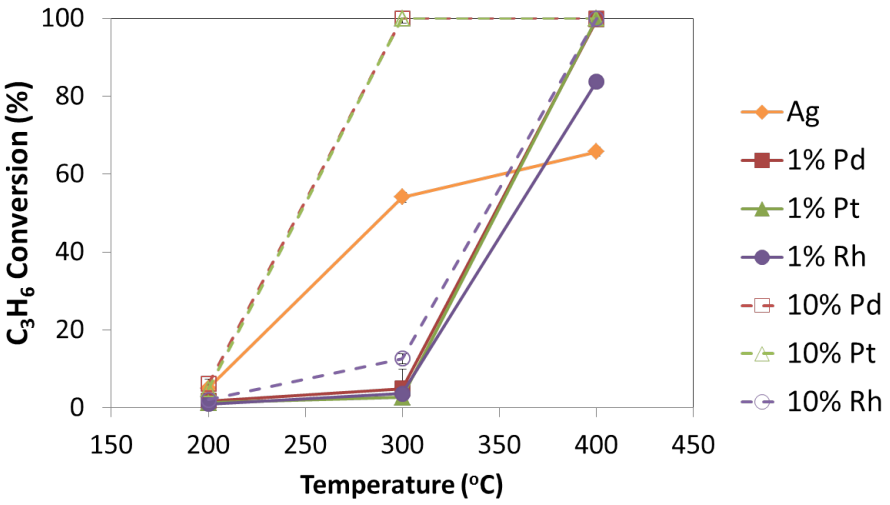

Figure 3.4: Effect of metal loading on C_3H_6 conversion for the monometallic catalysts supported on γ-Al_2O_3. The feed consisted of 600 ppm NO, 800 ppm CO, 3200 ppm H_2, 1800 ppm C_3H_6, 4% CO_2, 10% O_2, and 4% H_2O, with Ar as the balance gas.

3.4.3.2 HC-SCR Activity for Bimetallic Catalysts

The monometallic platinum group metal catalysts exhibited lower performance for NO_x conversion compared with Ag/Al_2O_3. Nevertheless, having both platinum group metal and Ag on the surface may result in improved performance for NO_x conversion. Based on this hypothesis, bimetallic catalysts were prepared through sequential dry impregnation, with the Ag precursor added before the platinum group metal precursor. Figure 3.5 illustrates the NO_x conversion performance for the bimetallic catalysts. At 200°C, the NO_x conversion over Ag/Al_2O_3 was 18%, and addition of 1% atomic loading of the platinum group metal onto the Ag/Al_2O_3 did not modify the NO_x conversion appreciably. The addition of 10% metal loading resulted in a decrease of about 7% over the Pt bimetallic catalyst at 200°C, but the conversions over the Pd and Rh bimetallic catalysts did not change significantly. At 300°C, the conversion over Ag/Al_2O_3 increased to 92%. Addition of 1% of the platinum group resulted in a slight increase in the conversion. This behavior was also observed by Wang *et al.* [20]. Addition of 10% of the platinum group metal resulted in a 10% decrease for the Pt and Rh bimetallic catalysts, but the conversion over the Pd bimetallic catalyst decreased nearly 60%. As described by Burch and Millington, Pd/Al_2O_3 has the most narrow temperature window and smallest maximum conversion of the three platinum group metals studied in this work [21]. It is possible that complete combustion of the C_3H_6 occurred at a much earlier temperature for Pd compared to Pt and Rh. Assuming that the platinum group metals did not interact with Ag, this behavior may explain the greater decrease in the NO_x conversion over the 10% Pd bimetallic catalyst compared with the Pt and Rh bimetallic catalysts. At 400°C, Ag/Al_2O_3, the Ag-1% Pd/Al_2O_3, and the Ag-1% Pt/Al_2O_3 maintain their activity. However, when 1% Rh is added, the conversion decreases to 69%. It is likely that the Rh became active for combustion at this temperature and began to unselectively consume C_3H_6. At 10% platinum group metal loading, the conversions for all the bimetallic catalysts

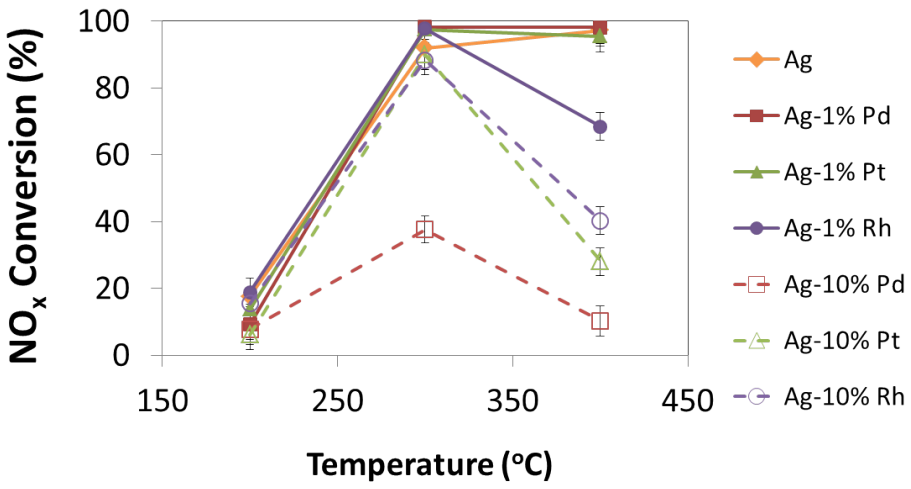

Figure 3.5: Effect of second metal loading on NO_x conversion for the bimetallic catalysts supported on γ-Al_2O_3. The feed consisted of 600 ppm NO, 800 ppm CO, 3200 ppm H_2, 1800 ppm C_3H_6, 4% CO_2, 10% O_2, and 4% H_2O, with Ar as the balance gas.

significantly decreased. The detrimental effect may be due to site blocking of the Ag or to an increased extent of unselective combustion of C_3H_6 due to the increased amount of metal on the surface.

Figure 3.6 illustrates the N_2 selectivity for the bimetallic catalysts. At 200°C, Ag/Al_2O_3 achieved 91% selectivity to N_2. Addition a second metal resulted in a slight increase in the selectivity. As temperature increased, the selectivity increased over the Ag/Al_2O_3 and the 1% bimetallic catalysts. However, when the loading of the platinum group metal was increased to 10%, the selectivity decreased. For platinum group metals, the greatest extent of N_2O formation happens between the FWHM temperature range for the NO_x conversion. Burch and Millington determined that for a 1% Rh/Al_2O_3, the range is in between 325°C - 400°C. In this temperature range, the extent of NO dissociation on the surface is at a minimum. The non-dissociated NO reacts with adsorbed N-atoms to form N_2O which then desorbs from the surface [8].

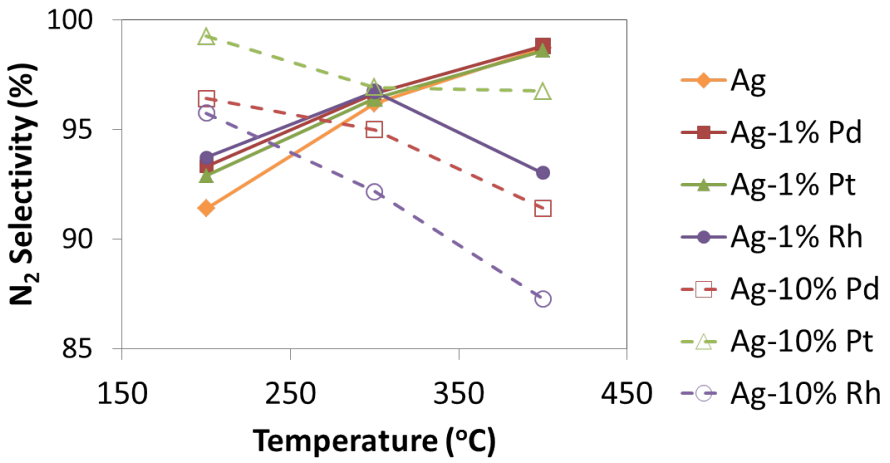

Figure 3.6: Effect of second metal loading on N_2 selectivity for the bimetallic catalysts supported on γ-Al_2O_3. The feed consisted of 600 ppm NO, 800 ppm CO, 3200 ppm H_2, 1800 ppm C_3H_6, 4% CO_2, 10% O_2, and 4% H_2O, with Ar as the balance gas.

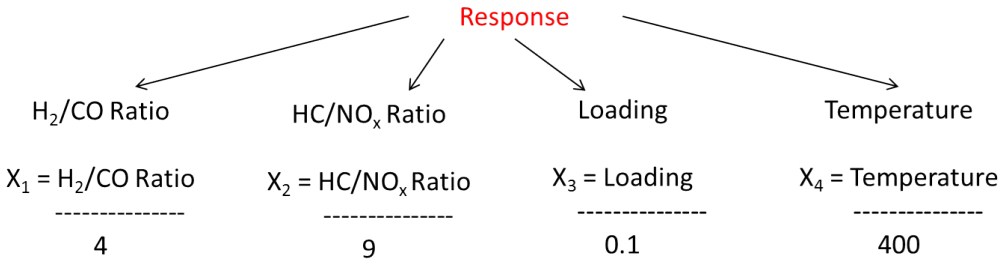

Figure 3.7: Illustration for the normalization of factor values.

3.4.4 Analysis of Experimental Design

3.4.4.1 NO_x Conversion

A 3^5 full factorial design was conducted and analyzed with the factors and levels listed in Table 3.2. The levels for the HC/NO_x ratio, H_2/CO ratio, second metal loading, and reaction temperature were normalized by dividing all factor levels by the largest factor level. Figure 3.7 illustrates the normalized factor level values used in this work. Tables 3.5, 3.6, 3.7, and 3.8 list the actual and normalized factor level values. The response values were normalized from 0 to 1.

The main effect plot and p-values for NO_x conversion are shown in Figure 3.8.

Table 3.5: Actual and normalized HC/NO_x ratio level values.

Actual Values	Normalized Values
3	0.33
6	0.66
9	1.00

Table 3.6: Actual and normalized H_2/CO ratio level values.

Actual Values	Normalized Values
0	0.00
2	0.50
4	1.00

Table 3.7: Actual and normalized second metal loading level values.

Actual Values	Normalized Values
0%	0.00
1%	0.10
10%	1.00

Table 3.8: Actual and normalized reaction temperature level values.

Actual Values	Normalized Values
200°C	0.50
300°C	0.75
400°C	1.00

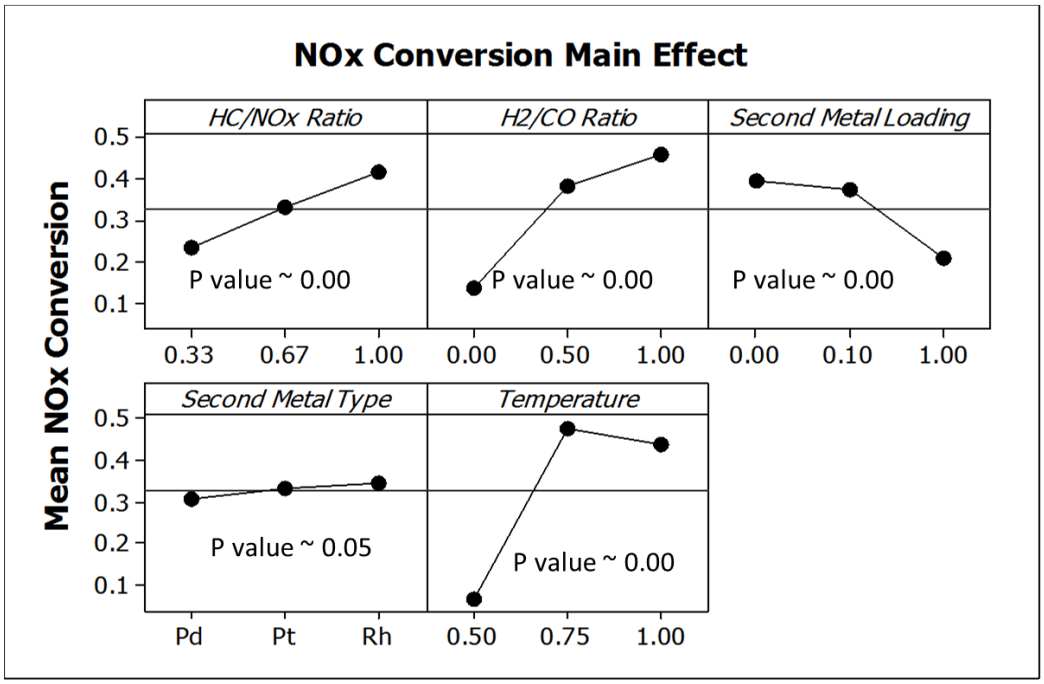

Figure 3.8: Main Effects for NO_x conversion. The standard error on the points is 1.3 units.

Based on the p-values, all the effects were significant. The trends showed that increasing HC/NO_x ratio, H_2/CO ratio, and reaction temperature all improved the NO_x conversion. However, the effect of second metal loading resulted in a detrimental effect on NO_x conversion, especially at high loadings. Also, the Pd bimetallic catalysts on average performed slightly worse than the Pt and Rh bimetallic catalysts. Burch and Millington observed that of the three platinum group metals, Pd was the least active for NO_x conversion [8]. Comparison of the Ag/Al_2O_3 and low-loading bimetallic catalysts yielded some notable results. Multiple papers have stated that a small amount of Pt improved the NO_x conversion [20, 22]. It was hypothesized that the overall NO_x conversion over Ag/Al_2O_3 would improve when platinum group metals were added to the surface because platinum group metals can reduce NO_x using H_2 and CO. This behavior was not observed in this study, as the NO_x conversion at high loadings decreased over all the bimetallic catalysts.

To illustrate other possible factors' influences on the second metal loading, the plots for significant interactions involving second metal loading are shown in Figure 3.9. The interactions of second metal loading with the HC/NO_x ratio and H_2/CO ratio showed that regardless of the amount of hydrocarbon or H_2, the NO_x conversion decreased with increasing loading. The most notable interactions are observed with the second metal type and reaction temperature. For the Pd and Pt bimetallic catalysts, the NO_x conversion did not change significantly at low loadings. However, at high loadings, the NO_x conversion decreased by approximately 30% for Pd and 20% for Pt. For the Rh bimetallic catalysts, the NO_x conversion decreased with the presence of the metal. However, the NO_x and C_3H_6 conversions at low and high loadings were identical. Hence on average, the decrease in NO_x conversion due to the second metal loading is observed on the Pd and Pt bimetallic catalysts. Concerning temperature, the NO_x conversion at 200°C was nearly identical at all loadings. However, at 300°C and 400°C, the NO_x conversion was significantly less at the high loadings compared to low loadings. In summary, the detrimental effect of NO_x conversion due to second metal loading is observed at temperatures of 300°C and higher over Pd and Pt bimetallic catalysts.

Concerning the factor of second metal type, the second metal loading and reaction temperature interactions were significant. The interactions are depicted in Figure 3.10. The interaction between the second metal type and reaction temperature showed that there is a significant difference in the NO_x conversion at 300°C. The average NO_x conversions over the Pd, Pt, and Rh bimetallic catalysts were 42%, 49%, and 54% respectively.

Table 3.9 displays the mean squares and p-values for NO_x conversion. The higher the value of the mean square, the more variance can be explained by the factor. Therein, the factor is responsible for a larger deviation from the proposed model. The reaction temperature and H_2/CO ratio were the most influential main effects,

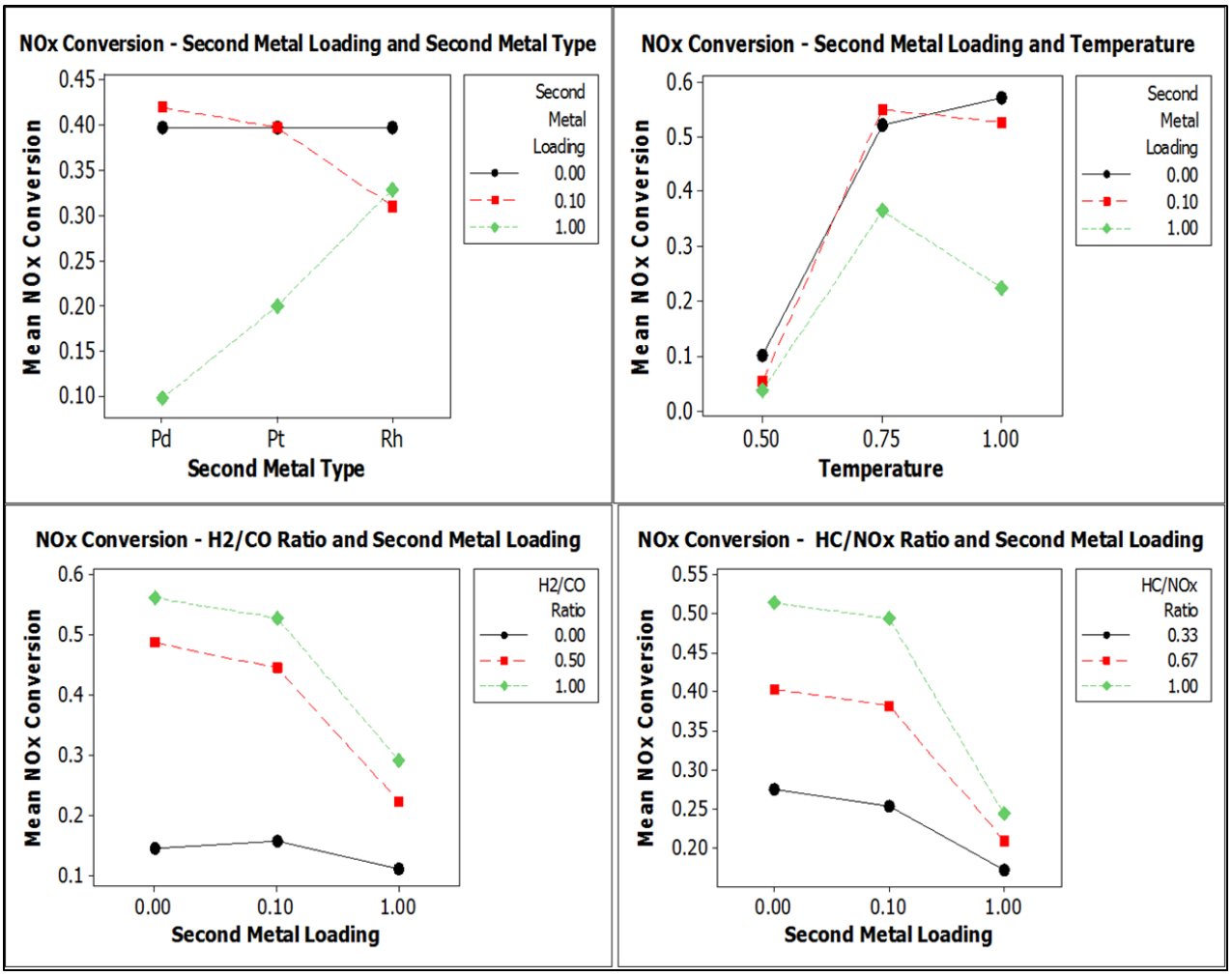

Figure 3.9: Significant interaction effects involving second metal loading for NO_x conversion. The standard error on the points is 2.3 units.

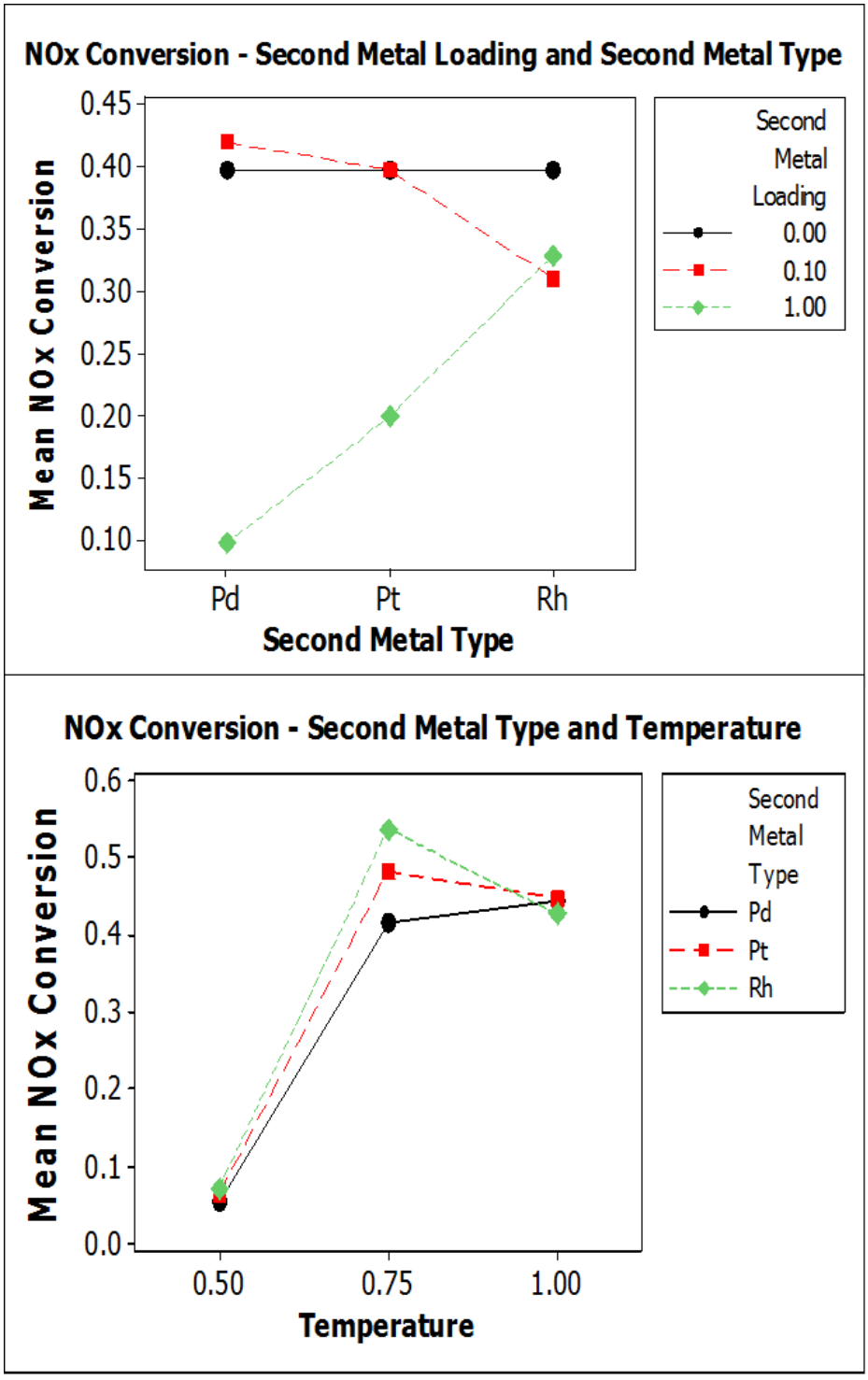

Figure 3.10: Significant interaction effects involving second metal type for NO_x conversion. The standard error on the points is 2.3 units.

Table 3.9: Significant factors and mean squares coefficients for NO_x conversion. The R-squared value was 0.9, suggesting the variance was well-captured by the main effects and 2-factor interaction effects.

Effect	Mean Square Coefficients	P-value
Temperature	31990	0.000
H_2/CO Ratio	16020	0.000
H_2/CO Ratio*Temperature	5855	0.000
Second Metal Loading	5802	0.000
HC/NO_x Ratio	5116	0.000
Second Metal Loading*Temperature	1811	0.000
HC/NO_x Ratio*Temperature	1697	0.000
Second Metal Loading*Second Metal Type	1055	0.000
HC/NO_x Ratio*Second Metal Loading	615.2	0.000
H_2/CO Ratio*Second Metal Loading	567.1	0.000
HC/NO_x Ratio*H_2/CO Ratio	469.4	0.001
Second Metal Type	379.9	0.022
HC/NO_x Ratio*Second Metal Type	305.9	0.016

and the interaction between reaction temperature and the H_2/CO ratio was the most influential interaction effect.

3.4.4.2 N_2 Selectivity

The main effect plot and p-values for N_2 selectivity are shown in Figure 3.11. Like the NO_x conversion, the presence of H_2 is required for the reaction to occur at lower temperatures. Thus, when the reaction begins, N_2 is produced. The presence of the platinum group metals on Ag/Al_2O_3 results in a similar trend. Concerning the second metal loading, the data shows that an increase in the platinum group metal concentration results in an increase in the N_2O formation, and therefore a decrease in the N_2 selectivity.

Figure 3.12 shows the significant interactions for N_2 selectivity related to second metal loading and second metal type. For Pd and Pt bimetallic catalysts, as the second metal loading increases, the selectivity to N_2 decreases. This decrease is likely due to the formation of N_2O caused by the presence of the platinum group metals. The Rh bimetallic catalysts behave differently in that the selectivity increases

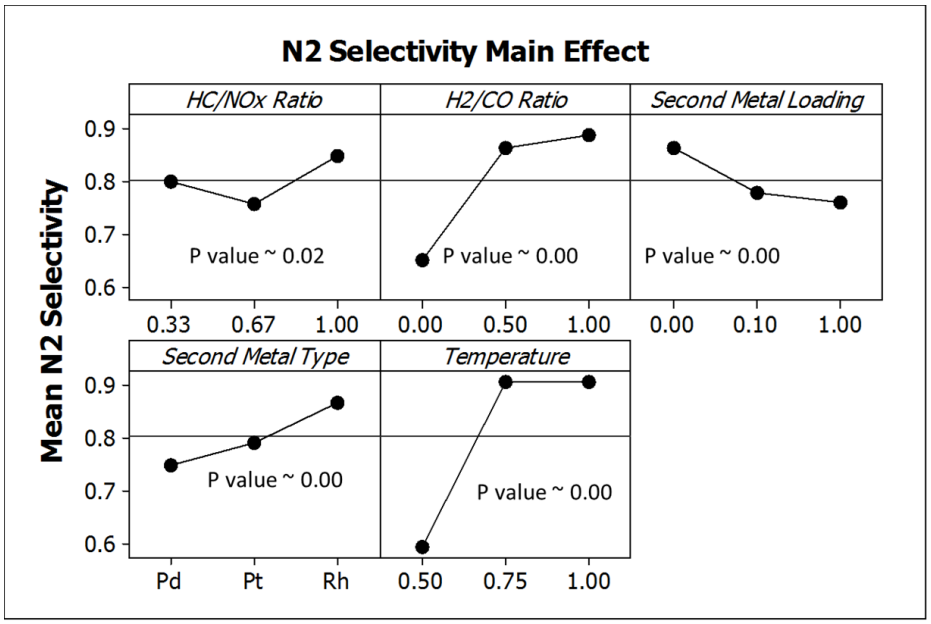

Figure 3.11: Main Effects for N_2 selectivity. The standard error on the points is 2.1 units.

dramatically at high loadings. This increase may be due to the observation that the Rh bimetallic catalysts are slightly more active for NO_x conversion compared to Pd and Pt bimetallic catalysts. The slight increase in activity is only observed at 200°C. The increase in NO_x conversion over the Rh bimetallic catalysts likely corresponds with the increase in selectivity to N_2 as shown in the interaction between metal type and reaction temperature.

Table 3.10 displays the mean squares and ANOVA p-values for N_2 selectivity. Similarly to the NO_x conversion, the reaction temperature and the H_2/CO ratio were the most influential main effects, and the interaction between reaction temperature and H_2/CO ratio was the most influential interaction effect.

3.4.5 Loading Order

3.4.5.1 Introduction

Because of the observed lack of improvement in the performance of the tested catalysts for NO_x reduction, the effect of loading order was studied. It was believed that

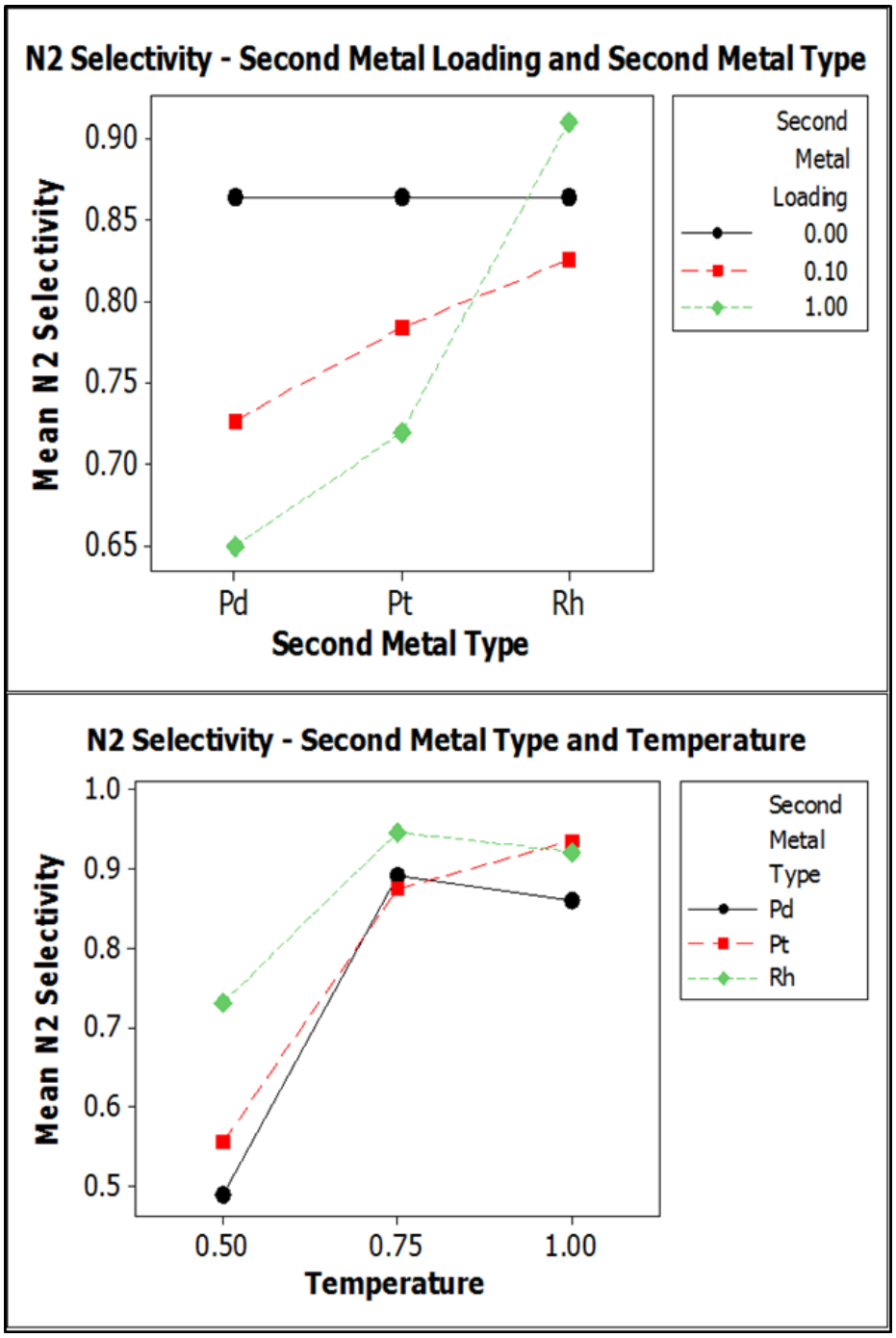

Figure 3.12: Significant interaction effects involving metal loading and metal type for N_2 selectivity. The standard error on the points is 3.6 units.

Table 3.10: Significant factors and mean squares coefficients for N_2 selectivity. The R-squared value was 0.86, suggesting the variance was well-captured by the main effects and 2-factor interaction effects.

Effect	Mean Square Coefficients	P-value
Temperature	22750	0.000
H_2/CO Ratio	12310	0.000
H_2/CO Ratio*Temperature	7899	0.000
Second Metal Type	3517	0.000
Second Metal Loading*Second Metal Type	3145	0.000
H_2/CO Ratio*Second Metal Loading	2300	0.000
Second Metal Loading	1888	0.001
HC/NO_x Ratio*Temperature	1697	0.000
HC/NO_x Ratio*Second Metal Type	1127	0.001
HC/NO_x Ratio	1037	0.014
HC/NO_x Ratio*Second Metal Loading	696.9	0.000
HC/NO_x Ratio*H_2/CO Ratio	602.6	0.001

by adding the Ag precursor after the platinum group metal precursor, the catalysts formed would consist of a surface with more exposed Ag surface atoms. Therein, the extent of NO_x reduction would likely be enhanced. Sato *et al.* added small amounts of Rh to a Ag/Al_2O_3 catalyst and studied the effect of the order. They found that impregnating the Ag after the Rh improved NO_x reduction compared to adding Ag first [23]. They attributed this effect to the presence of larger amounts of Ag clusters, which were the catalytic active species responsible for the formation of isocyanate species (-NCO), one of the key reaction intermediates in the NO_x reduction mechanism. Shu *et al.* studied the effect of loading order for bimetallic Pt-Ni mixtures for hydrogenation activity and selectivity. They used the disproportionation activity of cyclohexene and the hydrogenation selectivity of acetylene in ethylene as probe reactions to compare the effect of the impregnation sequence. The bimetallic Pt/Ni catalysts showed significantly higher activity toward the disproportionation of cyclohexene than either Pt/Al_2O_3 or Ni/Al_2O_3. The effect varied as the metal ratio of Pt to Ni changed [24]. Ren *et al.* studied the effect of the addition of Zn on the catalytic activity of a Co/HZSM-5 catalyst for the SCR of NO_x with CH_4. They

found that when Co was added first, the activity improved compared to when Zn was added first. However, the selectivity increased when the orders were switched. The co-impregnation method was better than both sequential impregnations [25]. These studies illustrate the complexity of the development of a highly active catalyst due to preparation methods.

The platinum group metal was loaded onto the support before adding the Ag metal precursor. Between each impregnation the samples were dried in a Fisher Scientific vacuum oven at a pressure of -30 mm Hg at 100°C for 8-12 hours and calcined in 90 cm^3/minute of dry-grade air in a horizontal quartz tube furnace at 600°C for 3 hours.. An ANOVA analysis was performed in which the loading order was added as an extra factor in addition to the other five factors employed in the full factorial analysis described previously.

3.4.5.2 Surface Area/Elemental Analysis

Table 3.11 shows the BET surface areas and metal loadings for the Ag second-loaded catalysts. Surface areas and elemental loadings were very similar among the catalysts and to their Ag-first counterparts.

3.4.6 Crystalline Structure

Figure 3.13 shows the diffraction patterns for the Ag-second loaded catalysts. Similar to the Ag-first loaded catalysts, the presence of γ-Al_2O_3 was visible with peaks at 39°, 46°, and 67°. Any peaks corresponding to the metal were not present, indicating that the metal particles were likely again well dispersed on the support.

3.4.6.1 NO_x Conversion

The effect of loading order on the conversion of NO_x is shown in the main effect plot displayed in Figure 3.14. The average NO_x conversion for the Ag-first loaded

Table 3.11: Surface areas and metal loadings for the Ag second-loaded catalysts.

Catalyst	Target Metal Loading	Actual Metal Loading	Surface Area (m^2/g)
Al_2O_3	-	-	67 ± 3
Ag/Al_2O_3	2.00% Ag	1.55 ± 0.03% Ag	58 ± 3
1% Pd-Ag/Al_2O_3	2.00% Ag, 0.02% Pd	1.78 ± 0.01% Ag, 0.01 ± 0.001% Pd	56 ± 3
1% Pt-Ag/Al_2O_3	2.00% Ag, 0.04% Pt	1.87 ± 0.02% Ag, 0.02 ± 0.003% Pt	56 ± 3
1% Rh-Ag/Al_2O_3	2.00% Ag, 0.02% Rh	1.44 ± 0.03% Ag, 0.01 ± 0.001% Rh	57 ± 3
10% Pd-Ag/Al_2O_3	2.00% Ag, 0.20% Pd	1.70 ± 0.03% Ag, 0.17 ± 0.01% Pd	58 ± 3
10% Pt-Ag/Al_2O_3	2.00% Ag, 0.40% Pt	1.78 ± 0.03% Ag, 0.21 ± 0.01% Pt	59 ± 3
10% Rh-Ag/Al_2O_3	2.00% Ag, 0.20% Rh	2.04 ± 0.03% Ag, 0.13 ± 0.01% Rh	58 ± 3

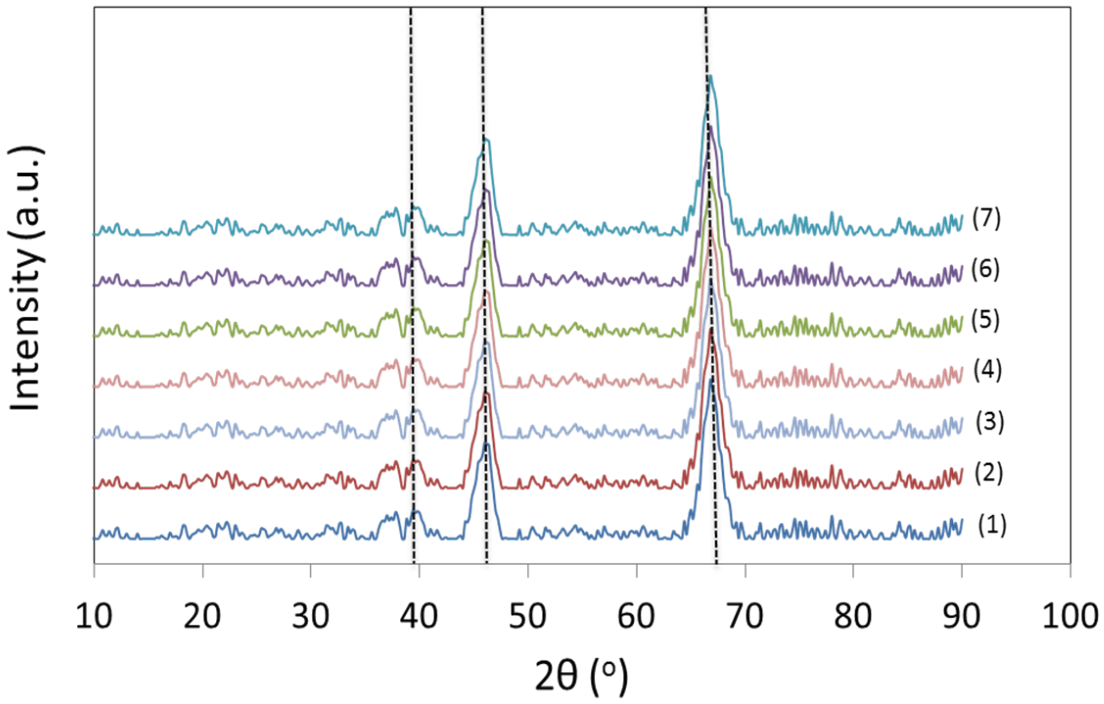

Figure 3.13: X-ray diffraction patterns for the Ag-second loaded catalysts. (1) Ag/Al_2O_3, (2) 1% Pd-Ag/Al_2O_3, (3) 1% Pt-Ag/Al_2O_3, (4) 1% Rh-Ag/Al_2O_3, (5) 10% Pd-Ag/Al_2O_3, (6) 10% Pt-Ag/Al_2O_3, (7) 10% Rh-Ag/Al_2O_3. The dotted lines correspond to the major peaks obtained in the γ-Al_2O_3 support.

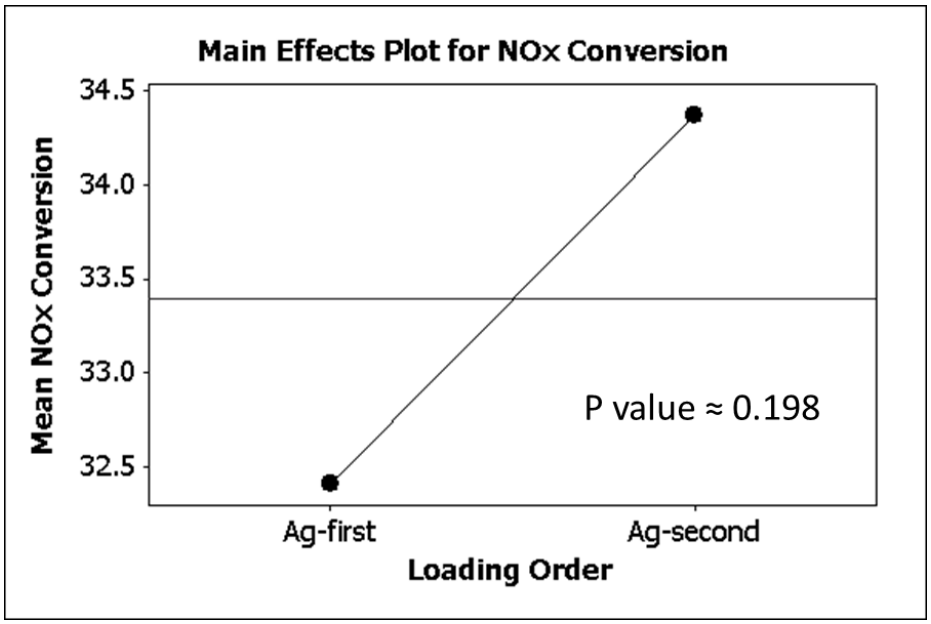

Figure 3.14: Main effect of loading order for NO_x conversion. The standard error on the points is 1.1 units.

catalysts was 32%, whereas the average NO_x conversion for the Ag-second loaded catalysts was 34%. The error was ± 1%, indicating that the conversion was the same regardless of the order of loading. This observation is also reflected in the ANOVA analysis, in which the p-value was 0.198, indicating that loading order itself was not a significant factor in affecting the NO_x conversion. However, the interaction between loading order and the second metal type was significant, as shown in Figure 3.15. The p-value was 0.023, indicating significance. The NO_x conversion performance of the Pt and Rh bimetallic catalysts did not vary with loading order. However, there was a significant increase in the NO_x conversion for the Pd bimetallic catalysts when Ag was loaded second.

3.4.6.2 N_2 Selectivity

The trends in N_2 selectivity follow the trends seen in the NO_x conversion. The effect of loading order on the selectivity to N_2 is shown in the main effect plot displayed in Figure 3.16. The average N_2 selectivity for the Ag-first loaded catalysts was 82%,

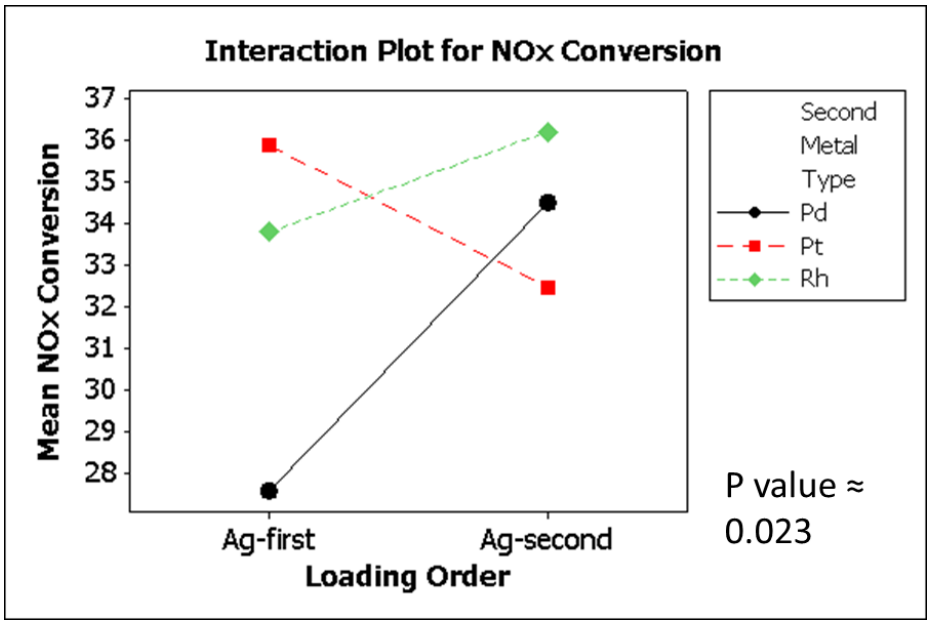

Figure 3.15: Interaction effect of NO_x conversion for loading order and second metal type. The standard error on the points is 1.8 units.

whereas the average N_2 selectivity for the Ag-second loaded catalysts was 83%. The error was ± 2%, indicating that the selectivity was the same regardless of the order of loading. The p-value was 0.639, indicating that loading order itself was not a significant factor in affecting the N_2 selectivity. The interaction between loading order and the metal type was significant, as shown in Figure 3.17. The p-value was 0.044, indicating significance. The N_2 selectivity performance of the Pt and Rh bimetallic catalysts did not vary with loading order. However, there was a significant increase in the N_2 selectivity for the Pd bimetallic catalysts when Ag was loaded second.

3.5 Conclusions

Five factors - HC/NO_x ratio, H_2/CO ratio, second metal loading, second metal type, and reaction temperature - were studied to determine the effects on NO_x conversion and N_2 selectivity. All main effects were statistically significant for NO_x conversion and N_2 selectivity. It was demonstrated that the addition of the platinum

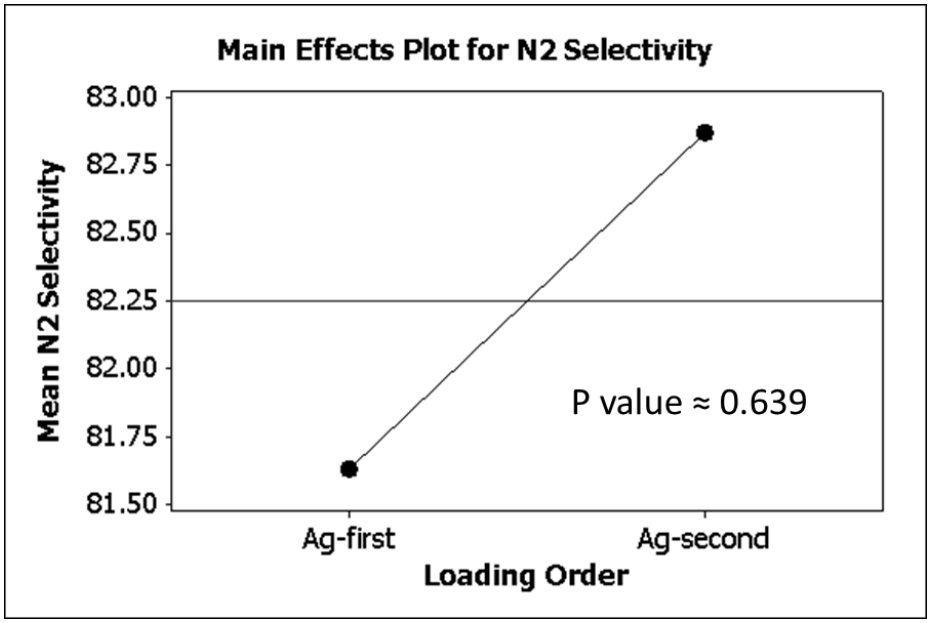

Figure 3.16: Main effect of loading order for N_2 selectivity. The standard error on the points is 1.9 units.

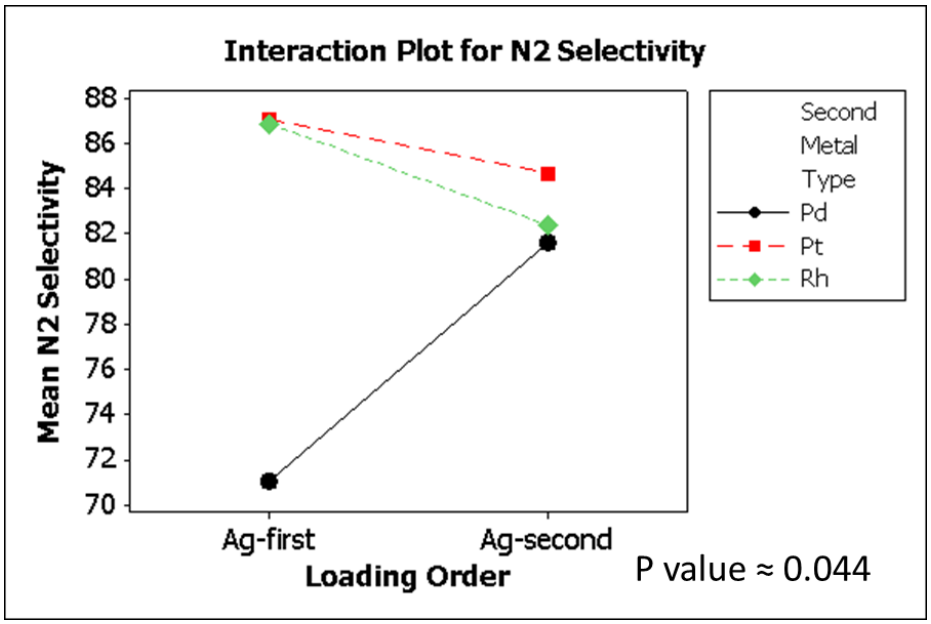

Figure 3.17: Interaction effect of N_2 selectivity for loading order and second metal type. The standard error on the points is 3.2 units.

group metal did not improve NO_x conversion or N_2 selectivity, contrary to the original hypothesis. Secondly, the second metal type was significant for NO_x conversion and N_2 selectivity. The Pd bimetallic catalysts performed worse than Pt and Rh bimetallic catalysts. For the N_2 selectivity, the Rh bimetallic catalysts performed better than the Pt and Pd bimetallic catalysts on average. All main effects were statistically significant for NO_x conversion and N_2 selectivity. In response to the detrimental effect by the second metal loading, the order of metal loading was reversed, in which the Ag metal precursor was added after the platinum group metal precursor. It was observed that the loading order alone did not have a significant effect on the NO_x conversion or N_2 selectivity. However, the interaction between the second metal type and loading order was significant for both NO_x conversion or N_2 selectivity. The Pd bimetallic catalyst behavior was the primary influence. The NO_x conversion and N_2 selectivity over the Pd bimetallic catalysts greatly improved when the Pd metal precursor was added first.

Bibliography

[1] R. Burch, J.P. Breen, and F.C. Meunier. A review of the selective reduction of NO_x with hydrocarbons under lean-burn conditions with non-zeolitic oxide and platinum group metal catalysts. *Applied Catalysis B: Environmental*, 39(4):283–303, 2002.

[2] Z. Liu and S.I. Woo. Recent advances in catalytic $DeNO_x$ science and technology. *Catalysis Reviews*, 48(1):43–89, 2006.

[3] T. Miyadera. Alumina-supported silver catalysts for the selective reduction of nitric oxide with propene and oxygen-containing organic compounds. *Applied Catalysis B: Environmental*, 2(2-3):199–205, 1993.

[4] T.E. Hoost, R.J. Kudla, K.M. Collins, and M.S. Chattha. Characterization of Ag/[gamma]-Al_2O_3 catalysts and their lean-NO_x properties. *Applied Catalysis B: Environmental*, 13(1):59–67, 1997.

[5] L.E. Lindfors, K. Eranen, F. Klingstedt, and D.Y. Murzin. Silver/alumina catalyst for selective catalytic reduction of NO_x to N_2 by hydrocarbons in diesel powered vehicles. *Topics in Catalysis*, 28(1):185–189, 2004.

[6] B. Wichterlova, P. Sazama, J.P. Breen, R. Burch, C.J. Hill, L. Capek, and Z. Sobalik. An *in situ* UV-vis and FTIR spectroscopy study of the effect of H_2 and CO during the selective catalytic reduction of nitrogen oxides over a silver alumina catalyst. *Journal of Catalysis*, 235(1):195–200, 2005.

[7] R. Burch, J.P. Breen, C.J. Hill, B. Krutzsch, B. Konrad, E. Jobson, L. Cider, K. Eranen, F. Klingstedt, and L.E. Lindfors. Exceptional activity for NO_x reduction at low temperatures using combinations of hydrogen and higher hydrocarbons on Ag/Al_2O_3 catalysts. *Topics in Catalysis*, 30(1-4):19–25, 2004.

[8] R. Burch and P.J. Millington. Selective reduction of NO_x by hydrocarbons in excess oxygen by alumina-and silica-supported catalysts. *Catalysis Today*, 29(1-4):37–42, 1996.

[9] N. Macleod and R.M. Lambert. An *in situ* DRIFTS study of efficient lean NO_x reduction with H_2 + CO over Pd/Al_2O_3: the key role of transient NCO formation in the subsequent generation of ammonia. *Applied Catalysis B: Environmental*, 46(3):483–495, 2003.

[10] T. Nakatsuji, T. Yamaguchi, N. Sato, and H. Ohno. A selective NO_x reduction on Rh-based catalysts in lean conditions using CO as a main reductant. *Applied Catalysis B: Environmental*, 85(1-2):61–70, 2008.

[11] G. Qi, R.T. Yang, and F.C. Rinaldi. Selective catalytic reduction of nitric oxide with hydrogen over Pd-based catalysts. *Journal of Catalysis*, 237(2):381–392, 2006.

[12] J.A. Anderson and M.F. Garcia. *Supported Metals in Catalysis*, volume 5. Imperial College Press London, 2005.

[13] J. Hagen. *Industrial Catalysis: A Practical Approach*. Wiley-VCH, 2006.

[14] Robert Hammerle. Urea SCR and DPF system for diesel sport utility vehicle meeting Tier II Bin 5. `http://www1.eere.energy.gov/vehiclesandfuels/pdfs/deer_2002/session10/2002_deer_hammerle.pdf`, August 2002.

[15] C.L. DiMaggio, G.B. Fisher, K.M. Rahmoeller, and M. Sellnau. Dual SCR aftertreatment for lean NO_x reduction. *SAE Technical Paper*, pages 01–0277, 2009.

[16] J. Shibata, M. Hashimoto, K. Shimizu, H. Yoshida, T. Hattori, and A. Satsuma. Factors controlling activity and selectivity for SCR of NO by hydrogen over supported platinum catalysts. *The Journal of Physical Chemistry B*, 108(47):18327–18335, 2004.

[17] Y.W. Lee and E. Gulari. Improved performance of NO_x reduction by H_2 and CO over a Pd/Al_2O_3 catalyst at low temperatures under lean-burn conditions. *Catalysis Communications*, 5(9):499–503, 2004.

[18] S. Roy, M.S. Hegde, S. Sharma, N.P. Lalla, A. Marimuthu, and G. Madras. Low temperature NO_x and N_2O reduction by H_2: Mechanism and development of new nano-catalysts. *Applied Catalysis B: Environmental*, 84(3-4):341–350, 2008.

[19] K.A. Bethke and H.H. Kung. Supported Ag catalysts for the lean reduction of NO with C_3H_6. *Journal of Catalysis*, 172(1):93–102, 1997.

[20] J. Wang, H. He, Q. Feng, Y. Yu, and K. Yoshida. Selective catalytic reduction of NO_x by C_3H_6 over Ag/Al_2O_3 catalyst with a small quantity of noble metal. *Catalysis Today*, 93:783–789, 2004.

[21] R. Burch, P.J. Millington, and A.P. Walker. Mechanism of the selective reduction of nitrogen monoxide on platinum-based catalysts in the presence of excess oxygen. *Applied Catalysis B: Environmental*, 4(1):65–94, 1994.

[22] H. He, J. Wang, Q. Feng, Y. Yu, and K. Yoshida. Novel Pd promoted Ag/Al_2O_3 catalyst for the selective reduction of NO_x. *Applied Catalysis B: Environmental*, 46(2):365–370, 2003.

[23] K. Sato, T. Yoshinari, Y. Kintaichi, M. Haneda, and H. Hamada. Rh-post-doped Ag/Al_2O_3 as a highly active catalyst for the selective reduction of NO with decane. *Catalysis Communications*, 4(7):315–319, 2003.

[24] Y. Shu, L.E. Murillo, J.P. Bosco, W. Huang, A.I. Frenkel, and J.G. Chen. The effect of impregnation sequence on the hydrogenation activity and selectivity of supported Pt/Ni bimetallic catalysts. *Applied Catalysis A: General*, 339(2):169–179, 2008.

[25] L. Ren, T. Zhang, D. Liang, C. Xu, J. Tang, and L. Lin. Effect of addition of Zn on the catalytic activity of a Co/HZSM-5 catalyst for the SCR of NO_x with CH_4. *Applied Catalysis B: Environmental*, 35(4):317–321, 2002.

CHAPTER IV

Characterization of Silver-Based Catalysts for the Reformate-Assisted Selective Catalytic Reduction of NO_x

4.1 Summary

In the previous chapter, a full factorial design was conducted to determine the effect of HC/NO_x ratio, H_2/CO ratio, second metal loading, second metal type, and reaction temperature on the NO_x conversion and N_2 selectivity. The effect of loading order was also analyzed. Increasing the second metal loading inhibited the NO_x conversion and N_2 selectivity. The NO_x conversion and N_2 selectivity were different between the platinum group metals. The NO_x conversion over the Pd bimetallic catalysts was marginally worse compared to the Pt and Rh bimetallic catalysts. In contrast, the Pd bimetallic catalysts were significantly worse for N_2 selectivity. Loading order was a significant factor for the Pd bimetallic catalysts. The NO_x conversion and N_2 selectivity performances improved when the Pd precursor was added before the Ag precursor. In this chapter, the observed trends are explained using various characterization techniques such as TPR and chemisorption of H_2 and O_2.

4.2 Introduction

It was hypothesized that NO_x reduction over Ag/Al_2O_3 could be improved at temperatures below 400°C by combining two modifications: (1) adding H_2 to the exhaust mixture and (2) impregnating Pd, Pt, or Rh onto the Ag/Al_2O_3. The presence of H_2 results in a significant decrease in the temperature at which the hydrocarbon reductant begins to react. Therein, the reaction NO_x begins to react at the same temperature [1–4]. Pd, Pt, and Rh-supported catalysts have exhibited activity for lean NO_x reduction on a number of supports [5–8]. Unlike Ag/Al_2O_3 without H_2, the platinum group metals are active below 400°C [5]. However, these metals also produce significant amounts of N_2O. Nevertheless, literature exists that details the improvement in NO_x reduction when a small amount of a platinum group metal is applied onto an Ag/Al_2O_3 catalyst [9, 10]. The improvement is minuscule however, and was only observed at temperatures above 400°C.

4.3 Experimental

4.3.1 Catalyst Characterization

For TPR experiments, approximately 150 mg of the catalyst was loaded into a U-tube reactor and heated from 25°C to 500°C at 40°C/min in a mixture of 10% H_2/Ar flowing at 90 mL/min. H_2 consumption was monitored using a thermal conductivity detector (TCD). For chemisorption, approximately 150 mg of the catalyst was first oxidized in air at 600°C for 1 hour, reduced in a mixture of 10% H_2/Ar at 250°C for 2 hours, degassed in an inert gas at 300°C for 30 minutes, and cooled to the desired temperature. Measurements for the Pt and Rh bimetallic catalysts were taken at ambient temperature, and Pd bimetallic catalytic measurements were taken at 70°C. This temperature was selected to avoid formation of Pd hydride [11, 12]. 20-30 pulses of 10% H_2/Ar or 1% O_2/He were then pulsed onto the catalyst surface until saturation

was reached. The loop size used was 300 μL.

4.4 Effect of Loading

4.4.1 NO_x Conversion

The detrimental effect on NO_x conversion with increasing second metal loading is possibly due to (1) the onset of the unselective combustion of the C_3H_6 to CO_2, and/or (2) site blocking of Ag sites by the noble metals. Figure 4.1 displays the NO_x and C_3H_6 conversions for Ag/Al_2O_3 and the bimetallic catalysts at 300°C. The conversion of NO_x over Ag/Al_2O_3 was 90%, with nearly 60% of the C_3H_6 being utilized. At high loadings, the extent of conversion to C_3H_6 increased to 100%, yet the NO_x conversion decreased significantly compared to Ag/Al_2O_3 and the low-loading catalysts. The behavior indicated that as the second metal loading was increased, unselective combustion of the C_3H_6 to CO_2 became dominant. Once the C_3H_6 reductant was used up, the NO_x conversion subsequently began to decline.

Another potential cause of the detrimental effect of second metal loading on NO_x conversion is site blocking. Because the noble metals were loaded after the Ag, some of the Ag sites could be covered by the noble metals. Chemisorption of O_2 was conducted to probe the surface of the catalysts. Table 4.1 lists the O_2 uptakes and dispersions for the bimetallic catalysts. The dispersion of Ag on the Ag/Al_2O_3 catalyst was not high, possibly due to the low surface area of the Al_2O_3 support. The presence of the noble metal did not result in a significant change in the O_2 uptake of the Ag. This observation signified that although there may be some covering of the Ag by noble metals, the significance of the effect was very small compared to the unselective combustion of C_3H_6.

The detrimental effect of second metal loading on NO_x conversion was not uniform across all the catalysts, as was shown in the interaction plots in Chapter 3. At low

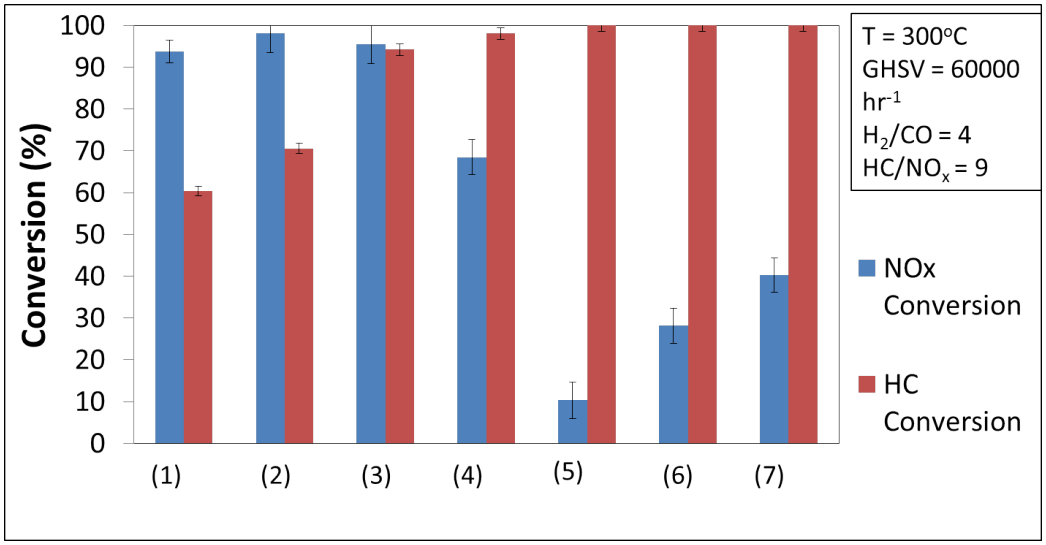

Figure 4.1: NO_x and C_3H_6 conversion for Ag/Al_2O_3 and the bimetallic catalysts. The HC/NO_x ratio and H_2/CO ratio are listed. The inlet H_2 concentration is 3200 ppm and the inlet C_3H_6 concentration is 1800 ppm. (1) Ag/Al_2O_3, (2) Ag-1% Pd/Al_2O_3, (3) Ag-1% Pt/Al_2O_3, (4) Ag-1% Rh/Al_2O_3, (5) Ag-10% Pd/Al_2O_3, (6) Ag-10% Pt/Al_2O_3, (7) Ag-10% Rh/Al_2O_3.

Table 4.1: O_2 uptakes and theoretical Ag dispersions for the Ag/Al_2O_3 and Ag-first bimetallic catalysts.

Catalyst	O_2 uptake (μmol/g)	Theoretical Ag Dispersion (%)
Ag/Al_2O_3	2 ± 1	2
Ag-10% Pd/Al_2O_3	1 ± 0	1
Ag-10% Pt/Al_2O_3	1 ± 0	2
Ag-10% Rh/Al_2O_3	3 ± 1	4

loadings, the Pd and Pt bimetallic catalysts performed similarly to the Ag/Al_2O_3. To attempt to explain these observations, interaction plots of loading with the HC/NO_x ratio, H_2/CO ratio, and reaction temperature were made with the data points from the loading levels of 0% (Ag/Al_2O_3) and 1% second metal loading. Figure 4.2 displays the plots for the Pd bimetallic catalysts. The largest change in the NO_x conversion was observed when comparing the Ag/Al_2O_3 to the low loading Pd bimetallic catalysts at 400°C. At this temperature, the conversion increased from 57% to 67% when a small amount of Pd was added onto the Ag/Al_2O_3 catalyst. The Ag/Al_2O_3 performed better at 200°C, but the overall NO_x conversion was negligible at this temperature. The same plots were developed to compare Ag/Al_2O_3 to the 1% Pt bimetallic catalysts and are shown in Figure 4.3. For all interactions, there were no significant differences between the Ag/Al_2O_3 and low loading Pt bimetallic catalysts. This behavior was also observed by Wang *et al.* in their study of HC-SCR using Ag-noble metal bimetallic catalysts. Although the most significant improvements were observed at temperatures above 400°C for the Pd bimetallic catalyst (they did not observe the same improvement for the Pt), they observed modest improvement in the NO_x conversion for both Pd and Pt bimetallic catlaysts between 200°C and 400°C. In this study, the presence of H_2 improved the overall NO_x conversions between all the catalysts between 200°C and 400°C. Wang *et al.* attributed the improvement of the NO_x conversion to the formation of a surface enolic species through the partial oxidation of C_3H_6 catalyzed by the platingum group metal. The species is very reactive for the formation of surface nitrates (NO_3^-) which form the isocyanate intermediate (-NCO). The formation isocyanate is widely accepted as the rate-determing step in the mechanism for NO_x reduction over Ag/Al_2O_3 [9].

At high loadings, the NO_x conversions over the Pd and Pt bimetallic catalysts decreased significantly compared to Ag/Al_2O_3. As shown in Figure 4.1, the C_3H_6 is completely converted to CO_2 and the NO_x conversion consequently declined over

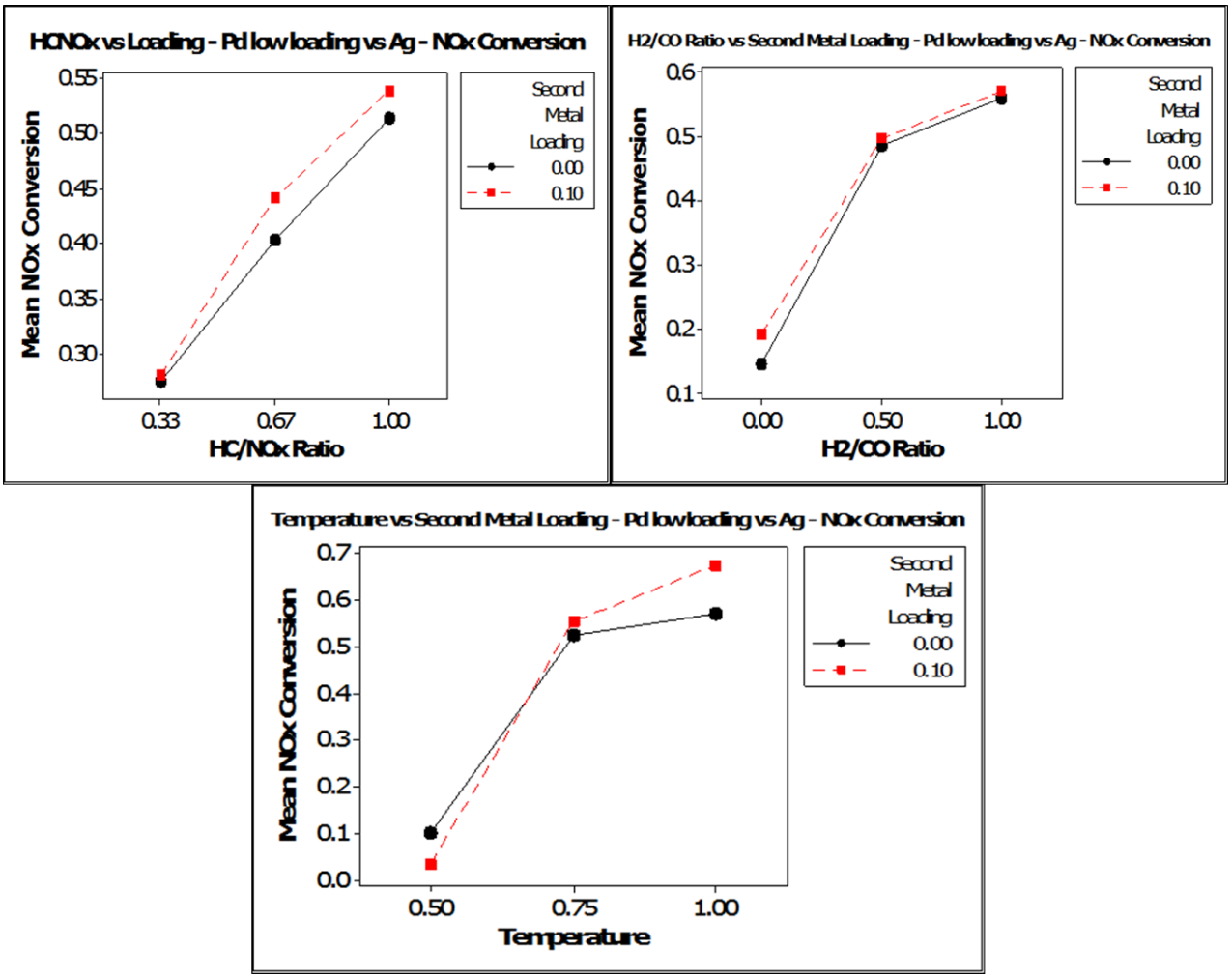

Figure 4.2: Interaction plots of the pure Ag and 1% Pd bimetallic catalysts for NO_x conversion for HC/NO_x ratio, H_2/CO ratio, and reaction temperature with second metal loading.

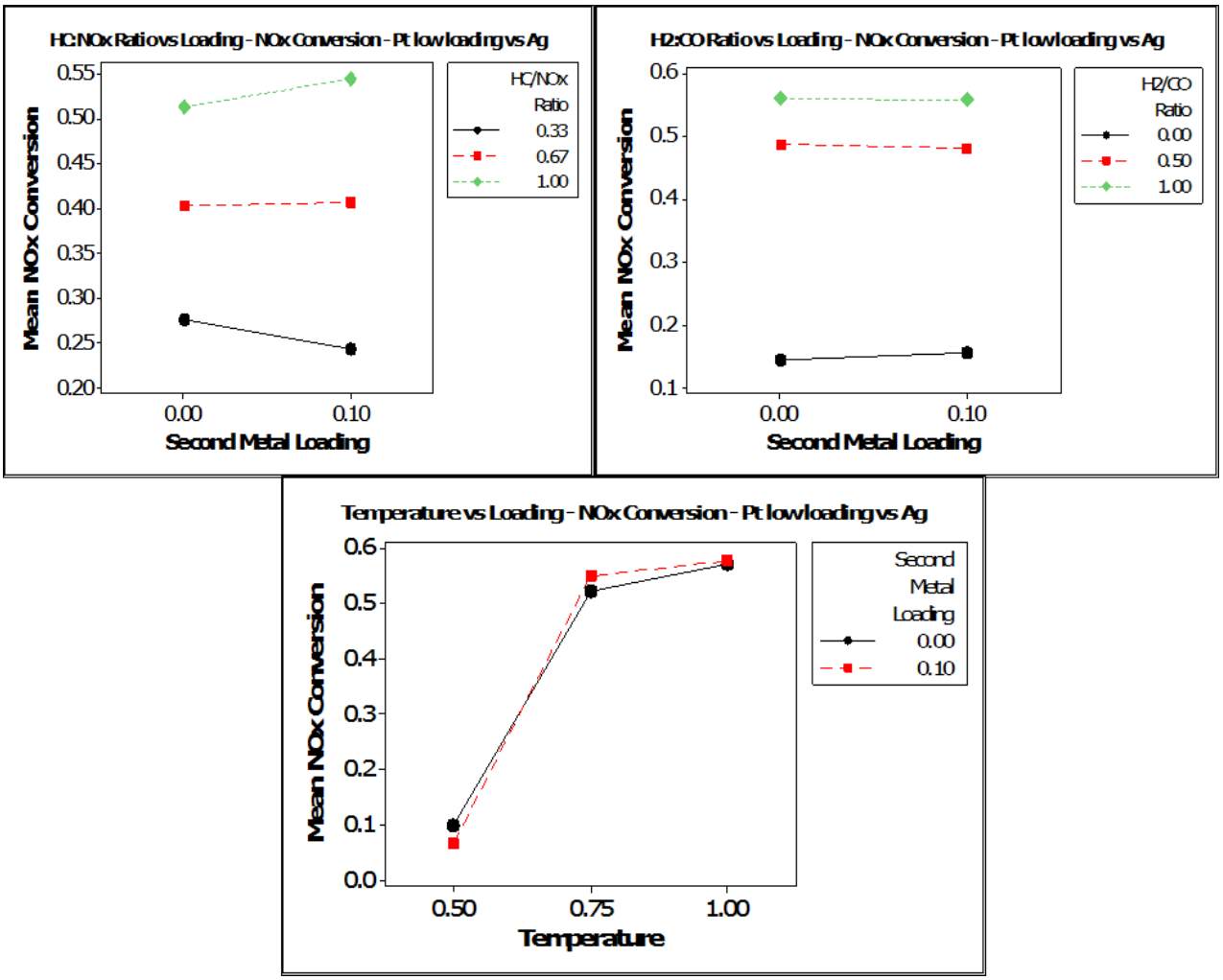

Figure 4.3: Interaction plots of the pure Ag and 1% Pt bimetallic catalysts for NO_x conversion for HC/NO_x ratio, H_2/CO ratio, and reaction temperature with second metal loading.

these catalysts. This decline is observed at 300°C and 400°C; the NO_x conversion was negligible over all the catalysts at 200°C.

Unlike the Pd and Pt bimetallic catalysts, the NO_x conversion performance for the Rh bimetallic catalysts was similar at both the low and high loadings. The presence of the Rh resulted in a decrease in the NO_x conversion when compared with Ag/Al_2O_3 alone. The similarity in NO_x conversion performance may be related to the dispersion of the Rh on the surface. A study by Hecker and Breneman compared various loadings of Rh on SiO_2 for the reduction of NO_x on CO. Two of the catalysts studied had weight loadings of 0.04% and 0.2%. The loadings of the catalysts were the two smallest amounts studied and are close to the actual measured loadings of the low and high-loading catalysts in this study. They found that the two catalysts had the same activity for NO_x reduction. They postulated, based on conclusions from Boudart *et al.* that as the weight loading of the Rh increased, the number of nearest neighbor sites increased, therein decreasing the activation energy of the rate-determining step for NO_x reduction [13, 14].

It was also observed that the NO_x conversion over the high-loading bimetallic catalysts reached a maximum at 300°C, before stagnating or decreasing at 400°C. The behavior is characteristic of the platinum group metals for which the conversion goes through a maximum as reaction temperature is increased. According to Obuchi *et al.*, the Pd is the least active of the three metals, achieving a maximum conversion of 10% at 250°C. Pt and Rh achieve a maximum conversion of 50% at 250°C and 300°C, respectively. At temperatures below the peak NO_x conversion temperature, the oxidation of the hydrocarbon does not occur at a substantial rate. The O_2 is able to react with the hydrocarbon and NO_x to form the partially oxidized hydrocarbon species which initiate the NO_x reduction. Above the peak temperature, the complete oxidation of the hydrocarbon proceeds too quickly and the formation of the partially oxidized hydrocarbons is minimized [15].

Table 4.2: H_2 uptakes and metal dispersions for the Ag-first bimetallic catalysts.

Catalyst	H_2 uptake (μmol/g)	Noble Metal Dispersion (%)
Ag-10% Pd/Al_2O_3	2 ± 1	16
Ag-10% Pt/Al_2O_3	1 ± 0	18
Ag-10% Rh/Al_2O_3	4 ± 1	37

4.4.2 N_2 Selectivity

The decrease in selectivity to N_2 due to the second metal loading is related to the amount of metal on the surface. Platinum group metals are known for producing significant amounts of N_2O [15, 16]. As the loading is increased, more of the PGM is exposed on the surface and the properties of the bimetallic catalysts begin to exhibit behavior similar to the PGMs.

4.5 Effect of Metal Type

4.5.1 NO_x Conversion

In the factorial analysis, the metal type was a significant factor in the NO_x conversion. The main effect plot of NO_x conversion for second metal type showed that the Pd bimetallic catalysts were slightly less active than the Pt or Rh bimetallic catalysts. The significance was observed in the interaction of second metal type with reaction temperature. There is no difference in NO_x conversion between the metals at 200°C and 400°C. However, at 300°C, the average NO_x conversion over the Pd bimetallics was 6% less than the Pt bimetallic catalysts and 10% less than the Rh bimetallic catalysts. It is hypothesized that the decrease in the Pd bimetallic catalyst performance is due to the reduced dispersion of the Pd compared with Pt and Rh. Table 4.2 displays the H_2 uptake for the Ag-first bimetallic catalysts. Pd bimetallic catalysts had the lowest dispersion of the three noble metals. Typically as the dispersion decreases, the particle size increases. The larger Pd particles possibly blocked some Ag sites and also therefore reduced the conversion.

4.5.2 N_2 Selectivity

The second metal type was significant for N_2 selectivity. According to the main effect plot, the ranking of metal type for selectivity was Rh > Pt > Pd. The ranking is maintained for the bimetallic catalysts at low loadings. However, there was a significant increase in the N_2 selectivity for Rh bimetallic catalysts at high loadings. The increase was observed in the interaction between metal type and reaction temperature. The Rh bimetallic catalysts performed much better than the Pt or Pd bimetallic catalysts at 200°C. However, the conversion to NO_x was less than 10% at this temperature, therein the overall improvement in N_2 selectivity was offset by the negligible conversion to NO_x for Rh bimetallic catalysts.

4.6 Effect of Loading Order

For NO_x conversion and N_2 selectivity, the main effect of loading order was not a significant factor. However, the interaction between second metal type and loading order was significant as a result of the behavior of the Pd bimetallic catalyst. When the Pd precursor was added before the Ag precursor, the NO_x conversion increased by 7% and the N_2 selectivity increased by 12%. There was no change in the NO_x conversion or N_2 selectivity for the Pt or Rh bimetallic catalysts.

The improvement in the NO_x conversion and N_2 selectivity when Pd is added before Ag may have indicated that some modification on the surface occurred. A number of papers have studied Ag-Pd bimetallic catalysts, particularly for ethylene epoxidation and detail the ability of Pd to alloy with Ag [17–20]. Although the phase diagram shown in Figure 4.4 depicts that Pd should alloy with Ag at temperatures of 900°C and above [21], Pd has shown to interact electronically with Ag at the nanoscale level. However, alloying can not explain the positive effect in the NO_x conversion and N_2 selectivity when Pd is added first. Shu *et al.* proposed a possible explanation

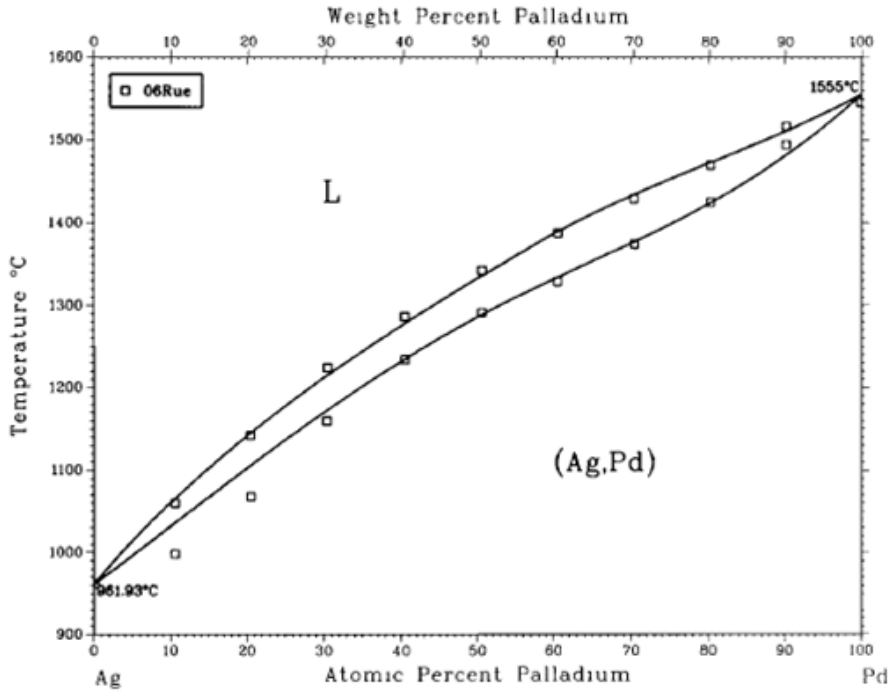

Figure 4.4: The phase diagram for Ag and Pd. The "'L"' signifies the aqueous phase.

for the improvement. They studied the effect of loading order on the hydrogenation activity of Pt/Ni catalysts. They observed that when the Pt was added first, the hydrogenation activity improved significantly compared to when Ni was added first. They used EXAFS to verify the formation of Pt-Ni bimetallic bonds when Pt was added first. The resulting interaction produced a modified active site that was more active for the target reaction [22]. Since Ag and Pd are known to interact, adding Pd first may increase the extent of interaction between the Pd and Ag, which in turn improves the NO_x conversion and N_2 selectivity. Pt and Rh will not alloy with Ag through impregnation preparation methods [23] as shown in Figure 4.5 [24] and Figure 4.6 [25]. The inability of Pt and Rh to alloy corroborates the theory that the exposed surface on Ag-Pt and Ag-Rh bimetallic catalysts is similar independent of the loading order, and therein the NO_x conversion and N_2 selectivity do not change.

To understand the nature of the surface, the surface energies of the individual metals need to be known. Vitos *et al.* conducted an extensive theoretical study to

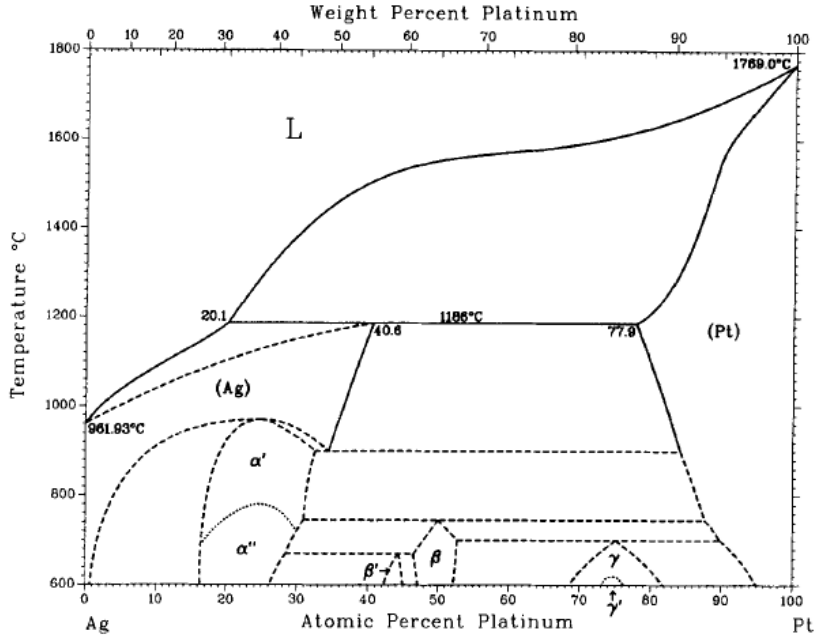

Figure 4.5: The phase diagram for Ag and Pt.

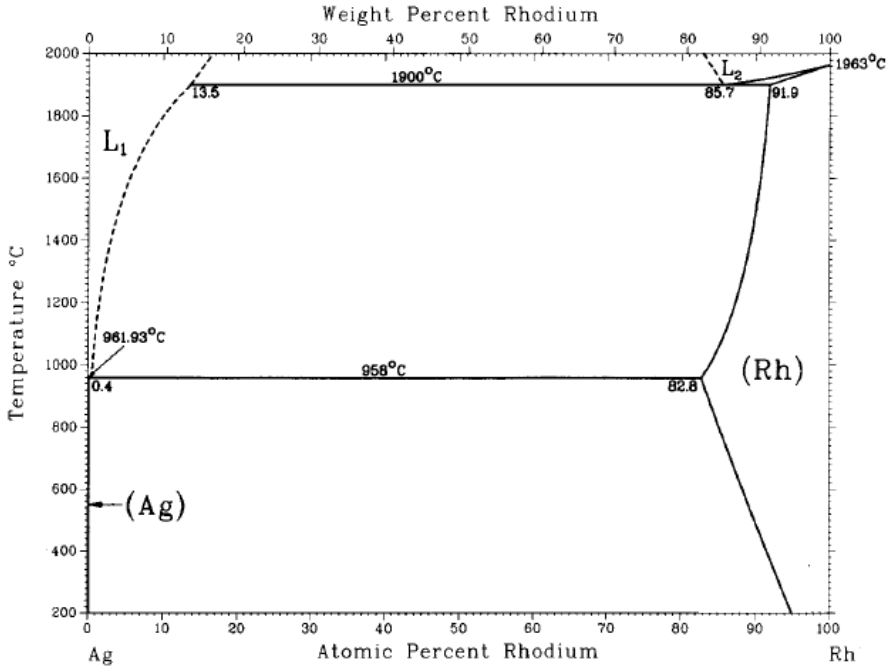

Figure 4.6: The phase diagram for Ag and Rh.

Table 4.3: Surface energies of the metals on the (111) crystal surface.

Metal	Surface Energies (J/m^2)
Ag	1.172
Pd	1.920
Pt	2.299
Rh	2.472

determine the surface energies of over 60 different metals [26]. Between two metals, the one with the lower the surface energy will migrate the surface. Table 4.3 displays the surface energies for Ag, Pd, Pt, and Rh for the (111) surface [26]. As observed, the Ag has the lowest surface energy, and will therefore tend the rise to the surface. This behavior was confirmed by a number of authors such as Jaatinen *et al.*, who used density functional theory (DFT) calculations to show that Pd lies 14 picometers (0.14 Angstroms) below the surface Ag atoms in the case of the (111) surface [17].

4.6.1 Temperature Programmed Reduction

Temperature programmed reduction (TPR) was used to determine the reduction temperatures for chemisorption. Figure 4.7 shows the H_2 TPR profiles for Pd-based catalysts. For Al_2O_3, a single peak is observed at 350°C, corresponding to weakly physisorbed O_2 being removed from the surface of the support. For Ag/Al_2O_3, a consumption peak is observed at 250°C. This peak is attributable to the reduction of Ag_2O [3]. This peak is convoluted with the Al_2O_3 reduction peak. At low loadings, it was difficult to see consumption of H_2. For the 10% Pd catalyst, a broad yet small H_2 consumption peak was observed at about 110-120°C corresponding to the reduction of PdO to Pd [27, 28]. For the bimetallic catalysst, the reduction behavior changed significantly. The absence of the peak attributed to the reduction of Ag_2O in the Ag-10% Pd sample implies that H_2 may have spilled over from reduced Pd to Ag_2O during the reduction of PdO [29]. The peak profiles changed significantly with loading order. For Ag-1% Pd and Ag-10% Pd, there was no visible Ag reduction peak. However,

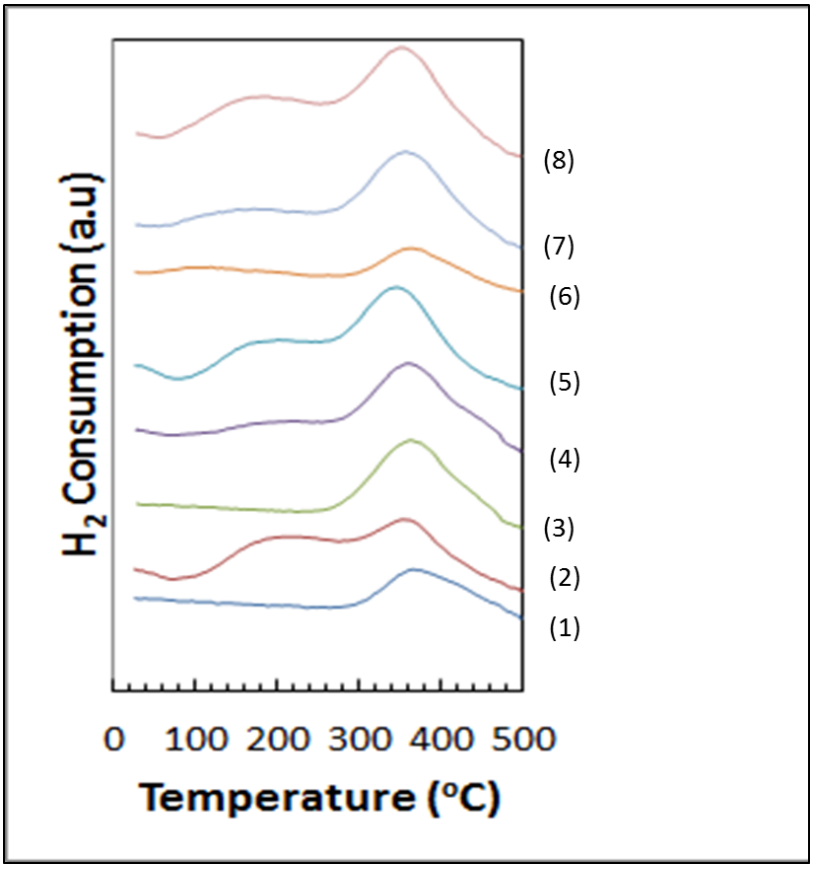

Figure 4.7: H_2 TPR profiles for Pd-based catalysts.(1) Al_2O_3, (2) Ag/Al_2O_3, (3) 1% Pd/Al_2O_3, (4) Ag-1% Pd/Al_2O_3, (5) 1% Pd-Ag/Al_2O_3, (6) 10% Pd/Al_2O_3, (7) Ag-10% Pd/Al_2O_3, (8) 10% Pd-Ag/Al_2O_3.

with 1% Pd-Ag and 10% Pd-Ag, a peak was observed around 250°C. The TPR shows that loading order did affect the exposed surface for the Pd bimetallic catalysts, as the Ag_2O reduction was significantly larger. The nature of the surface explains the behavior seen in the NO_x conversion and N_2 selectivity interaction effects between second metal type and loading order in which switching the loading order resulted in a 7% increase in the NO_x conversion and 12% increase in the N_2 selectivity.

Figure 4.8 shows the H_2 TPR profiles for Pt-based catalysts. For 1% Pt, no peaks are observed, likely because of the low concentration of the metal. The peak attributed to Ag_2O reduction is the only peak observable on the Ag-1% Pt catalyst. For 10% Pt, a broad, but small H_2 consumption peak was observed at about 180°C corresponding

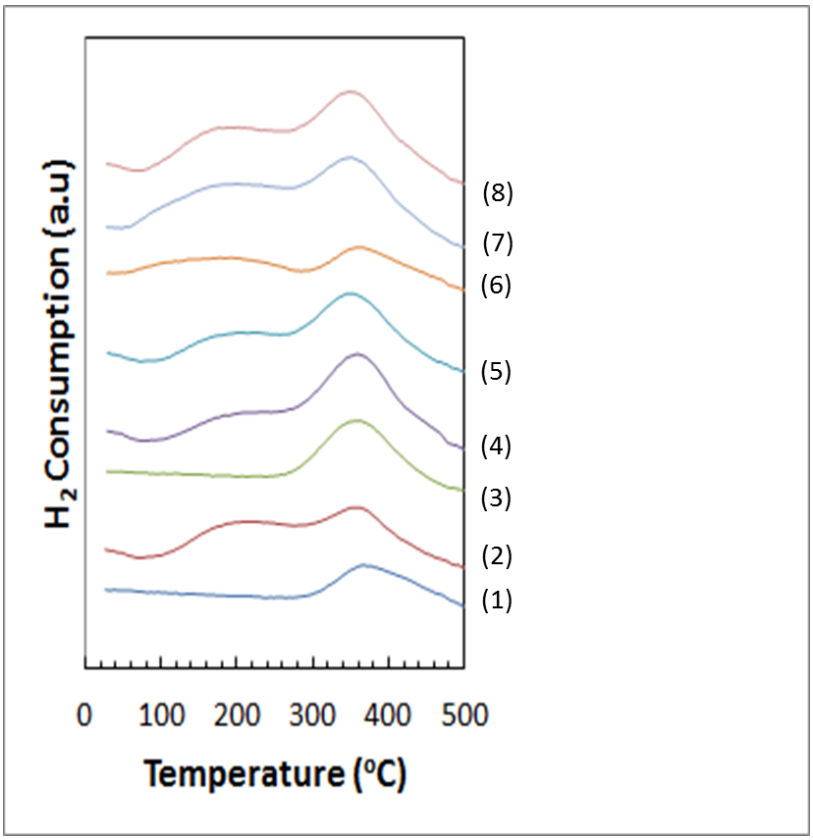

Figure 4.8: H_2 TPR profiles for Pt-based catalysts.(1) Al_2O_3, (2) Ag/Al_2O_3, (3) 1% Pt/Al_2O_3, (4) Ag-1% Pt/Al_2O_3, (5) 1% $Pt\text{-}Ag/Al_2O_3$, (6) 10% Pt/Al_2O_3, (7) Ag-10% Pt/Al_2O_3, (8) 10% $Pt\text{-}Ag/Al_2O_3$.

to the reduction of PtO_2 [30]. On Ag-10% Pt, a convoluted peak, probably due to a combination of the reduction of PtO_2 and Ag_2O, was noted at 210°C. The presence of the Pt decreased the temperature at which the Ag reduces, implying that the Pt promoted the reducibility of Ag_2O to metallic Ag. Reversing the loading order did not appear to change the peak profiles of the Pt bimetallic catalysts, which also may explain why the NO_x conversion and N_2 selectivity remained unchanged.

Figure 4.9 shows the H_2 TPR profiles for Rh-based catalysts. For 1% Rh, no peaks are observed, due to the low concentration of the metal. When Ag is added, the only peak present is related to the reduction of Ag_2O to Ag. For 10% Rh, there is a sharp H_2 consumption peak at 120°C, corresponding with the reduction of Rh_2O_3 [31]. The profile for the Ag-10% Rh displays that the presence of the Rh shifted the

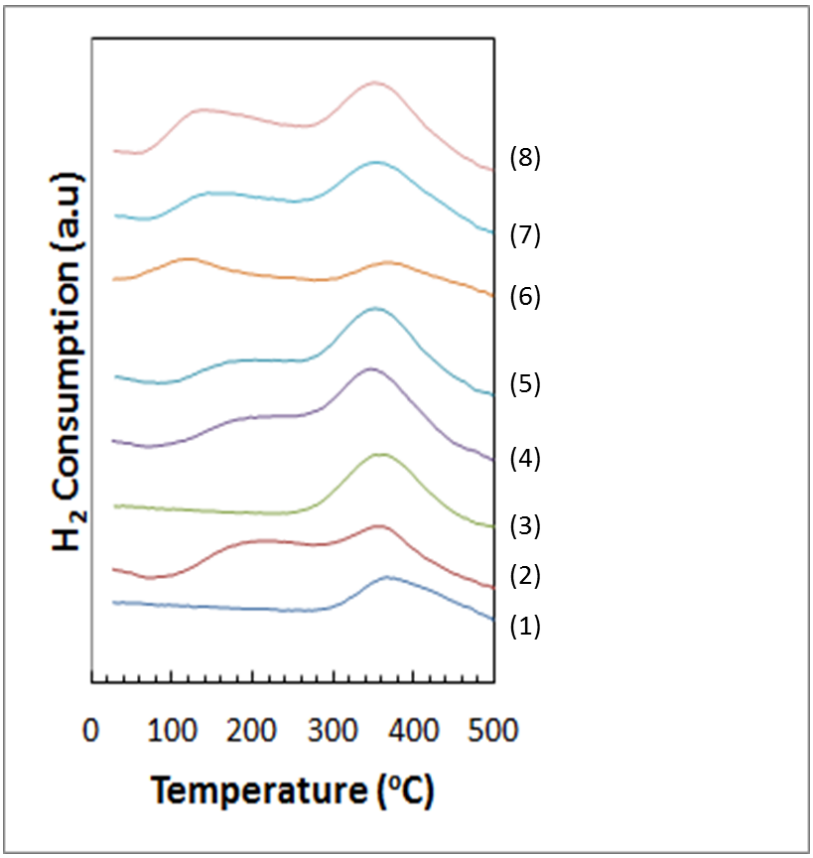

Figure 4.9: H_2 TPR profiles for Rh-based catalysts.(1) Al_2O_3, (2) Ag/Al_2O_3, (3) 1% Rh/Al_2O_3, (4) Ag-1% Rh/Al_2O_3, (5) 1% Rh-Ag/Al_2O_3, (6) 10% Rh/Al_2O_3, (7) Ag-10% Rh/Al_2O_3, (8) 10% Rh-Ag/Al_2O_3.

reduction of Ag_2O to 230°C. This same shift was also observed for the 10% Rh-Ag catalyst. The shift showed that the presence of the Rh helped to reduce the Ag at a slightly lower temperature. However, the change in the Ag reduction temperature did not result in a significant change to the NO_x conversion or N_2 selectivity.

4.6.2 Chemisorption

Based on the TPR results, all catalysts were pretreated by reduction at 250°C in 10% H_2/Ar before being exposed to the chemisorbate gas. A stoichiometry of O/Ag = 1 was assumed [32] and a stoichometry of H/Pd, H/Pt, and H/Rh = 1 was assumed. Table 4.4 shows the H_2 uptakes and metal dispersions for the Ag-first and Ag-second bimetallic catalysts. Experiments with Al_2O_3 and Ag indicated that

Table 4.4: H_2 uptakes and metal dispersions for the Ag-first and Ag-second bimetallic catalysts.

Catalyst	H_2 uptake (μmol/g)	Noble Metal Dispersion (%)
Ag/Al_2O_3	-	-
Ag-10% Pd/Al_2O_3	2 ± 1	16
10% Pd-Ag/Al_2O_3	6 ± 1	42
Ag-10% Pt/Al_2O_3	1 ± 0	18
10% Pt-Ag/Al_2O_3	1 ± 0	18
Ag-10% Rh/Al_2O_3	4 ± 1	37
10% Rh-Ag/Al_2O_3	9 ± 1	79

Table 4.5: O_2 uptakes and metal dispersions for the Ag-first and Ag-second bimetallic catalysts.

Catalyst	O_2 uptake (μmol/g)	Theoretical Ag Dispersion (%)
Ag/Al_2O_3	2 ± 1	2
Ag-10% Pd/Al_2O_3	1 ± 0	1
10% Pd-Ag/Al_2O_3	6 ± 1	9
Ag-10% Pt/Al_2O_3	1 ± 0	2
10% Pt-Ag/Al_2O_3	2 ± 1	3
Ag-10% Rh/Al_2O_3	3 ± 1	4
10% Rh-Ag/Al_2O_3	3 ± 1	4

neither the support nor the Ag surface sites chemisorbed H_2 under the conditions employed. Except for Pt, switching the order had a positive impact on the surface noble metal density. This indicated that there was surface promotion of the Pd and Rh by the Ag through the formation of a Pd-Ag solid solution or an Ag-rich Rh alloy. Yuvaraj *et al.* observed the formation of Rh-Ag alloys [33]. Table 4.5 shows the O_2 uptakes and metal dispersions for the Ag-first and Ag-second bimetallic catalysts. O_2 chemisorption showed that switching the order of loading helped to promote the surface dispersion of Ag, particularly with the Pd bimetallic catalysts. This promotion of the Ag can possibly be attributed to the ability of Pd to interact electronically with Ag. Pt and Rh have been shown not to interact with Ag, and therefore the metals are likely oriented in separate domains.

4.7 Conclusions

The effects of loading, platinum group metal type, and loading order on the NO_x conversion and N_2 selectivity were described. The detrimental effect on NO_x conversion and N_2 selectivity due to increasing second metal loading was caused by the increased extent of the unselective combustion of C_3H_6. Pd bimetallic catalysts performed slightly worse than the Pt or Rh bimetallic catalysts. The difference in performance was observed at 300°C and at high loadings. H_2 chemisorption experiments showed that the noble metal dispersion of Pd was the smallest compared to Pt and Rh. The low dispersion resulted in larger particles on the surface of the Ag/Al_2O_3, possibly blocking Ag sites and enhancing the unselective combustion of the C_3H_6 to CO_2. The loading order was reversed, with the platinum group metal impregnated first. As a main effect, the loading order was not significant in affecting the NO_x conversion. However, the interaction of loading order with the metal type was significant. The NO_x conversion and N_2 selectivity over the Pt and Rh bimetallic catalysts were similar regardless of the loading order, but Pd bimetallic catalysts displayed a significantly larger conversion to NO_x and selectivity to N_2 when Ag was added second. The improvement was attributed to the significant increase in dispersion of the Ag when it was added after the Pd and possibly by electronic interactions between the Pd and Ag.

Bibliography

[1] R. Burch, J.P. Breen, C.J. Hill, B. Krutzsch, B. Konrad, E. Jobson, L. Cider, K. Eranen, F. Klingstedt, and L.E. Lindfors. Exceptional activity for NO_x reduction at low temperatures using combinations of hydrogen and higher hydrocarbons on Ag/Al_2O_3 catalysts. *Topics in Catalysis*, 30(1-4):19–25, 2004.

[2] S. Satokawa. Enhancing the NO/C_3H_8 reaction by using H_2 over Ag/Al_2O_3 catalysts under lean-exhaust conditions. *Chemistry Letters*, 29(3):294–295, 2000.

[3] M. Richter, U. Bentrup, R. Eckelt, M. Schneider, M.M. Pohl, and R. Fricke. The effect of hydrogen on the selective catalytic reduction of NO in excess oxygen over Ag/Al_2O_3. *Applied Catalysis B: Environmental*, 51(4):261–274, 2004.

[4] S. Satokawa, J. Shibata, K. Shimizu, A. Satsuma, and T. Hattori. Promotion effect of H_2 on the low temperature activity of the selective reduction of NO by light hydrocarbons over Ag/Al_2O_3. *Applied Catalysis B: Environmental*, 42(2):179–186, 2003.

[5] R. Burch and P.J. Millington. Selective reduction of NO_x by hydrocarbons in excess oxygen by alumina-and silica-supported catalysts. *Catalysis Today*, 29(1-4):37–42, 1996.

[6] M. Huuhtanen, T. Kolli, T. Maunula, and R.L. Keiski. *In situ* FTIR study on NO reduction by C_3H_6 over Pd-based catalysts. *Catalysis Today*, 75(1-4):379–384, 2002.

[7] A. Kotsifa, D.I. Kondarides, and X.E. Verykios. Comparative study of the chemisorptive and catalytic properties of supported Pt catalysts related to the selective catalytic reduction of NO by propylene. *Applied Catalysis B: Environmental*, 72(1-2):136–148, 2007.

[8] E.A. Efthimiadis, S.C. Christoforou, A.A. Nikolopoulos, and I.A. Vasalos. Selective catalytic reduction of NO with C_3H_6 over Rh/alumina in the presence and absence of SO_2 in the feed. *Applied Catalysis B: Environmental*, 22(2):91–106, 1999.

[9] J. Wang, H. He, Q. Feng, Y. Yu, and K. Yoshida. Selective catalytic reduction of NO_x by C_3H_6 over Ag/Al_2O_3 catalyst with a small quantity of noble metal. *Catalysis Today*, 93:783–789, 2004.

[10] K. Sato, T. Yoshinari, Y. Kintaichi, M. Haneda, and H. Hamada. Rh-post-doped Ag/Al_2O_3 as a highly active catalyst for the selective reduction of NO with decane. *Catalysis Communications*, 4(7):315–319, 2003.

[11] P.C. Aben. Palladium areas in supported catalysts:: Determination of palladium surface areas in supported catalysts by means of hydrogen chemisorption. *Journal of Catalysis*, 10(3):224–229, 1968.

[12] J.E. Benson, H.S. Hwang, and M. Boudart. Hydrogen-oxygen titration method for the measurement of supported palladium surface areas. *Journal of Catalysis*, 30(1):146–153, 1973.

[13] W.C. Hecker and R.B. Breneman. The effect of weight loading and reduction temperature on Rh/silica catalysts for NO reduction by CO. In *Catalysis and automotive pollution control: proceedings of the First International Symposium (CAPOC I), Brussels, September 8-11, 1986*, volume 30, page 257. Elsevier Science Ltd, 1987.

[14] M. Boudart. Catalysis by supported metals. *Adv. Catal. Relat. Subj.*, 20:153–166, 1969.

[15] A. Obuchi, A. Ohi, M. Nakamura, A. Ogata, K. Mizuno, and H. Ohuchi. Performance of platinum-group metal catalysts for the selective reduction of nitrogen oxides by hydrocarbons. *Applied Catalysis B: Environmental*, 2(1):71–80, 1993.

[16] R. Burch, J.P. Breen, and F.C. Meunier. A review of the selective reduction of NO_x with hydrocarbons under lean-burn conditions with non-zeolitic oxide and platinum group metal catalysts. *Applied Catalysis B: Environmental*, 39(4):283–303, 2002.

[17] S. Jaatinen, P. Salo, M. Alatalo, V. Kulmala, and K. Kokko. Structure and reactivity of Pd doped Ag surfaces. *Surface Science*, 529(3):403–409, 2003.

[18] Q. Zhang, J. Li, X. Liu, and Q. Zhu. Synergetic effect of Pd and Ag dispersed on Al_2O_3 in the selective hydrogenation of acetylene. *Applied Catalysis A: General*, 197(2):221–228, 2000.

[19] R.N. Lamb, B. Ngamsom, D.L. Trimm, B. Gong, P.L. Silveston, and P. Praserthdam. Surface characterisation of Pd-Ag/Al_2O_3 catalysts for acetylene hydrogenation using an improved XPS procedure. *Applied Catalysis A: General*, 268(1-2):43–50, 2004.

[20] JC Dellamorte, J. Lauterbach, and MA Barteau. Palladium-silver bimetallic catalysts with improved activity and selectivity for ethylene epoxidation. *Applied Catalysis A: General*, 391(1-2):281–288, 2011.

[21] I. Karakaya and W.T. Thompson. The Ag-Pd (Silver-Palladium) system. *Journal of Phase Equilibria*, 9(3):237–243, 1988.

[22] Y. Shu, L.E. Murillo, J.P. Bosco, W. Huang, A.I. Frenkel, and J.G. Chen. The effect of impregnation sequence on the hydrogenation activity and selectivity of supported Pt/Ni bimetallic catalysts. *Applied Catalysis A: General*, 339(2):169–179, 2008.

[23] V.K. Tzitzios, V. Georgakilas, and T.N. Angelidis. Catalytic reduction of N_2O with CH_4 and C_3H_6 over Ag-Rh/Al_2O_3 bimetallic catalyst in the presence of oxygen. *Journal of Chemical Technology & Biotechnology*, 80(6):699–704, 2005.

[24] I. Karakaya and W.T. Thompson. The Ag-Pt (Silver-Platinum) system. *Journal of Phase Equilibria*, 8(4):334–340, 1987.

[25] I. Karakaya and W.T. Thompson. The Ag-Rh (Silver-Rhodium) system. *Journal of Phase Equilibria*, 7(4):362–365, 1986.

[26] L. Vitos, A.V. Ruban, H.L. Skriver, and J. Kollar. The surface energy of metals. *Surface Science*, 411(1-2):186–202, 1998.

[27] F.B. Noronha, D.A.G. Aranda, A.P. Ordine, and M. Schmal. The promoting effect of Nb_2O_5 addition to Pd/Al_2O_3 catalysts on propane oxidation. *Catalysis Today*, 57(3-4):275–282, 2000.

[28] R.J. Wu, T.Y. Chou, and C.T. Yeh. Enhancement effect of gold and silver on nitric oxide decomposition over Pd/Al_2O_3 catalysts. *Applied Catalysis B: Environmental*, 6(2):105–116, 1995.

[29] C.W. Chou, S.J. Chu, H.J. Chiang, C.Y. Huang, C. Lee, S.R. Sheen, T.P. Perng, and C. Yeh. Temperature-programmed reduction study on calcination of nano-palladium. *The Journal of Physical Chemistry B*, 105(38):9113–9117, 2001.

[30] L.S. Carvalho, P. Reyes, G. Pecchi, N. Figoli, C.L. Pieck, and M. do Carmo Rangel. Effect of the solvent used during preparation on the properties of Pt/Al_2O_3 and Pt-Sn/Al_2O_3 catalysts. *Industrial and engineering chemistry research*, 40(23):5557–5563, 2001.

[31] H.C. Yao, S. Japar, and M. Shelef. Surface interactions in the system Rh/Al_2O_3. *Journal of Catalysis*, 50(3):407–418, 1977.

[32] T.E. Hoost, R.J. Kudla, K.M. Collins, and M.S. Chattha. Characterization of Ag/[gamma]-Al_2O_3 catalysts and their lean-NO_x properties. *Applied Catalysis B: Environmental*, 13(1):59–67, 1997.

[33] S. Yuvaraj, S.C. Chow, and C.T. Yeh. Characterization of Silver-Rhodium Bimetallic Nanocrystallites Dispersed on [gamma]-Alumina. *Journal of Catalysis*, 198(2):187–194, 2001.

CHAPTER V

Conclusions and Future Work

5.1 Summary

The reduction of vehicle exhaust emissions is of primary concern in the field of pollution reduction, particularly for NO_x emissions from diesel engines. Increasingly stringent emissions standards set by the U.S. Environmental Protection Agency and the desire to reduce photochemical smog has made the development of technologies for NO_x reduction a key focus in the catalysis community. Many technologies have been researched such as NO_x decomposition, NO_x storage reduction, selective catalytic reduction with urea, and selective catalytic reduction with hydrocarbons (HC-SCR). Each technology has advantages and disadvantages. Hydrocarbon selective catalytic reduction of NO_x is one of the most promising methods. Ag/Al_2O_3 has been one of the most researched catalysts for this reaction due to its high activity for NO_x reduction and high selectivity to N_2. However, the catalyst is not active below 400°C [1]. The addition of H_2 to the exhaust system has shown to reduce the temperature at which NO_x starts to react by nearly 150-200°C, depending on the concentration of H_2 [2]. In addition, Pd, Pt, and Rh have demonstrated NO_x reduction activity at temperatures below 400°C [3]. In this work a full factorial analysis was conducted with five factors and three levels. Using MINITAB^{TM} software, the data was analyzed to determine factor significance on the NO_x conversion and N_2 selectivity. In addition, the order of

metal loading was studied. In this chapter the major conclusions stated in this thesis are outlined and discussion of possible future directions is presented.

5.2 General Conclusions

Increasing the second metal loading affected the NO_x conversion detrimentally. The effect of the loading was unexpected as multiple papers have stated that a small amount of noble metal can improve the NO_x conversion [4, 5]. It was believed that the overall NO_x conversion would have been improved with the ability of platinum group metals to reduce NO_x using H_2 and CO, but this trend was not observed in this dissertation. It was hypothesized that the unselective combustion of C_3H_6 to CO_2 was enhanced by the presence of the platinum group metal. This trend was displayed by analyzing the NO_x and C_3H_6 conversions with respect to second metal loading. Unlike the bimetallic catalysts at low loadings, which exhibited high activity to NO_x and did not completely combust C_3H_6, the high-loading catalysts completely exhausted the C_3H_6, and the NO_x conversion subsequently decreased. O_2 chemisorption was also used to measure the Ag dispersion. The dispersions decreased when the platinum group metal was added, but the change was not significant. Therefore, it was concluded that the unselective combustion of the C_3H_6 was the primary cause of the reduction in the conversion of NO_x due to second metal loading. There were also significant interactions that involved the second metal loading, particularly with reaction temperature and second metal type. The decrease in conversion of NO_x due to the increase of the second metal loading was observed at 300°C and above at high loadings. The behavior observed in the interaction was also attributed to the unselective combustion of C_3H_6 as well. Concerning the second metal type, at low loadings, the Pd and Pt bimetallic catalysts performed similarly to Ag/Al_2O_3 whereas the Rh bimetallic catalysts did not perform as well. At high loadings, the NO_x conversions of the Pd and Pt bimetallic catalysts dropped significantly while the

NO_x conversion over the Rh bimetallic catalysts increased, although not to the same level as the Ag/Al_2O_3.

The selectivity to N_2 also decreased as the second metal loading was increased. The decrease was observed in the performance of the Pd and Pt bimetallic catalysts. At low loadings, although the Pd and Pt bimetallic catalysts had similar NO_x activities to Ag/Al_2O_3, they produced more N_2O. At high loadings, the extent of N_2O formation increased, resulting in a further decrease in the selectivity to N_2. The same decrease in selectivity was observed for Rh, although not as significant. The behavior changes significantly at high loadings, where the Rh bimetallic catalyst displayed a higher average N_2 selectivity than Ag/Al_2O_3. However, the improvement was observed only at 200°C, at which the NO_x conversion was less than 10%.

The loading order was also studied, in which Ag was impregnated after the Pd, Pt, or Rh. The surface areas and metal loadings were similar to the Ag-first catalysts. For NO_x conversion and N_2 selectivity, the main effect of loading order by itself was not significant. However, the interaction between second metal type and the loading order was significant, as the Pd bimetallic catalysts performed worse than the Pt and Rh bimetallic catalysts when Ag was added first. When Ag was added after the Pd, the NO_x conversion and N_2 selectivity significantly improved. When comparing the bimetallic catalysts when Ag was added second compared to Ag added first, the O_2 uptake increased significantly, indicating the surface was populated with more Ag atoms. The extra exposed Ag results in a higher NO_x conversion and N_2 selectivity over the Ag secondly-loaded Pd bimetallic catalysts.

5.3 Future Research Directions

The presence of the platinum group metal on the surface of the Ag/Al_2O_3 did not improve HC-SCR of NO_x conversion due to unselective combustion of the C_3H_6 to CO_2 as the loading increases. In addition, the second metal type was a significant

factor with the Pd bimetallic catalysts performing worse that the Pt or Rh bimetallic catalysts. For the N_2 selectivity, the increase in PGM loading also resulted in a significant decrease in the selectivity. The Rh bimetallic catalysts performed better than the Pd or Pt bimetallic catalysts, but the improvement was seen only at 200°C where the NO_x conversion was negligible. Loading order was only significant for the Pd bimetallic catalysts, in which loading Pd first improved the NO_x conversion and N_2 selectivity compared with loading Ag first.

Because the PGMs appeared to hinder the NO_x conversion and N_2 selectivity, one suggestion is the modify the preparation method. The metals can be co-impregnated instead of sequentially impregnated; a number of papers focusing on bimetallic catalysts have stated that co-impregnating the two metals possibly improves the interaction between the two metals. Another suggestion is to explore the addition of base metals instead of platinum group metals. Like Ag, base metals have high selectivity to N_2 but low NO_x activity at low temperatures. Investigating the possibility of electronic interactions occurring between the Ag and the base metals that could potentially modify the nature of the active site and possibly improve the performance of the Ag/Al_2O_3 catalyst would be of some interest to study. Quantifying the utilization of the hydrocarbon is also important to study, as doing so would be helpful to know how much of the hydrocarbon participated in the reduction of NO_x and how much was unselectively combusted to CO_2. Furthermore, the behavior observed with respect to loading order on the Pd bimetallic catalysts should be analyzed using EXAFS to determine any electronic interaction that could be occurring between the Pd and Ag.

In addition, real-time characterization of the intermediates is important to understand the mechanistic behavior for these catalysts under the tested conditions. Although there is general consensus on the mechanisms for base and PGMs, the possibility of the involvement of both mechanisms is worth investigating. *In-situ* DRIFTS can

characterize the intermediates on the catalyst surface at specific times and temperatures. Future experiments over the high-loading bimetallic catalysts should be conducted at 300°C to explain possible reasons for the different performances. Moreover, conducting NO temperature-programmed desorption (TPD) experiments at 300°C could provide more insight into the differences between the bimetallic catalysts. In addition, utilizing transient techniques such as temporal analysis of products (TAP) or isotopic labeling could provide real-time monitoring of the intermediates and products that would provide a better understanding of the surface behavior. Finally, any desired formulation must be able to tolerate real-world conditions, and one of the most damaging molecules to the metals in a mobile exhaust aftertreatment system is SO_2. For example, Xie *et al.* found that the presence of SO_2 inhibited the NO_x conversion over Ag-Pd/Al_2O_3 [6]. Investigating and discovering conditions that will strengthen the tolerance of the catalysts to the presence of SO_2 will enhance the possibility of developing new formulations that are active for NO_x and selective to N_2.

Bibliography

[1] R. Burch, J.P. Breen, C.J. Hill, B. Krutzsch, B. Konrad, E. Jobson, L. Cider, K. Eranen, F. Klingstedt, and L.E. Lindfors. Exceptional activity for NO_x reduction at low temperatures using combinations of hydrogen and higher hydrocarbons on Ag/Al_2O_3 catalysts. *Topics in Catalysis*, 30(1-4):19–25, 2004.

[2] M. Richter, U. Bentrup, R. Eckelt, M. Schneider, M.M. Pohl, and R. Fricke. The effect of hydrogen on the selective catalytic reduction of NO in excess oxygen over Ag/Al_2O_3. *Applied Catalysis B: Environmental*, 51(4):261–274, 2004.

[3] R. Burch, P.J. Millington, and A.P. Walker. Mechanism of the selective reduction of nitrogen monoxide on platinum-based catalysts in the presence of excess oxygen. *Applied Catalysis B: Environmental*, 4(1):65–94, 1994.

[4] J. Wang, H. He, Q. Feng, Y. Yu, and K. Yoshida. Selective catalytic reduction of NO_x by C_3H_6 over Ag/Al_2O_3 catalyst with a small quantity of noble metal. *Catalysis Today*, 93:783–789, 2004.

[5] H. He, J. Wang, Q. Feng, Y. Yu, and K. Yoshida. Novel Pd promoted Ag/Al_2O_3 catalyst for the selective reduction of NO_x. *Applied Catalysis B: Environmental*, 46(2):365–370, 2003.

[6] S. Xie, J. Wang, and H. He. Poisoning effect of sulphate on the selective catalytic reduction of NO_x by C_3H_6 over Ag-Pd/Al_2O_3. *Journal of Molecular Catalysis A: Chemical*, 266(1-2):166–172, 2007.